

Cyclopentadiene Based Low-Valent Group 13 Metal Compounds: Ligands in Coordination Chemistry and Link between Metal Rich Molecules and Intermetallic Materials

Sandra González-Gallardo,[†] Timo Bollermann,[‡] Roland A. Fischer,^{*,‡} and Ramaswamy Murugavel^{*,§}

[†]Karlsruhe Institute of Technology (KIT), Institute of Inorganic Chemistry, 76131 Karlsruhe, Germany

[‡]Lehrstuhl für Anorganische Chemie II, Organometallics & Materials Chemistry, Ruhr-University Bochum, D-44780 Bochum, Germany

[§]Department of Chemistry, Indian Institute of Technology Bombay, Powai, Mumbai-400076, India

CONTENTS

1. Introduction	3136
1.1. Scope	3136
1.2. Coverage	3137
2. Low-Valent RE ^I Organyls	3137
2.1. Synthesis of Low-Valent RE ^I Organyls	3137
2.2. Electronic Properties of the RE ^I Species As Ligands	3138
3. Main-Group Metal Complexes	3139
3.1. s-Block Compounds	3139
3.2. p-Block Compounds	3140
4. Transition-Metal Complexes	3142
4.1. Synthetic Methods	3142
4.1.1. Substitution of Labile Ligands	3142
4.1.2. Addition Reactions	3148
4.1.3. Redox Reactions	3148
4.1.4. Insertion Reactions	3150
4.1.5. Hydrogenolysis and Cluster Growth	3154
5. f-Block Complexes	3154
5.1. Lanthanide Compounds	3154
5.2. Actinide Compounds	3155
6. Coordination Chemistry of Substituent-Free Ga ⁺	3156
7. Removal of Cp* from Coordinated Cp*E Ligands	3158
7.1. Protolysis	3158
7.2. Oxidation	3158
7.3. Hydrogenolysis	3159
8. Reactions at [M(ECp*) _n] Fragments	3160
8.1. Bond-Activation Reactions	3160
8.2. Substitution of Cp*E Ligands	3161
8.3. Exchange of the Two-Electron Ligands Cp*E against One-Electron Ligands MR'	3162
9. Precursor Chemical Nanometallurgy: From Fundamentals to Applications	3164
10. Conclusions and Perspectives	3166
Author Information	3167
Corresponding Author	3167
Notes	3167
Biographies	3167
References	3167

1. INTRODUCTION

1.1. Scope

Design and development of synthetic strategies for the isolation of lower-valent compounds of p-block elements in the 1980s and 1990s marked the arrival of new classes of ligands in organometallic chemistry and cluster synthesis. Especially interesting among these are the isolation of synthetically useful quantities of stable *bottleable* carbenes¹ and the kinetically stabilized monovalent compounds of aluminum, gallium, and indium, RE^I, with R typically being a steric demanding monoanionic alkyl or aryl substituent and most prominently R = pentamethylcyclopentadienyl (Cp*).^{2,3} If the substituent R is chosen as a *N,N'* chelating system, such as bulky amidinates, guanidinates, diazabutadienides, or β -diketiminates, the resulting family of RE^I species represent analogues to the nitrogen heterocyclic carbenes (NHCs). The chemistry of these type of compounds of group 13 and 14 elements including their ligand properties has recently been comprehensively reviewed by Asay, Jones, and Driess.⁴ Although the initial interest in the monovalent compounds RE^I of Al and Ga in particular has mainly been due to the challenge of the stabilization of such species and understanding of their structure and bonding, these compounds are being increasingly used as 2-electron donor ligands in coordination chemistry during the last 10 years. Over 150 publications employing RE^I as ligands for the formation of metal–metal bonds, clusters, and more recently molecular alloys have appeared in the literature. The coordination chemistry of RE^I ligands initially focused on transition-metal carbonyl substitution reactions yielding very stable and kinetically inert complexes that simultaneously contain both CO and RE^I ligands. This chemistry was further expanded later to the synthesis of carbonyl-free d-block complexes. More recently the coordination chemistry of these ligands have been expanded to complexes of s-, p-, and f-block metals, even stabilizing very electrophilic metal centers such as Ca, Mg, and lanthanides. From a situation where most of the published work primarily dealt with the synthesis, structure, and bonding aspects about 5 years ago, the current interest in this area is moving toward the exploration of the *reactivity* of the compounds that contain the RE^I ligands, and in particular if R = Cp*. A notable outcome of these studies is the activation

Received: April 9, 2011

Published: February 24, 2012

or selective splitting of Cp^*-E bonds. Accordingly, a separate section in the review will deal with the coordination chemistry of naked, substituent-free Ga^+ , highlighting its strong σ - as well as π -acceptor characteristics but no significant donor capabilities. The soft and flexible binding mode of the Cp^* group combined with the reducing power of Al^{I} or Ga^{I} provides an entry to the novel chemistry of the related monovalent MR^{I} metal ligands as one-electron ligands whose chemistry is also briefly summarized ($\text{M} = \text{Zn}, \text{Cd}, \text{R}' = \text{Me}, \text{Et}, \text{Cp}^*$; and $\text{M} = \text{Au}, \text{R}' = \text{PMe}_3, \text{PPh}_3$). The review closes with the perspectives on using the unique ligand and reactive properties of Cp^*E at transition metals for developing a soft chemical precursor chemistry for intermetallic nanomaterials, such as NiAl alloy phases.

1.2. Coverage

The above developments clearly indicate the arrival of low-valent group 13 compounds as an important class of ligands in organometallic/coordination chemistry since 1994. Although the monovalent chemistry of RE^{I} compounds has been developed for many types of substituents R , most noteworthy being the N,N' chelating systems,⁴ the present article is mainly focused on $\text{R} = \text{Cp}^*$ (and related organyls), largely because of the special features of Cp^* as a removable protecting group in contrast to the other choices of R . There have been some general reviews including the chemistry of $\text{Al}^{\text{I}}, \text{Ga}^{\text{I}},$ and In^{I} compounds but without emphasis on the coordination chemistry of Cp^*E .^{2,3,5,6} A few reviews on the use of group 13 monovalent compounds as ligands have also appeared in the last 15 years.⁷⁻⁹ We like to highlight a recent review by P. W. Roesky concerning the ECp^* complexes at electron-poor metal centers.¹⁰ Our presentation will deal with the synthesis, structure, and subsequent chemistry of the compounds and will only briefly summarize the results of the theoretical bonding analysis on the density functional theory (DFT) level, wherever appropriate.

2. LOW-VALENT RE^{I} ORGANYLs

Although the existence of stable low-valent organyls of relatively lighter group 13 elements such as aluminum and gallium was more of a laboratory curiosity in the late 1980s and early 1990s, today this area has grown into a separate discipline within low-valent organometallic chemistry. By 2010, a large variety of RE^{I} ($\text{E} = \text{Al}, \text{Ga}, \text{In}$) compounds have already been synthesized, and their utility as ligands has been explored in great detail. The nature of the R group in low-valent group 13 compounds influences strongly both the electronic and steric properties of these ligands. All monovalent group 13 compounds have been demonstrated to be strong σ -donors with an ability to also act as relatively weak π -acids. The π -acidity in particular has been found to be largely dependent on the nature of the organic substituent R .

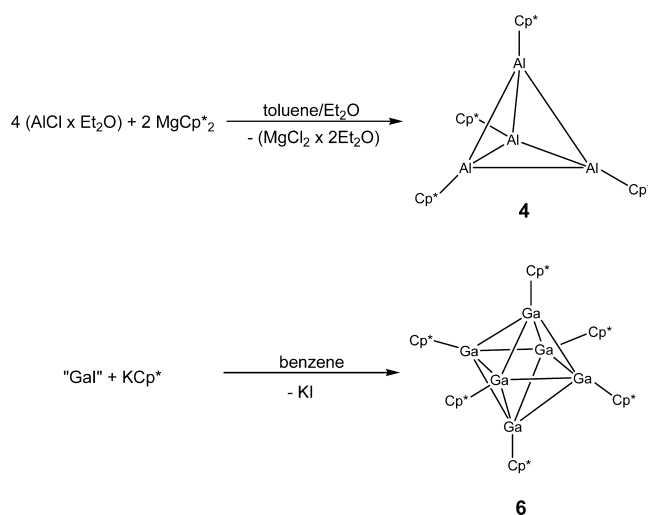
Over the years, many synthetic routes to sterically shielded RE^{I} compounds have been developed (section 2.1), and this topic has been previously reviewed.^{5,8} Thus, the accessibility of such thermodynamically stable species represents a big step toward the tailored synthesis of mixed metal coordination compounds. Because of its unique steric and electronic properties, the Cp^*E ($\text{E} = \text{Al}$ or Ga) species have been one of the extensively used two-electron donor ligands for elements across the periodic table, covering s-, p-, d-, and f-block metals.

2.1. Synthesis of Low-Valent RE^{I} Organyls

Because of their relative stability, the first group 13 low-valent species reported in 1957 were those of the heavier elements In and Tl .^{11,12} The derivatives CpIn (**1**) and CpTl (**2**) were obtained by direct reaction of the halogenides with $\text{Mg}(\text{C}_5\text{H}_5)_2$. CpIn (**1**) and $\text{In}(\text{C}_5\text{H}_4\text{Me})$ (**3**) were later obtained in good yields when InCl was reacted with the corresponding alkyl lithium derivatives.^{13,14}

Schnöckel and co-workers reported in 1991 the successful synthesis of a stable Al^{I} organyl by isolating Cp^*Al (**4**) in the solid state. The synthetic strategy employed involved the reaction of metastable AlCl with Cp^*_2Mg (Scheme 1).¹⁵

Scheme 1. Routes of Synthesis of $\text{Cp}^*\text{E}^{\text{I}}$ Organyls



However, the generation and storing of AlCl starting material is rather difficult as it is obtained from HCl and Al at 1200 K.¹⁶ Therefore, the development of more convenient methods for the synthesis of low-valent RE^{I} ($\text{E} = \text{Al}, \text{Ga}, \text{In}$) organyls was sought soon after. Nowadays these compounds are accessible by other, less tedious laboratory methods. The first method uses the reduction of the trivalent organyls through metathesis reaction involving alkaline or alkaline-earth metals. However, the choice of starting materials is often not trivial, because their nature and availability determine their usefulness as precursors for the isolation of stable RE^{I} species. As highlighted in previous reviews,^{2,5,6,8} the nature of the R substituent is a critical factor in determining whether the RE^{I} species will be monomeric, dimeric, or oligomeric (Figure 1).^{8,17}

In 1992, the synthesis of the first low-valent Ga organyl, CpGa (**5**), was reported.¹⁸ Early work in this area has shown that the 6π -electron-cyclopentadienyl anions ($\text{Cp}, \text{Cp}^*, \text{Cp}(\text{SiMe}_3)_3, \text{Cp}(\text{Benzyl})_5$) are sterically demanding electron donors and hence suitable for stabilization of the low-valent group 13 species.^{19,20} In the following years, new routes to obtain Cp^*Al (**4**) and Cp^*Ga (**6**) were developed. The first alternative method involves the reduction of Cp^*AlCl_2 or Cp^*GaI_2 with a small excess of potassium.^{21,22} To increase the yield, this method underwent numerous modifications, such as the use of Na/K alloy as reducing agent or employing different Cp^*AlX_2 ($\text{X} = \text{Br}, \text{I}$) halides as starting materials.²³ These modifications provided means to optimize this route and obtain many alkyl-substituted RE^{I} compounds ($\text{E} = \text{Al}, \text{Ga}, \text{In}; \text{R} = \text{C}(\text{SiMe}_3)_3, \text{CH}(\text{SiMe}_3)_2, \text{Si}(\text{SiMe}_3)_3, \text{C}(\text{SiMe}_2\text{Et})_3, \text{C}_5\text{Me}_4\text{Ph}$).²⁴⁻³⁰

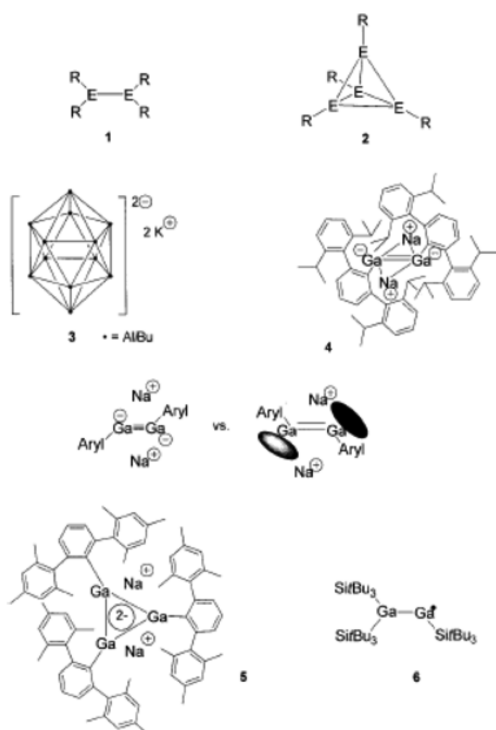


Figure 1. Aggregation of various RE^I species. Reprinted with permission from Linti, G.; Schnöckel, H. Low valent aluminum and gallium compounds—Structural variety and coordination modes to transition metal fragments. *Coord. Chem. Rev.* **2000**, *206–207*, 285–319.⁸ Copyright 2000 Elsevier.

The second alternative route involves the reaction of alkali-metal cyclopentadienides with “GaI”, to yield Cp^*Ga (**6**) and $Ga(C_5EtMe_4)$ (**7**).³¹ The silyl- Ga^I compound $GaSi(SiMe_3)_3$ (**8**) can also be prepared using a similar synthetic protocol.³² Although the above-mentioned group 13 organyls are aggregated oligomers (typically tetramers or hexamers) in the solid state, the use of even bulkier organic groups like substituted arenes can afford monomeric,^{33–35} dimeric,^{36,37} or trimeric complexes.³⁸ The late introduction of β -diketiminate ligands in low-valent group 13 chemistry opened the doors for the isolation of stable monomeric species.^{39,40}

RE^I compounds contain an E element in sp -hybridization with two unoccupied p -orbitals. The stability, isolability, and ease of handling of the low-coordinated compounds RE^I ($E = Al, Ga, In$) provides them with enormous potential as ligands toward transition metals, as opposed to the related B^I organyls.⁴¹ For a deeper understanding of their ligating characteristics, it is necessary to analyze the frontier orbitals of the RE^I compounds, as well as their interaction with the corresponding orbitals of the appropriate symmetry at the transition metals.

2.2. Electronic Properties of the RE^I Species As Ligands

The nature of the bonding between a transition metal and a RE^I ligand in complexes $[L_nM]-ER$ and $[M(ER)_4]$ ($E = B, Al, Ga, In, Tl$; $R = Me, Cp, Cp^*, N(SiH_3)_2$) has been the topic of numerous theoretical studies.^{42–48} Some reviews summarizing the present knowledge in the field have appeared in the literature.^{49,50} The low-valent group 13 organyls RE^I formally possess a free electron-pair located in a σ -orbital (highest occupied molecular orbital (HOMO)) and two degenerate unoccupied p -orbitals (lowest unoccupied molecular orbital

(LUMO)), which lie perpendicular to the axis of the $E-C$ bond (Figure 2). Therefore, their electronic state can be described as

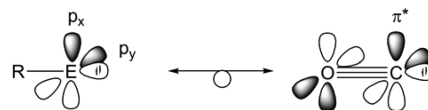


Figure 2. Isolability of RE^I species and CO.

a singlet state, which results in their isolability to CO.^{42,51,52} The HOMO of the group 13 ligand can interact with the corresponding dz^2 orbital on the transition metal, resulting in a σ -donation. Because of the increasing s -contribution and the unfavorable hybridization, the free electron pair at the group 13 center turns gradually inert with increasing atomic number (going down the group), so that the $M-E$ bonding energy decreases correspondingly. In principle, the free p -orbitals remain available for a $M \rightarrow RE^I$ back-donation. However, it has been shown that the electronic properties of the organic substituent R have a strong influence on the ability of the group 13 center to accept π -back-donation, because there is a competing π -donation of the organic substituents R into the free p -orbitals (Figures 2 and 3).

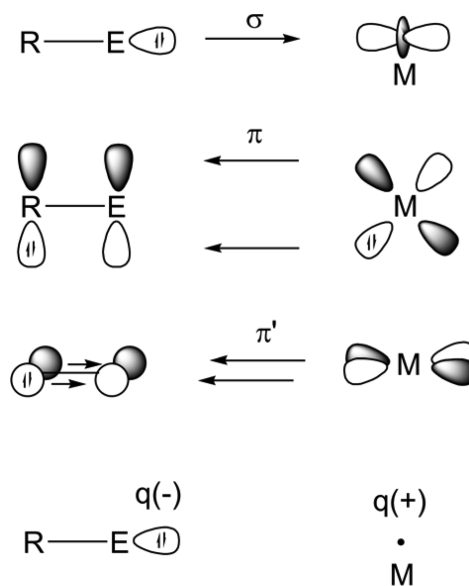


Figure 3. Interactions in $M-ER^I$ complexes.^{45,48} Reprinted and adapted with permission from refs 45 and 48. Copyright 2001 and 2000 American Chemical Society.

For instance, the Cp^* substituent donates electron density from its π -orbitals into both p -orbitals of the group 13 metal and therefore Cp^*E ligands show a diminished ability to accept π -back-donation. However, the Cp -substituted RE^I fragments may increase their ability to accept π -back-donation by changing the hapticity of the C_5 ring from η^5 to η^3 or even η^1 .²² On the other hand, weak π -donor ligands such as the bulky aryl $Ar^* = 2,6-(2,4,6\text{-triisopropylphenyl})phenyl$ ⁵³ and $-C(SiMe_3)_3$ also have the ability to form complexes as seen in $[(CO)_4Fe-GaAr^*]$ (**9**) and $[Ni(Ga-C(SiMe_3)_3)_4]$ (**10**).⁴² In spite of the presence of a rather short $Fe-Ga$ bond in $[(CO)_4Fe-GaAr^*]$ (**9**) (which led the authors to suggest that there is strong $Fe \rightarrow Ga$ π -back-donation), a charge and energy decomposition analysis (EDA) of the model complex

$[(\text{CO})_4\text{Fe}-\text{GaPh}]$ (Ph = phenyl) (**11**) showed that the π -back-donation is not much stronger than in $[(\text{CO})_4\text{Fe}-\text{GaCp}]$ (**12**). The shorter and stronger Fe–Ga bond in **12** arises mainly from the stronger σ -bond and from the enhanced electrostatic attraction (Figure 3).⁴⁵ Such an analysis of the $[(\text{CO})_4\text{Fe}-\text{GaR}]$ bonds (R = Cp, N(SiH₃)₂, Ph, CH₃) in comparison with the data for the $[\text{Fe}(\text{CO})_4-\text{CO}]$ (**13**) bond showed that the relative strength of the π -contribution to the $[(\text{CO})_4\text{Fe}-\text{GaR}]$ bond for the strong π -donor substituents R = Cp, N(SiH₃)₂ (13.2% and 18.2%, respectively) is comparable with that for the weak π -donors Ph and CH₃ (17.2% and 16.0%). The π -orbital contribution to ΔE_{orb} for all $[(\text{CO})_4\text{Fe}-\text{GaR}]$ systems is significantly lower than that for the carbonyl bond in $[\text{Fe}(\text{CO})_4-\text{CO}]$ (**13**) (47.9%). In the case of the homoleptic complexes $[\text{M}(\text{GaR})_n]$ such as $[\text{Fe}(\text{GaCH}_3)_5]$ (**14**) (37.3%) and $[\text{M}(\text{GaCH}_3)_4]$ (M = Ni, Pd, Pt; 39.4%, 39.2%, and 35.3%), the π -orbital contribution to ΔE_{orb} is considerably stronger than for the complexes where the ligand GaCH₃ competes with CO for π -back-donation from the metal.^{45,47,54}

3. MAIN-GROUP METAL COMPLEXES

Although the major development in the use of RE^I organyls as ligands has happened in the d-block, some examples of complexes involving main-group elements (both s- and p-block) have also been reported. The details of both s- and p-block complexes of group 13 ligands are described in this section.

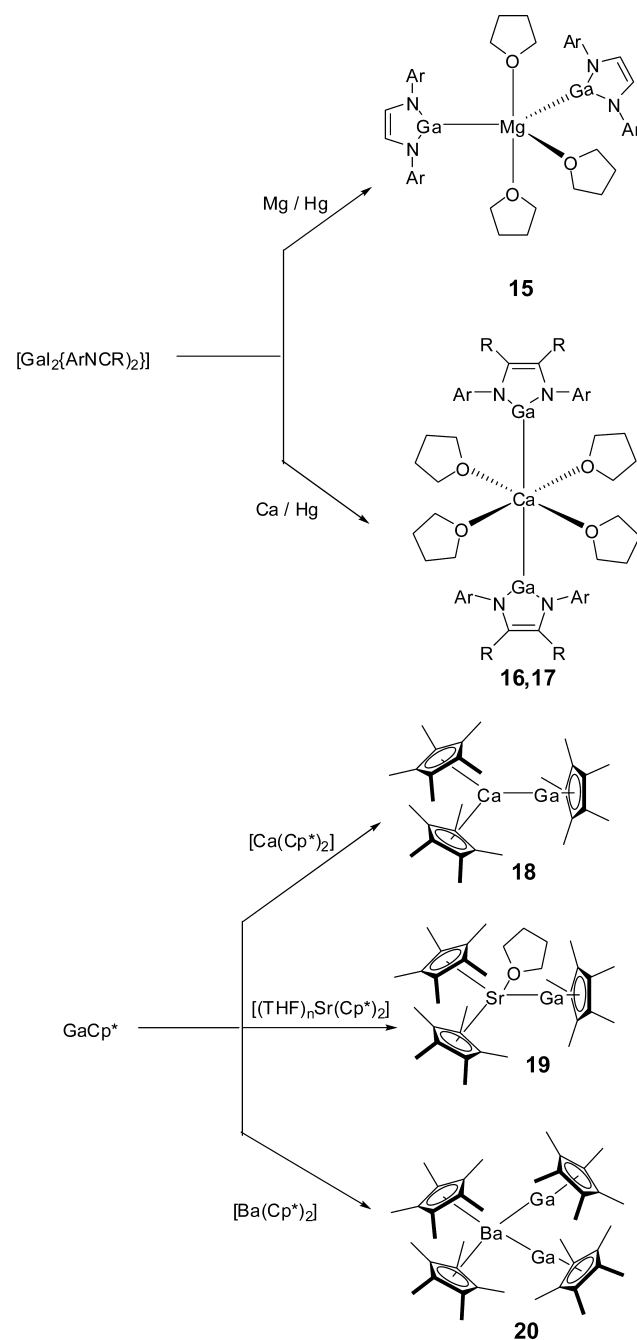
3.1. s-Block Compounds

Only a handful of examples of complexes containing bonds between a s-block metal and a group 13 low-valent donor atom are known. Such derivatives can be more easily stabilized by the charged diazabutadienido ligands $[\text{Ga}(\text{N}(\text{R})\text{C}(\text{H}))_2]^-$ than by the neutral organyls because of the highly electropositive nature of s-block elements as seen from the isolation of the complexes $[\text{Mg}(\text{Ga}(\text{ArNCH})_2)_2(\text{THF})_3]$ (**15**) and $[\text{Ca}(\text{Ga}(\text{ArNCR})_2)_2(\text{THF})_4]$ (R = H (**16**) or Me (**17**), Ar = 2,6-ⁱPr₂C₆H₃) via the reduction of $[\text{I}_2\text{Ga}(\text{ArNCR})_2]$ with the group 2 metal in tetrahydrofuran (THF) (Scheme 2).⁵⁵ As mentioned above, the formation of donor–acceptor adducts containing alkaline-earth metals and neutral RE^I ligands had not been observed previously but was predicted to be feasible by two recent theoretical studies.^{56,57} In accordance with these calculations, P. W. Roesky and co-workers reported in 2007 the synthesis of the complexes $[\text{Cp}^*_2\text{Ca}(\text{GaCp}^*)]$ (**18**), $[\text{Cp}^*_2(\text{THF})\text{Sr}(\text{GaCp}^*)]$ (**19**), and $[\text{Cp}^*_2\text{Ba}(\text{GaCp}^*)_2]$ (**20**), by direct coordination of Cp^{*}Ga (**6**) to the corresponding alkaline-earth metallocenes (Scheme 2).⁵⁸

In the case of strontium, a mixture of **19** and the solvent-free adduct is obtained. However, it was possible to isolate and crystallize **19** only. Remarkably, when $[\text{Cp}^*_2\text{Sr}(\text{THF})_2]$ was used as a starting material, neither **19** nor any complex of composition $[\text{Cp}^*_2\text{Sr}(\text{GaCp}^*)_x]$ was identified. Complexes **18–20** are relatively stable in toluene solutions. In the solid state, all three compounds consist of Lewis acid–base adducts, without any unusually short intermolecular contacts. In accordance with their ionic radii, only one Cp^{*}Ga unit is coordinated in **18**, whereas one Cp^{*}Ga and one THF molecule are bonded to the Sr center in **19**, and two Cp^{*}Ga units are coordinated to the Ba atom in **20** (Figure 4).

Despite the different coordination geometry, it can be said that the Ga–Ca bond in $[\text{Cp}^*_2\text{Ca}(\text{GaCp}^*)]$ (**18**) (3.183(2) Å) is similar to the corresponding distance observed in $[\text{Ca}(\text{Ga}(\text{ArNCR})_2)_2(\text{THF})_4]$ (3.1587(6) Å for R = H (**16**), 3.1988(6) Å for R = Me (**17**)) but is slightly longer than the sum of the covalent radii (Ga–Ca 2.96 Å) (Figures 4 and 5).^{59a} The Cp^{*}_{centr}–Ga–Ca angle is slightly bent (173.31(1)°), as a result of packing effects. Bond distances and angles of **19** and **18** are similar in spite of the different coordination environments of the Ca and Sr atoms. The Cp^{*}_{centr}–Ga–Sr angle is also quasi-linear (175.15(10)°), and the Ga–Sr distance is 3.4348(7) Å. The Ga–Ba distances in **20** are 3.6024(6) and 3.5798(7) Å (Figure 4). Jones and co-workers have more recently reported newer examples of complexes featuring Ga–Ca, Ga–Sr, and Ga–Ba bonds, *trans*- $[\text{M}(\text{Ga}(\text{ArNCH})_2)_2(\text{tmeda})_2]$ (Ar = 2,6-diisopropylphenyl; tmeda = N,N,N',N'-tetramethyl ethylenedi-

Scheme 2. Synthesis of Gallium^I–Alkaline-Earth Metal Complexes



$(\text{ArNCR})_2)_2(\text{THF})_4]$ (3.1587(6) Å for R = H (**16**), 3.1988(6) Å for R = Me (**17**)) but is slightly longer than the sum of the covalent radii (Ga–Ca 2.96 Å) (Figures 4 and 5).^{59a} The Cp^{*}_{centr}–Ga–Ca angle is slightly bent (173.31(1)°), as a result of packing effects. Bond distances and angles of **19** and **18** are similar in spite of the different coordination environments of the Ca and Sr atoms. The Cp^{*}_{centr}–Ga–Sr angle is also quasi-linear (175.15(10)°), and the Ga–Sr distance is 3.4348(7) Å. The Ga–Ba distances in **20** are 3.6024(6) and 3.5798(7) Å (Figure 4). Jones and co-workers have more recently reported newer examples of complexes featuring Ga–Ca, Ga–Sr, and Ga–Ba bonds, *trans*- $[\text{M}(\text{Ga}(\text{ArNCH})_2)_2(\text{tmeda})_2]$ (Ar = 2,6-diisopropylphenyl; tmeda = N,N,N',N'-tetramethyl ethylenedi-

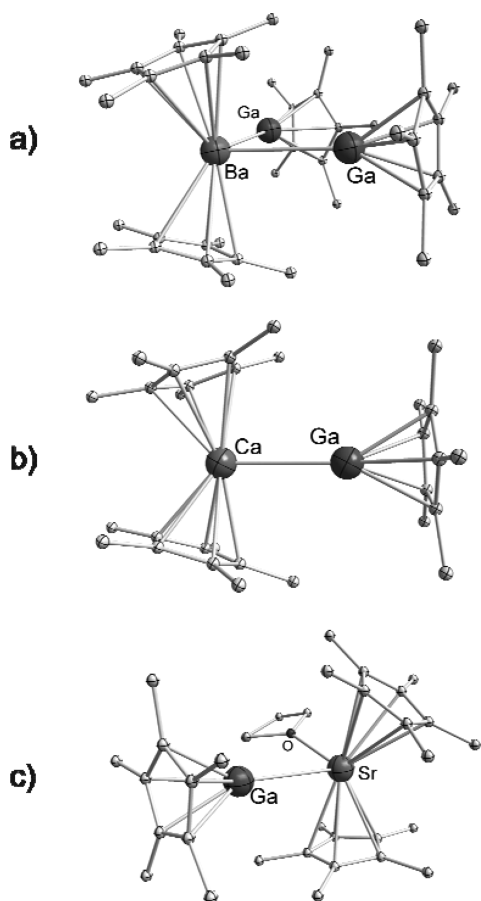


Figure 4. Molecular structures of gallium^I-alkaline-earth metal adducts: (a) $[\text{Cp}^*_2\text{Ba}(\text{GaCp}^*)_2]$ (**20**), (b) $[\text{Cp}^*\text{Ca}(\text{GaCp}^*)]$ (**18**), and (c) $[\text{Cp}^*_2\text{Sr}(\text{GaCp}^*)(\text{THF})]$ (**19**).

amine; $M = \text{Ca}, \text{Sr}, \text{Ba}$ ($\text{Ca}-\text{Ga}$ 3.2568(8) and 3.1983(8) Å; $\text{Sr}-\text{Ga}$ 3.324(1) Å; $\text{Ba}-\text{Ga}$ 3.4625(6) and 3.4658(6) Å).^{59b}

As one would expect, the nature of the bonding for both classes of group 2 complexes, containing either anionic or neutral RE^{I} ligands, is different. A significant ionic character was confirmed from experimental and theoretical data for the complexes **16** and **17**, which contain the charged $[\text{Ga}(\text{NRCH}_2)_2]^-$ ligand.⁵⁵ The calculations performed on the alkaline-earth adducts suggest that the van der Waals dispersive forces are responsible for the weak interactions between the Cp^*Ga and Cp^*_2M ($M = \text{Mg}, \text{Ca}, \text{Sr}$) moieties.

3.2. p-Block Compounds

Whereas the NHC analogue $(\text{DDP})\text{Ga}$ (**21**)⁴⁰ ($\text{DDP} = [(2,6\text{-}^i\text{Pr}_2\text{C}_6\text{H}_3)\text{NC}(\text{Me})\text{CHC}(\text{Me})\text{N}(2,6\text{-}^i\text{Pr}_2\text{C}_6\text{H}_3)]$) has been used as a reducing agent for the isolation of tin clusters $[\{(\text{DDP})\text{ClGa}\}_2\text{Sn}_7]$ (**22a**) and $[\{(\text{DDP})\text{ClGa}\}_4\text{Sn}_{17}]$ (**22b**) with strong metal–metal interactions⁶⁰ and the stabilization of $[(\text{OSO}_2\text{CF}_3)(\text{DDP})\text{GaBi}=\text{BiGa}(\text{DDP})(\text{OSO}_2\text{CF}_3)]$ (**22c**) and $[(\text{OC}_6\text{F}_5)(\text{DDP})\text{GaBi}=\text{BiGa}(\text{DDP})(\text{OC}_6\text{F}_5)]$ (**22d**) with $\text{Bi}=\text{Bi}$ bonds (Figure 6),⁶¹ only two classes of p-block complexes of the $\text{Cp}^*\text{E}^{\text{I}}$ ligands have been reported: the heteropolyhedral compounds of the heavy main-group elements As and Sb, and the homo- and heteronuclear group 13 Lewis acid–base adducts.

The first examples of p-block compounds containing low-valent $\text{Cp}^*\text{E}^{\text{I}}$ ligands, $[(\text{Cp}^*\text{Al})_3\text{Sb}_2]$ (**23a**)⁶² and $[(\text{Cp}^*\text{Al})_3\text{As}_2]$ (**23b**),⁶³ were reported by the groups of H. W. Roesky

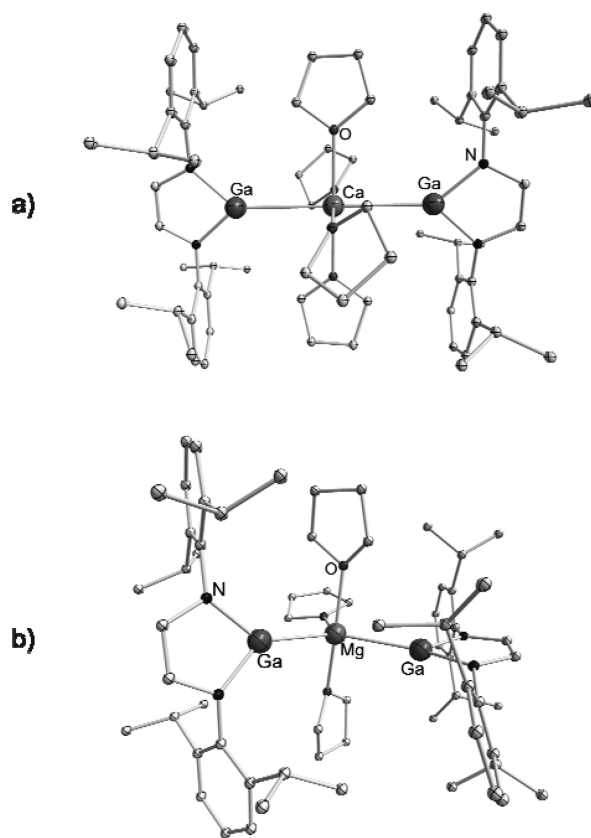


Figure 5. Molecular structures of alkaline-earth metal Ga^{I} -diazabutenido complexes: (a) $[\text{Ca}(\text{Ga}(\text{ArNCR})_2)_2(\text{THF})_4]$ (**16**) and (b) $[\text{Mg}(\text{Ga}(\text{ArNCH})_2)_2(\text{THF})_3]$ (**15**).

and H.-G. Schnöckel, respectively. The first of them was obtained when Cp^*Al was first recognized as a carbene analogue and the feasibility of this species to couple with other carbenoids was explored. Thus, Cp^*Al was reacted with an equimolar amount of $[(^t\text{BuSb})_4]$ in toluene at 60 °C. The reaction did not proceed stoichiometrically, because elemental antimony and various other decomposition products were formed in addition to the orange–brown crystals of composition **23a** (Scheme 3). This early attempt to obtain compounds containing novel aluminum–element bonds proved challenging, because the reaction conditions had to be chosen carefully, in order for the reaction to proceed with the minimum degree of decomposition.⁶³ Following this result, the reaction of Cp^*Al with $[(^t\text{BuAs})_4]$ in toluene led to the isolation of the analogous heteropolyhedral compound **23b**, along with the formation of 2-methylpropane and isobutene as byproducts (Scheme 3).

To understand the bonding in **23b**, self-consistent field (SCF) calculations were carried out, using the model molecules $[(\text{RAL})_3\text{As}_2]$ ($\text{R} = \text{H}, \text{Cl}, \text{NH}_2, \text{Cp}$). The population analysis for these species confirms a clear electron delocalization, supporting the hypothesis that heavy main-group elements can form heteropolyhedral compounds of the closo-borane type. Therefore, this compound contains a substantial three-center $\text{Al}-\text{As}-\text{Al}$ population, while the shared electron number (SEN ≈ 0.2) for the $\text{Al}-\text{Al}$ interaction is low, as expected for this kind of compound.

The second class of complexes of the low-valent group 13 ligands with p-block elements are the Lewis acid–base adducts.⁶⁴ As previously mentioned, RE^{I} ($\text{E} = \text{Al}, \text{Ga}, \text{In}$)

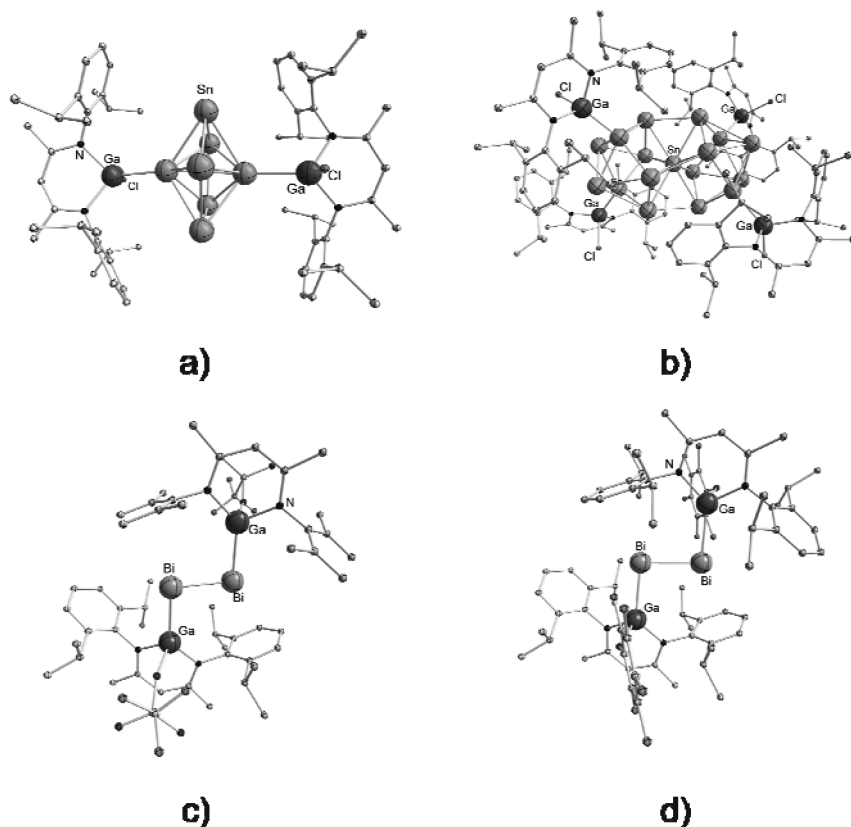
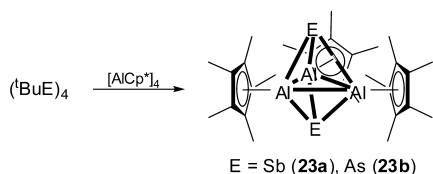


Figure 6. p-Block compounds stabilized by GaDDP moieties: (a) $[(\text{DDP})\text{ClGa}]_2\text{Sn}_7$ (**22a**), (b) $[(\text{DDP})\text{ClGa}]_4\text{Sn}_{17}$ (**22b**), (c) $[(\text{OSO}_2\text{CF}_3)(\text{DDP})\text{GaBi}=\text{BiGa}(\text{DDP})(\text{OSO}_2\text{CF}_3)]$ (**22c**), and (d) $[(\text{OC}_6\text{F}_5)(\text{DDP})\text{GaBi}=\text{BiGa}(\text{DDP})(\text{OC}_6\text{F}_5)]$ (**22d**).

Scheme 3. Synthesis of Heteropolyhedral p-Block Compounds **23a** and **23b**



were found to exhibit a strong Lewis basicity, and their electronic ground state is singlet with the singlet–triplet energy gap increasing with increasing atomic number. Furthermore, the increase of π -donor capability of the R group leads to an increase of the Lewis basicity of group 13 diyls. The first example of this class of complexes was the boron–aluminum adduct $[\text{Cp}^*\text{Al}-\text{B}(\text{C}_6\text{F}_5)_3]$ (**24**), which was reported by A. H. Cowley and co-workers in 2000 (Figure 7).⁶⁵ This adduct was readily obtained at room temperature, by adding toluene to a mixture of Cp^*Al and the highly electrophilic fragment $[\text{B}(\text{C}_6\text{F}_5)_3]$. In this complex a shortened Al–C average distance was observed, which was ascribed to the coordination of the aluminum lone pair into the donor–acceptor bond with the consequent development of a partial positive charge, as first suggested in the case of the transition-metal complex $[(\text{CO})_4\text{Fe}-\text{AlCp}^*]$ (**25**).⁶⁶ The E–C bond length can be regarded as an indicator for the degree of σ -donation from the RE^1 to the metal, and hence the polarization of the E–M bond.

Following a similar synthetic procedure, $[\text{Cp}^*\text{E}-\text{E}'(\text{C}_6\text{F}_5)_3]$ (E = E' = Al (**26**);⁵² E = Ga, E' = B (**27**),^{67,68} E' = Al (**28**)⁶⁹) have been obtained while the borafluorene derivatives $[\text{Cp}^*\text{Al}-\text{B}(\text{R})(\text{C}_{12}\text{F}_8)]$ (R = C_6F_5 (**29**), C_6H_5 (**30**), CH_3 (**31**)) are

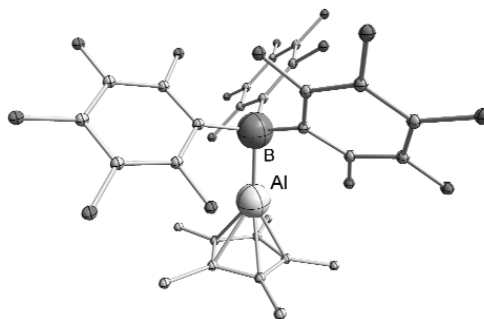


Figure 7. Molecular structure of $[\text{Cp}^*\text{Al}-\text{B}(\text{C}_6\text{F}_5)_3]$ (**24**).

isolated from toluene or bromobenzene solutions.⁷⁰ Among the known Lewis acid–base complexes, $[\text{Cp}^*\text{Al}-\text{Ga}(\text{tBu})_3]$ (**32**), recently reported by Schulz and co-workers,⁷¹ is the only example where the E^1 element has a lower atomic number than the E^{III} acceptor element. The analogous species containing Al–In bonds have not been reported, which has been associated with the disparity in the $\text{M}^{\text{I}}/\text{M}^{\text{III}}$ oxidation potentials for these elements, along with the relatively modest In–C bond energy.⁶⁵ To compare the relative Lewis basicity of the group 13 diyls, the adduct $[\text{Cp}^*\text{Al}-\text{Ga}(\text{tBu})_3]$ (**32**) has been isolated along with a series of complexes $[\text{Cp}^*\text{E}-\text{E}'(\text{tBu})_3]$ (E = E' = Ga (**33**),⁷⁰ Al (**34**); E = Ga, E' = Al (**35**); E = In, E' = Al (**36**), E' = Ga (**37**)).⁷² These complexes are chosen since the structural and spectroscopic parameters of the $[\text{E}'(\text{tBu})_3]$ fragments are well-established.⁷³ Upon adduct formation, the sum of the C–E–C bond angles decreases from 360° to lower values as the coordination geometry of the group 13 Lewis acid changes from trigonal planar to distorted tetrahedral.⁷² Thus, the

Table 1. Structural and NMR Spectroscopic Data of Cp*E–E'(tBu)₃ Adducts

compound	E–E'(Å)	E–Cp* _{centr} (Å)	$\delta_{\text{H}}^{\text{tBu}_3}$ (ppm)	$\Delta(\delta_{\text{H}}^{\text{tBu}_3})$ (ppm)	sum C–E–C (°)
Cp*Al–Ga(tBu) ₃ (32)	2.620(2)	1.861	1.3	0.14	348.5
Cp*Ga–Ga(tBu) ₃ (33)	<i>a</i>	<i>a</i>	1.26	0.10	<i>a</i>
Cp*Al–Al(tBu) ₃ (34)	2.689(2)	1.858	1.24	0.16	348.3
Cp*Ga–Al(tBu) ₃ (35)	2.629(2)	1.913	1.18	0.10	351.4
Cp*In–Al(tBu) ₃ (36)	2.843(2)	2.173(2)	1.12	0.04	353.1
Cp*In–Ga(tBu) ₃ (37)	2.845(2)	2.187	1.18	0.02	353.9

^aSingle crystal structure not determined.

stronger the Lewis acid–base interaction, the more pronounced the deviation from planarity, which leads to smaller C–E–C bond angles and a consequent E–C bond length increase (Table 1). The smallest deviation from planarity was observed for adducts containing Cp*In as ligand, indicating it to be the weakest Lewis base. The Al(tBu)₃ adduct exhibits a C–Al–C sum of 353.1°, whereas the corresponding Ga(tBu)₃ adduct exhibits the smallest deviation from planarity (353.9°).

The ¹H NMR spectra show that the resonances of the tBu groups are shifted to lower field. (free Al(tBu)₃, 1.08 ppm; free Ga(tBu)₃, 1.16 ppm). These chemical shifts reflect the different Lewis basicities of the Cp*E species, because the largest downfield shift is observed for complexes containing the strongest Lewis base, Cp*Al (Figure 8).

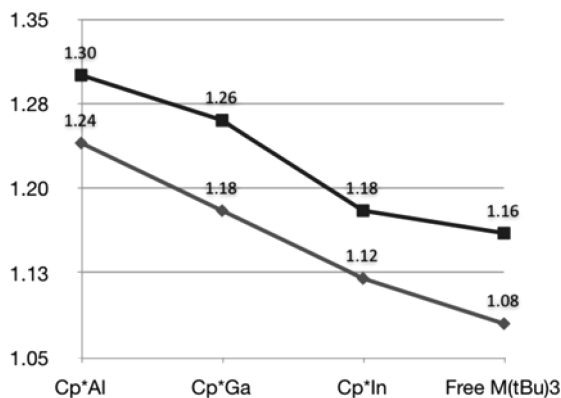


Figure 8. ¹H NMR chemical shifts of the tBu group in [Cp*E–E'(tBu)₃] adducts and uncomplexed E'(tBu)₃.⁷¹ Reprinted with permission from ref 71. Copyright 2006 American Chemical Society.

According to these structural data and spectroscopic parameters, the Lewis basicity of the Cp*E species (E = Al, Ga, In) decreases with increasing atomic number of the central group 13 atom, as previously reported for the B(C₆F₅)₃ adducts, and is comparable to that of trialkylstilbines and -bismuthines ER₃. Additionally, when the group 13–group 13 intermetallic distances in [Cp*E–Al(C₆F₅)₃] and [Cp*E–Al(tBu)₃]^{68,71} are considered, it can be observed that the latter are significantly elongated (Al–Al, 2.689(2) Å (34); Ga–Al, 2.629(2) Å (35)) compared to those in the perfluorinated complexes (Al–Al, 2.591(2) Å (26); Ga–Al, 2.515(11) Å (28)). This elongation reflects the different electronic and steric properties of the organic residues in the AlR₃ fragment, namely, the higher Lewis acidity and lower steric demand of the Al(C₆F₅)₃ moiety, relative to the Al(tBu)₃ one.

4. TRANSITION-METAL COMPLEXES

The bulk of the coordination chemistry that has been carried out using RE^I donors involves the use of transition metals.

Because the RE^I donors behave very similar to π -acidic carbonyl and phosphine ligands, they normally tend to stabilize low-valent transition-metal ions, and hence not much chemistry has been developed for titanium and vanadium group metals. RE^I complexes of late transition metals on the other hand have been extensively investigated. The following subsections describe the various synthetic strategies that led to the development of transition-metal RE^I chemistry.

4.1. Synthetic Methods

4.1.1. Substitution of Labile Ligands. Among the various types of synthetic strategies developed, the substitution of labile ligands on the metal center has been the most productive route for the synthesis of transition-metal complexes with low-valent group 13 organyls as ligands. Because of the isolability of RE^I ligands to CO, the first reports in this direction focused on their reactivity toward transition-metal carbonyl complexes (Scheme 4).

Uhl and co-workers studied the reactivity of [InC(SiMe₃)₃]₄ (38) toward various transition-metal carbonyl complexes. The reaction of this low-valent precursor with the dinuclear metallic carbonyl [Mn₂(CO)₁₀] leads to the isolation of [Mn₂(CO)₈(μ_2 -InC(SiMe₃)₃)₂] (39).⁷⁴ It has also been demonstrated that the partial and selective substitution of the CO ligands in binuclear metallic carbonyls is feasible. For example, when [Co(CO)₃(μ_2 -CO)]₂ was reacted with 1 equiv of [InC(SiMe₃)₃]₄ (38), only one bridging CO ligand was substituted to yield [(Co(CO)₃)₂(μ_2 -CO)(μ_2 -InC(SiMe₃)₃)] (40). On the other hand, the same reaction with 2 equiv of the low-valent indium species results in the formation of [Co(CO)₃(μ_2 -InC(SiMe₃)₃)₂]₂ (41).⁷⁵ It has also been established that the partial substitution of CO ligands in [Mn₂(CO)₁₀] and [Fe₃(CO)₁₂] by [GaC(SiMe₃)₃] (42) yields the complexes [Mn₂(CO)₈(μ_2 -GaC(SiMe₃)₃)₂] (43) and [Fe₃(CO)₉(μ_2 -CO)(μ_2 -GaC(SiMe₃)₃)₂] (44), respectively. Neither of these two products is isostructural to the respective starting carbonyl compound (Figure 9).⁷⁶

The RGa^I ligands in 43 bridge both manganese atoms whereas all carbonyl groups occupy terminal coordination sites. The two edges of the central Fe₃ triangle in 44 are occupied by GaC(SiMe₃)₃ units, whereas the third one is bridged by carbon monoxide. In the case of [Co₂(CO)₈], the reaction with Cp*E (E = Al, Ga) yields the analogous complexes [Co₂(CO)₆(μ_2 -ECp*)₂] (E = Al (45), E = Ga (46)).^{77,22} Interestingly, a similar reaction with binuclear iron nonacarbonyl [Fe₂(CO)₉] with Cp*Ga does not result in the formation of a binuclear complex but affords mononuclear [(Cp*Ga)Fe(CO)₄] (47) through elimination of [Fe(CO)₅] (Scheme 5a). Contrasting to this observation, the reaction of [Ni(CO)₄] with Cp*Ga yields the tetranuclear cluster [Ni₄(GaCp*)₄(CO)₆] (48). It has been suggested that the formation of tetranuclear [Ni₄(GaCp*)₄(CO)₆] (48) proceeds via the unstable inter-

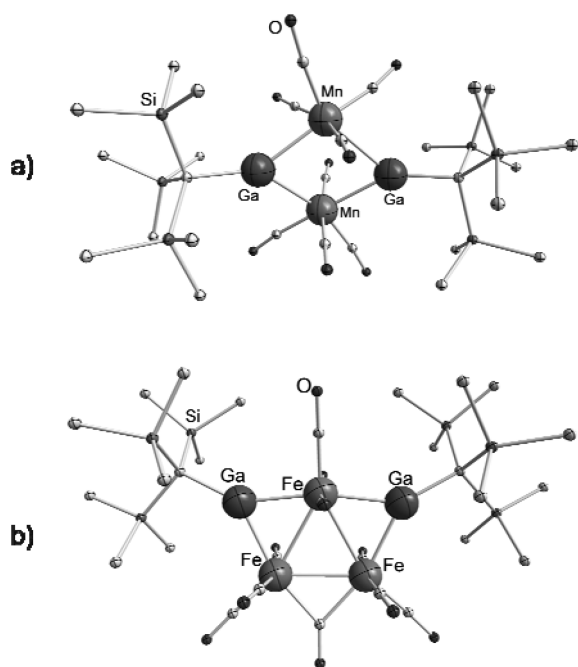
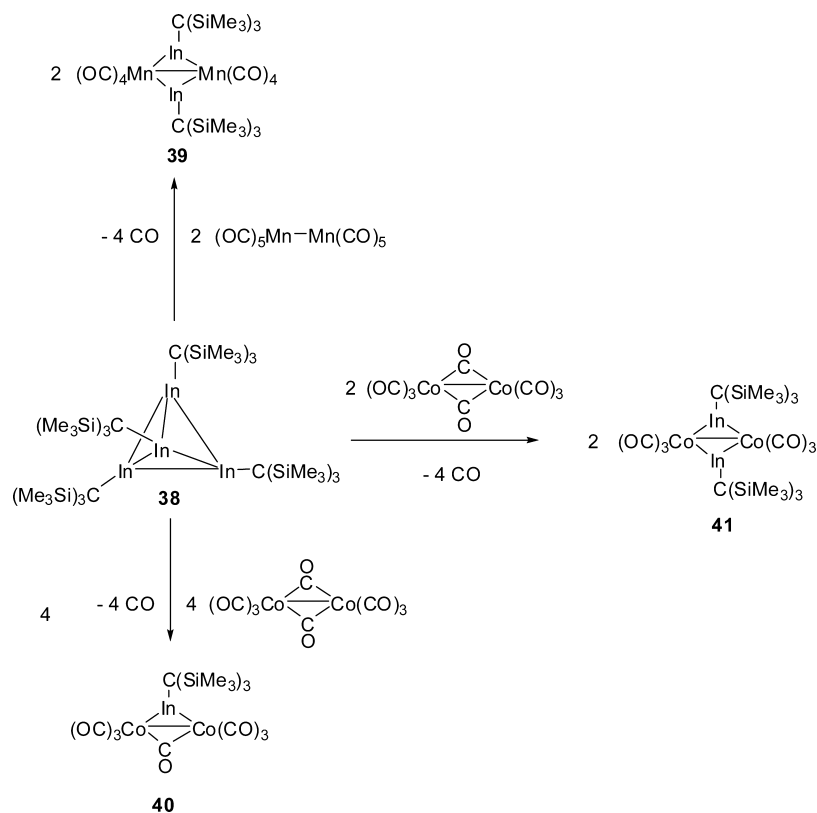
Scheme 4. Substitution of CO Ligands by $[\text{InC}(\text{SiMe}_3)_3]_4$ (38)

Figure 9. Molecular structure of (a) $[\text{Mn}_2(\text{CO})_8(\mu_2\text{-GaC}(\text{SiMe}_3)_3)_2]$ (43) and (b) $[\text{Fe}_3(\text{CO})_9(\mu_2\text{-CO})(\mu_2\text{-GaC}(\text{SiMe}_3)_3)_2]$ (44).

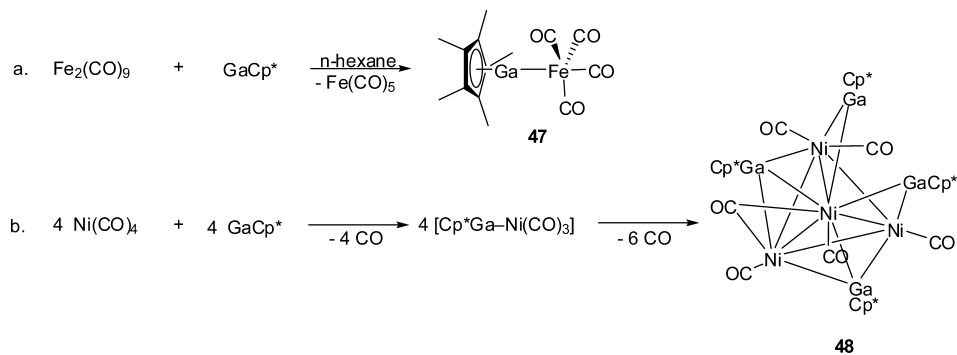
mediate $[\text{Ni}(\text{GaCp}^*)(\text{CO})_3]$ (49), as has been established by spectroscopic studies (Scheme 5b).²²

The substitution of CO by RE^I ligands in polynuclear carbonyl clusters such as $[\text{Rh}_6(\text{CO})_{16}]$ has also been studied. The reaction of this rhodium hexanuclear cluster or $[\text{Rh}_6(\text{CO})_{15}(\text{MeCN})]$ with Cp*Ga leads to the selective substitution of the face bridging CO to yield all four possible

cluster derivatives $[\text{Rh}_6(\mu_3\text{-CO})_{4-x}(\mu_3\text{-GaCp}^*)_x(\text{CO})_{12}]$ ($x = 1-4$) (50–53) (Scheme 6), depending on the amount of Cp*Ga used and the Rh-precursor chosen.⁷⁸ All four cluster derivatives have been isolated in pure form after column chromatography and characterized by single-crystal X-ray diffraction studies.

The formation of the $[\text{Rh}_6(\mu_3\text{-CO})_{4-x}(\mu_3\text{-GaCp}^*)_x(\text{CO})_{12}]$ ($x = 1-3$) (50–53) clusters can be formally regarded as the result of a stepwise substitution of face-bridging carbonyl ligands for Cp*Ga fragments. However, it has been shown that the presence of $\mu_3\text{-CO}$ ligands in the coordination environment of the starting cluster is not an essential condition for the formation of a substituted cluster complex with triply bridging Cp*Ga ligands. Thus, the reaction of $[\text{Ru}_6(\eta^6\text{-C})(\mu_2\text{-CO})(\text{CO})_{16}]$ cluster with a slight excess of Cp*Ga in hexane results initially in the formation of an intermediate $[\text{Ru}_6(\eta^6\text{-C})(\text{CO})_{16}(\mu_3\text{-GaCp}^*)]$ (54), which has been detected by both IR and ¹H NMR spectral studies but has not been isolated (Scheme 6). This intermediate complex reacts further and yields the cluster $[\text{Ru}_6(\eta^6\text{-C})(\mu_2\text{-CO})(\text{CO})_{13}(\mu_3\text{-GaCp}^*)_2(\mu_2\text{-GaCp}^*)]$ (55), where the parent Ru₆C octahedral core is preserved (Figure 10). Similarly, the reaction of $[\text{Rh}_6(\text{CO})_{10}(\mu_3\text{-CO})_4(\mu_2\kappa^3\text{-Ph}_2\text{PC}_2\text{H}_3)]$ with a 2-fold excess of Cp*Ga affords the clusters $[\text{Rh}_6(\text{CO})_{10}(\mu_3\text{-CO})_3(\mu_2\kappa^3\text{-Ph}_2\text{PC}_2\text{H}_3)(\mu_3\text{-GaCp}^*)]$ (56) and $[\text{Rh}_6(\text{CO})_{10}(\mu_3\text{-CO})_3(\kappa^1\text{-Ph}_2\text{PC}_2\text{H}_3)(\mu_3\text{-GaCp}^*)_2]$ (57) (Figure 11), where evidence of the hemilabile behavior of the diphenylvinylphosphane ligand has been established.⁷⁹

The hexanuclear cluster 56 possesses 86 valence electrons. This is consistent with the *closo* octahedral structure of the metal framework, which has been preserved from the metallic precursor $[\text{Rh}_6(\text{CO})_{10}(\mu_3\text{-CO})_4(\mu_2\kappa^3\text{-Ph}_2\text{PC}_2\text{H}_3)]$. In 57, however, the phosphane ligand is coordinated through the

Scheme 5. Formation of (a) $[(\text{Cp}^*\text{Ga})\text{Fe}(\text{CO})_4]$ (47) and (b) $[\text{Ni}_4(\text{GaCp}^*)_4(\text{CO})_6]$ (48)

Scheme 6. Substitution of Triply Bridging CO Ligands in Polynuclear Rh Carbonyl Clusters

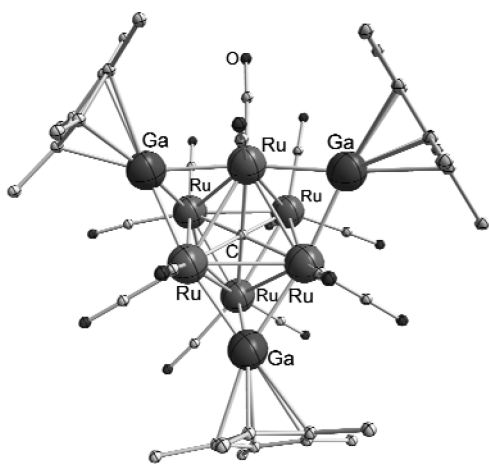
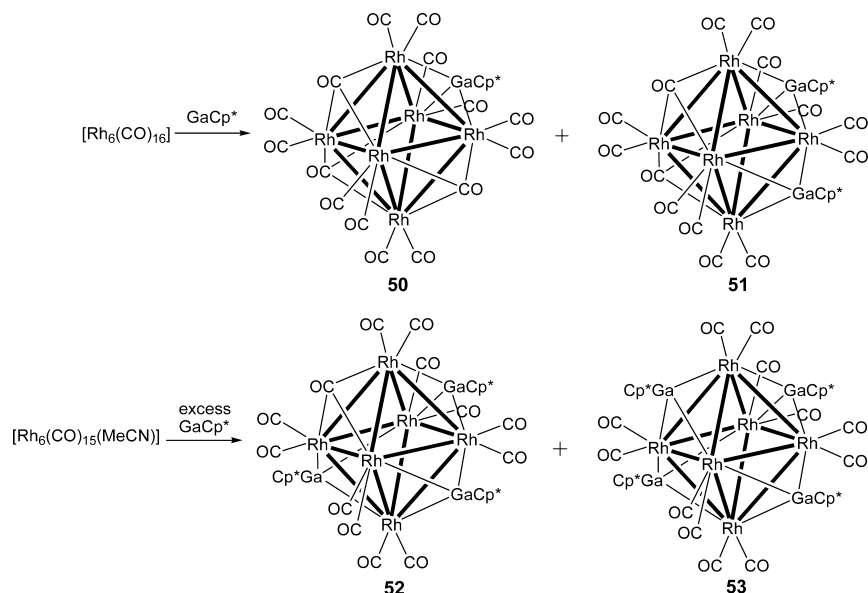


Figure 10. Molecular structure of $[\text{Ru}_6(\eta^6\text{-C})(\mu_2\text{-CO})(\text{CO})_{13}(\mu_3\text{-GaCp}^*)_2(\mu_2\text{-GaCp}^*)]$ (55).

phosphorus atom, occupying a terminal position, where the coordination of the vinyl double bond is presumably prevented by the steric hindrance rendered by the second $[\mu_3\text{-GaCp}^*]$ ligand (Figure 11).

Apart from the above-described homoleptic metal carbonyls, several heteroleptic metal carbonyl complexes, which bear even more labile ligands such as olefins, have been employed in the

reactions with RE^I . For example, the reaction of heteroleptic transition-metal carbonyl $[\text{Fe}(\text{CO})_3(\text{COT})]$ with $[\text{InC}(\text{SiMe}_3)_3]_4$ affords the complex $[\{\text{Fe}(\text{CO})_3\}_2(\mu_2\text{-InC}(\text{SiMe}_3)_3)_3]$ (58). The isolation of this complex reveals the preferred substitution of olefin ligands as well as the predisposition of RE^I to occupy bridging positions.⁸⁰ The substitution of olefin ligands like cyclooctene (COT), norbornadiene (NBD), cyclooctatetraene, and cycloheptatriene on heteroleptic carbonyl complexes was also observed in the formation of $[\text{Cr}(\text{CO})_5(\text{ECp}^*)]$ ($\text{E} = \text{Al}$ (59), Ga (60), In (61)),^{81,82} $[(\text{Cp}^*\text{Ga})_2\text{M}(\text{CO})_4]$ ($\text{M} = \text{Cr}$ (62), Mo (63)),⁸³ $[\text{Fe}_2(\text{CO})_6(\mu_2\text{-InC}(\text{SiMe}_3)_3)_3]$ (64)⁸⁰ and $[\text{Fe}_2(\text{CO})_6(\mu_2\text{-GaCp}^*)_3]$ (65).²² The synthetic protocols used for the preparation of 61–64 are shown in Scheme 7.

The concept of labile ligand substitution on this kind of complexes can also be extended to the substitution of solvent molecules as observed in the case of $[\text{CpMn}(\text{CO})_2(\text{THF})]$, which reacts with $\text{InC}_6\text{H}_3\text{-2,6-Trip}_2$ to yield $[\text{Cp}(\text{CO})_2\text{Mn-InC}_6\text{H}_3\text{-2,6-Trip}_2]$ (66) ($\text{Trip} = \text{-C}_6\text{H}_2\text{-2,4,6-}^i\text{Pr}_3$).³⁴ Similarly, the acetonitrile-containing compounds $[\text{fac}(\text{RCN})_3\text{M}(\text{CO})_3]$ ($\text{R} = \text{Me}$, $\text{M} = \text{Mo}$; $\text{R} = \text{Et}$, $\text{M} = \text{W}$) on reaction with Cp^*Ga yield monomeric complexes $[\text{fac}(\text{Cp}^*\text{Ga})_3\text{M}(\text{CO})_3]$ ($\text{M} = \text{Mo}$ (67), W (68)) (Scheme 8).

In an extension of this type of reaction, the treatment of $[\text{fac}(\text{Cp}^*\text{Ga})_3\text{Mo}(\text{CO})_3]$ (67) with a second equivalent of $[\text{fac}(\text{MeCN})_3\text{Mo}(\text{CO})_3]$ affords the dinuclear derivative $[(\text{Mo}$

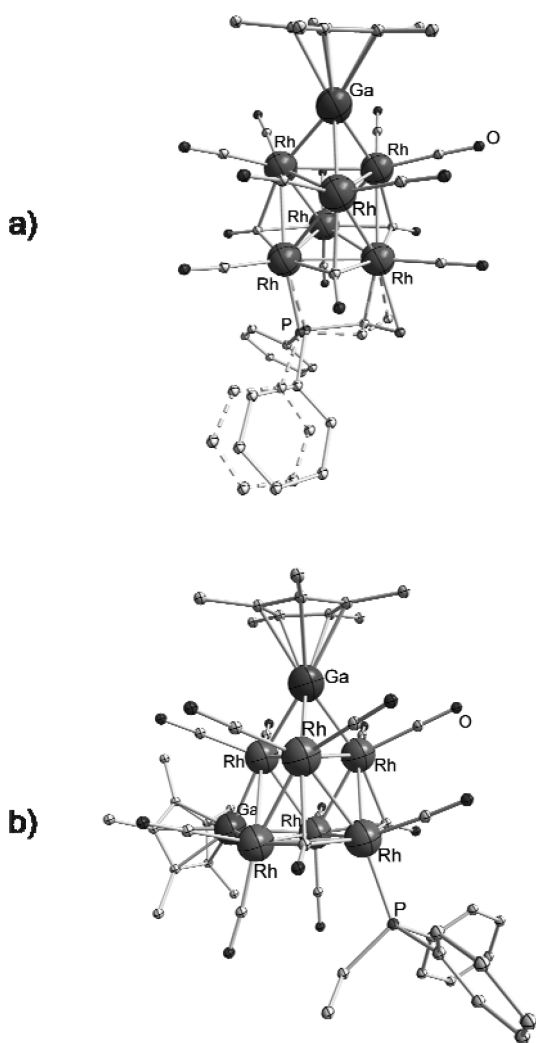


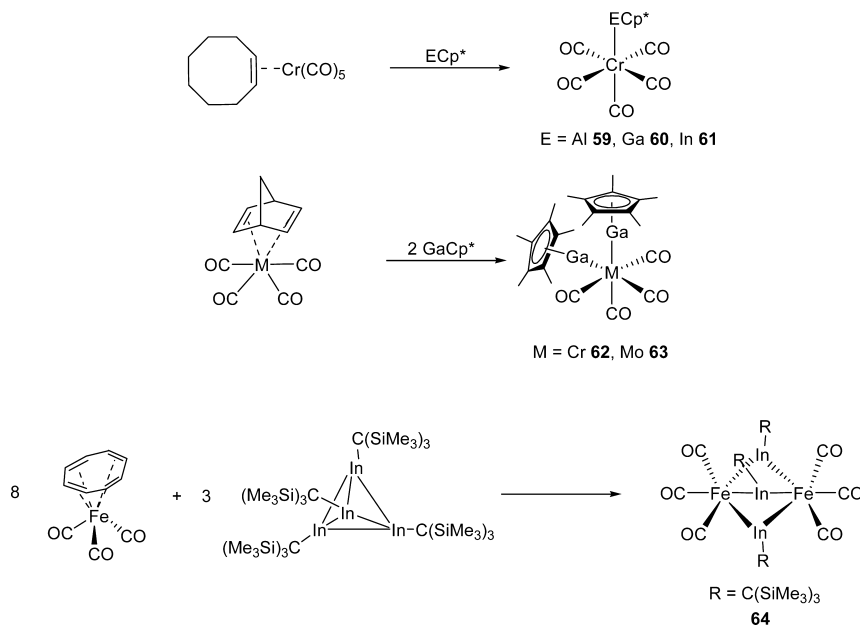
Figure 11. Molecular structures of (a) $[\text{Rh}_6(\text{CO})_{10}(\mu_3\text{-CO})_3(\mu_2, \kappa^3\text{-Ph}_2\text{PC}_2\text{H}_3)(\mu_3\text{-GaCp}^*)]$ (**56**) and (b) $[\text{Rh}_6(\text{CO})_{10}(\mu_3\text{-CO})_3(\kappa^1\text{-Ph}_2\text{PC}_2\text{H}_3)(\mu_3\text{-GaCp}^*)_2]$ (**57**).

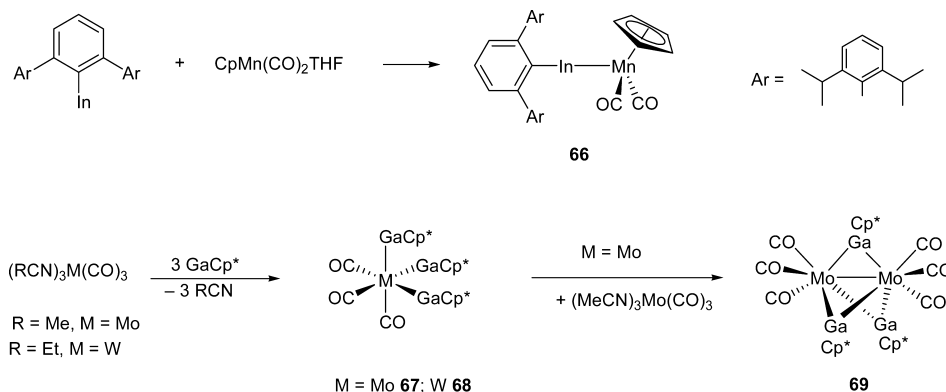
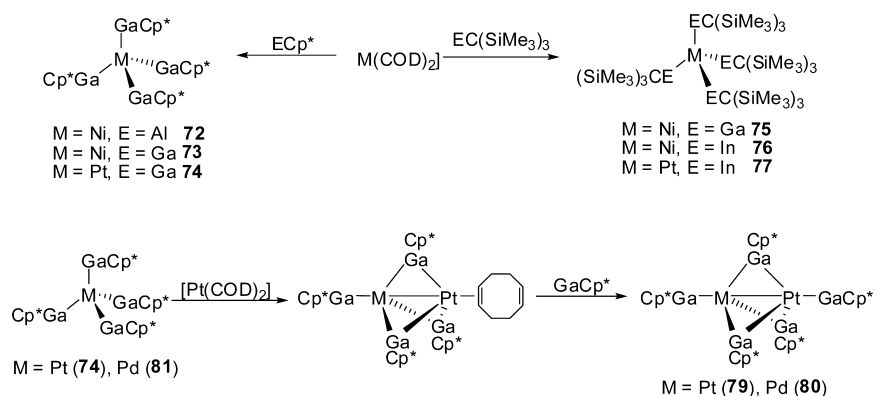
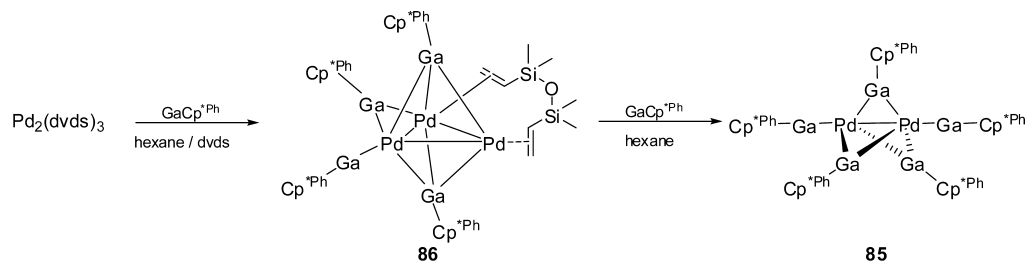
$(\text{CO})_3(\mu_2\text{-GaCp}^*)_3]$ (**69**) (Scheme 8). The formation of **69** can be understood as a substitution reaction, where the acetonitrile molecules in $[\text{fac}(\text{MeCN})_3\text{Mo}(\text{CO})_3]$ are replaced by the Cp*Ga ligands from complex $[\text{fac}(\text{Cp}^*\text{Ga})_3\text{Mo}(\text{CO})_3]$ (**67**).⁸⁴

On the other hand, heteroleptic carbonyl complexes containing more tightly bound ancillary ligands such as Cp, undergo the expected CO substitution when reacted with alkylgallium¹ or alkylindium¹ derivatives. An example of this type is the reaction of $[(\text{CpNi})_2(\mu_2\text{-CO})_2]$ with $[\text{EC}(\text{SiMe}_3)_3]_4$ (E = Ga (**42**), In (**38**)) affording complexes $[(\text{CpNi})_2(\mu_2\text{-E}(\text{C}(\text{SiMe}_3)_3)_2)]$ (E = Ga (**70**), In (**71**)).⁸⁵ In the case of RIn^{I} ligands, it has been established that the ligand insertion into the Ni–Ni bond takes place depending on the stoichiometry of the reaction, while the gallium derivative yields the substitution products regardless of the reaction conditions.

Despite the proven feasibility of the substitution of strong π -back-bonding CO ligands with strong σ -donors Cp*E, as showcased by the reactions described above, clearly successive substitutions of the CO groups on the metal become more difficult. In other words, this substitution reaction leads to an intrinsic drawback. Thus, when a CO ligand is substituted by a Cp*E (E = Al, Ga) ligand, the π -back-donation from the transition-metal center to the remaining CO ligands is significantly increased, leading to an increasingly difficult substitution of the latter. Therefore, for the synthesis of homoleptic $[\text{M}_x(\text{ECp}^*)_y]$ complexes, it is necessary to employ precursor complexes that do not contain CO ligands, but contain labile ligands such as olefins. For example, the cyclooctadiene (COD) ligands in $[\text{Ni}(\text{COD})_2]$ and $[\text{Pt}(\text{COD})_2]$ can be easily substituted by Cp*E or $\text{EC}(\text{SiMe}_3)_3$, leading to the formation of tetrahedral homoleptic complexes $[\text{M}(\text{ECp}^*)_4]$ (M = Ni, E = Al (**72**), Ga (**73**); M = Pt, E = Ga (**74**)) and $[\text{M}(\text{EC}(\text{SiMe}_3)_3)_4]$ (M = Ni, E = Ga (**75**), E = In (**76**); M = Pt, E = In (**77**)) (Scheme 9).^{29,42,83,86–89} In some cases, it may be necessary to use hydrolytic conditions to ensure clean removal of the olefin ligands. In this way, the reaction of $[\text{Mo}(\eta^4\text{-C}_4\text{H}_6)_3]$ (C_4H_6 = butadiene) with six

Scheme 7. Substitution of Olefin Ligands by Cp*E Ligands in Heteroleptic Olefin–Carbonyl Complexes



Scheme 8. Substitution of Solvent Ligands By RE^I Ligands in Heteroleptic ComplexesScheme 9. Preparation of [Pt₂(GaCp^{*})₂(μ₂-GaCp^{*})₃] (79) and [PtPd(GaCp^{*})(μ₂-GaCp^{*})₃] (80)Scheme 10. Formation of Palladium Di- And Trinuclear Complexes (Cp^{*Ph} = C₅Me₅Ph)

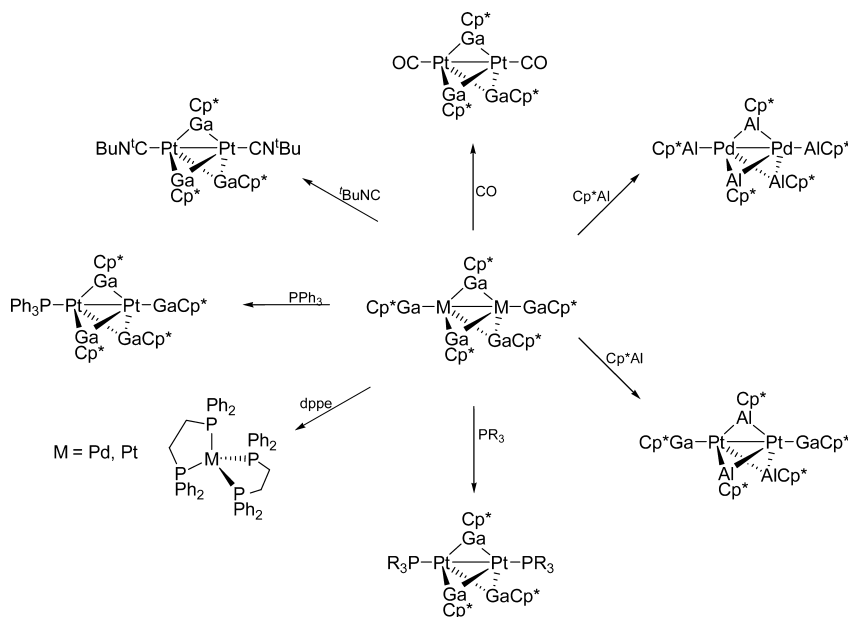
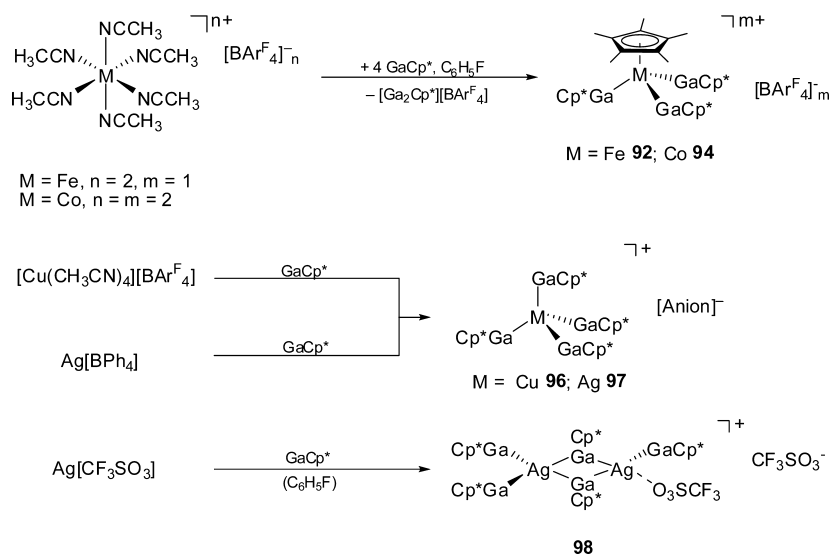
equivalents of Cp^{*}Ga in toluene under H₂ atmosphere (3 bar) yields the homoleptic, six-coordinated transition-metal–gallium complex [Mo(GaCp^{*})₆] (**78**).⁹⁰

The formation of the first homoleptic diplatinum complex [Pt₂(GaCp^{*})₂(μ₂-GaCp^{*})₃] (**79**) was achieved when the mononuclear olefin complex tris(ethylene)platinum(0) was reacted with an excess of Cp^{*}Ga.⁹¹ Complex **79** exhibits a central unit of two platinum atoms coordinated by five Cp^{*}Ga groups acting as terminal as well as bridging ligands. The dinuclear compounds **79** and [PtPd(GaCp^{*})(μ₂-GaCp^{*})₃] (**80**) could also be isolated from the reaction of the homoleptic [M(GaCp^{*})₄] (M = Pt (**74**), Pd (**81**)) with 1 equiv of [Pt(COD)₂] and subsequent addition of Cp^{*}Ga. The examination of the reaction mixture by variable-temperature ¹H and ¹³C NMR spectroscopic studies revealed that the intermediates of these reactions are dimeric clusters with a Pt₂ or a PtPd core, bearing four Cp^{*}Ga ligands and one η²-coordinated COD ligand (Scheme 9).⁸⁹

The analogous binuclear complex [Pd₂(GaCp^{*})₂(μ₂-GaCp^{*})₃] (**82**) has been obtained when [Pd₂(dvds)₃] (dvds

= 1,3-divinyl-1,1,3,3-tetramethyldisiloxane) was reacted with Cp^{*}Ga in hexane at –30 °C. Under different reaction conditions, the reaction of [Pd₂(dvds)₃] with Cp^{*}E ligands, leads to the formation of various products (Scheme 10).⁹² For instance, the reaction in toluene with Cp^{*}Ga at 25 °C yields the trinuclear, heterometallic cluster [Pd₃(GaCp^{*})₄(μ₂-GaCp^{*})₄] (**83**) in good yield. When the bulkier ligand [GaCp^{*Ph}] (Cp^{*Ph} = C₅Me₅Ph) (**84**) is used under similar reaction conditions, the binuclear complex [Pd₂(Cp^{*Ph})₂(μ₂-Cp^{*Ph})₃] (**85**) is obtained.³⁰ Furthermore, the isolation of an intermediate in this reaction was possible. It has been shown that the trinuclear complex [Pd₃(Cp^{*Ph})(μ₂-Cp^{*Ph})(μ₃-Cp^{*Ph})₂(dvds)] (**86**) containing a labile olefinic ligand is the intermediate, which further reacts with [Ga(C₅Me₅Ph)] to yield **85** (Scheme 10).

These observations show the importance of the kinetic control in the formation of products of different nuclearity. For example, the known trinuclear complex, [Pd₃(InCp^{*})₄(μ₂-InCp^{*})₄] (**87**) is obtained under gentle heating conditions. However, under the same conditions, the reaction involving

Scheme 11. Ligand Exchange of the Homoleptic Binuclear Complexes $[M_2(\text{GaCp}^*)_5]$ ($M = \text{Pd}$ (82), Pt (79))Scheme 12. Reaction of $[M(\text{CH}_3\text{CN})_n]^{m+}$ ($m = 2$, $M = \text{Fe}$, Co ; $m = 1$, $M = \text{Cu}$, Ag) with Cp^*Ga 

Cp^*Al yields $[\text{Pd}_3(\text{AlCp}^*)_2(\mu_2\text{-AlCp}^*)_2(\mu_3\text{-AlCp}^*)_2]$ (88). The reactivity of the mentioned binuclear complexes with a variety of ligands (Cp^*Al , Cp^*Ga , CO , phosphines, isonitriles), to yield bi- and trinuclear substitution products has also been extensively studied (Scheme 11).⁹²

It is also possible to isolate ionic homoleptic transition-metal complexes containing Cp^*Ga ligands by substitution of labile solvent molecules such as diethyl ether or acetonitrile. The compound $[\text{Zn}(\text{GaCp}^*)_4][\text{BARF}_4]_2$ (89) ($\text{Ar}^F = \text{C}_6\text{H}_3(\text{CF}_3)_2$) is the first example of a Cp^*Ga adduct with a strongly electrophilic metal center.⁹⁴ It was obtained by reacting ZnMe_2 with $[\text{H}(\text{OEt})_2][\text{BARF}_4]$ with subsequent addition of Cp^*Ga . This complex contains the $[\text{Zn}(\text{GaCp}^*)_4]^{2+}$ cation, which is both isostructural and isoelectronic to $[\text{M}(\text{GaCp}^*)_4]$ ($M = \text{Ni}$ (73), Pd (81), Pt (74)).^{83,89}

Also, reactions of Cp^*Ga with stabilized classical Werner type complexes have also been recently confirmed by the synthesis of the homoleptic cations $[\text{M}(\text{GaCp}^*)_4]^+$ ($M = \text{Cu}$

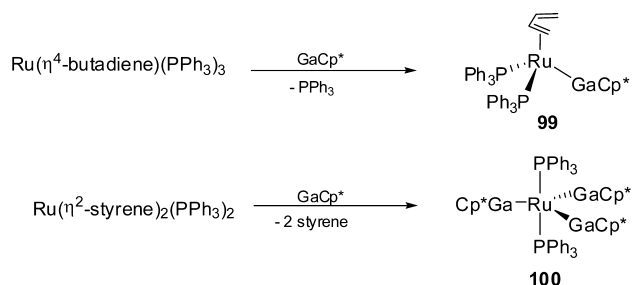
(90), Ag (91)).⁹⁵ The reactions of the cationic transition-metal acetonitrile complexes $[\text{M}(\text{CH}_3\text{CN})_n]^{m+}$ ($m = 2$, $M = \text{Fe}$, Co ; $m = 1$, $M = \text{Cu}$, Ag) with Cp^*Ga yield this type of cationic species with Cp^*Ga ligands (Scheme 12).

The reaction of $[\text{Fe}(\text{CH}_3\text{CN})_6][\text{BARF}_4]_2$ with Cp^*Ga proceeds with a redox neutral Cp^* transfer and the substitution of all acetonitrile ligands by three Cp^*Ga ligands to afford $[\text{Cp}^*\text{Fe}(\text{GaCp}^*)_3][\text{BARF}_4]$ (92) (Scheme 12), which is a stable 18 electron complex. $[Ga_2\text{Cp}^*][\text{BARF}_4]$ (93)⁹⁶ is obtained as the byproduct in this reaction. On the other hand, the formation of $[\text{Cp}^*\text{Co}(\text{GaCp}^*)_3][\text{BARF}_4]_2$ (94) (Scheme 12) from $[\text{Co}(\text{CH}_3\text{CN})_6][\text{BARF}_4]_2$ is accompanied by oxidation of $\text{Co}(\text{II})$ to $\text{Co}(\text{III})$, where Cp^*Ga is reduced to elemental gallium. Interestingly, an intermediate product of this reaction, $[\text{Cp}^*\text{Co}(\text{GaCp}^*)_2(\text{CH}_3\text{CN})][\text{BARF}_4]_2$ (95), where only a partial substitution is effected, could also be isolated when the reaction conditions were slightly modified. The softer, less electrophilic, group 10 precursors $[\text{Cu}(\text{CH}_3\text{CN})_4][\text{BARF}_4]$ and

Ag(BPh₄) react with four equivalents of Cp*Ga to afford the homoleptic complexes [Cu(GaCp*)₄][BAR^F₄] (**96**) and [Ag(GaCp*)₄][BPh₄] (**97**), respectively (Scheme 12). Interestingly, when Ag(CF₃SO₃) is used, the reaction with Cp*Ga in fluorobenzene leads to a dimeric species, which was spectroscopically identified as [Ag₂(GaCp*)₃(μ₂-GaCp*)₂(CF₃SO₃)][CF₃SO₃] (**98**) (Scheme 12). This difference could be attributed to the nature of the [CF₃SO₃]⁻ anion in **98** (not coordinatively innocent like [BPh₄]⁻ anion), which is a rather good ligand for the soft cationic transition-metal centers.

The above-described chemistry clearly establishes the use of olefin complexes as precursors for the synthesis of homoleptic [M(RE^I)₄] species. This is not necessarily true for olefin-containing basic d⁸ transition-metal complexes, which undergo only a partial substitution when reacted with Cp*Ga and Cp*Al ligands, owing to the high basicity of the metallic centers Ru(0) and Rh^I. Thus, the reaction of [Ru(η⁴-butadiene)(PPh₃)₃] with Cp*Ga yields the substitution product [Ru(η⁴-butadiene)-(PPh₃)₂(GaCp*)] (**99**) (Scheme 13). This product is stable

Scheme 13. Reaction of d⁸ Transition-Metal Complexes with Cp*E (E = Al, Ga)



even under hydrogenolytic conditions in presence of additional amounts of Cp*Ga. In contrast, the reaction of the 16 electron complex [Ru(PPh₃)₂(styrene)₂] with three equivalents of Cp*Ga undergoes complete substitution of the olefin ligands, to yield [Ru(PPh₃)₂(GaCp*)₃] (**100**) (Scheme 13), while the reaction of the Rh^I compounds [Rh(η², η²-NBD)(PCy₃)₂][BAR^F₄] and [Rh(η², η²-COD)₂][BAR^F₄] with the corresponding Cp*E ligand (E = Al, Ga) led to the complexes [Rh(η², η²-NBD)(PCy₃)₂](GaCp*)₂][BAR^F₄] (**101**), [Rh(η², η²-COD)(GaCp*)₃][BAR^F₄] (**102**) and [Rh(η², η²-COD)(AlCp*)₃][BAR^F₄] (**103**).⁹⁷ Because of the coordination of the strong σ-donors Cp*E, the π-back-donation from the transition-metal center to the olefin ligands is increased, which reflects, for example, on the C–C bond distances of the coordinated olefins. Therefore, the solid-state structure of the butadiene complex **99** is more accurately described as a metallacycle than as a simple π-complex.

There are a few examples of heteroleptic precursors that do not contain CO ligands, which may also undergo facile ligand substitution when reacted with RE^I organyls. In the case of [Ru(η⁴-COD)(η³-CH₂CMeCH₂)₂],⁹⁸ the reaction proceeds with the formation of a TMM (TMM = η⁴-C(CH₂)₃) ligand by hydrogen transfer from a coordinated 2-methylallyl moiety,⁹⁹ yielding [Ru(GaCp*)₃(η³-TMM)] (**104**) (Figure 12).¹⁰⁰

There are only a few reports in the literature on the reactivity of Cp*E (E = Al, Ga) ligands toward complexes with anionic ligands, such as hydrides, like Chaudret's ruthenium polyhydride [Ru(PCy₃)₂(H₂)₂(H)] (Cy = C₆H₁₁)¹⁰¹ and [Ru(COD)(H)(NH₂NMe₂)₃][BAR^F₄]. These complexes undergo

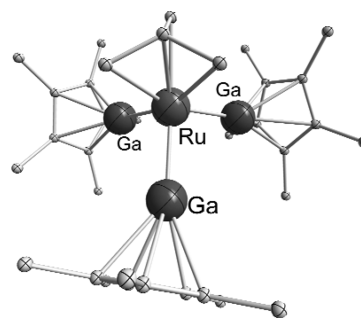


Figure 12. Molecular structure of [Ru(GaCp*)₃(η³-TMM)] (**104**).

the substitution of the labile ligands such as hydrazine or H₂ by Cp*Ga to afford [Ru(PCy₃)₂(GaCp*)₂(H)₂] (**105**) and [Ru(COD)(H)(GaCp*)₃][BAR^F₄] (**106**), respectively (Scheme 14).^{100,102}

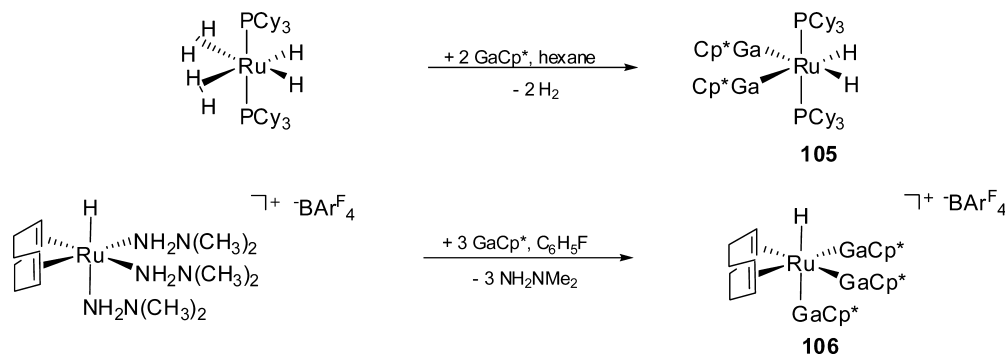
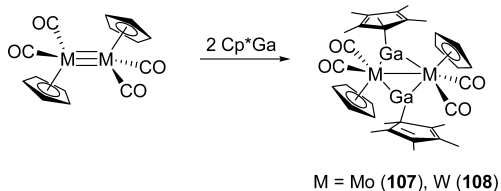
4.1.2. Addition Reactions. In contrast to the “classical” reactivity of transition-metal carbonyls toward RE^I compounds (E = Al, Ga, In), where the CO ligands can be stepwise and selectively substituted, the reaction of [CpM(CO)₂]₂ (M = Mo, W) with Cp*Ga yields the addition products [(OC)₂CpM(μ₂-η¹-GaCp*)₂] (M = Mo (**107**), W (**108**)) (Scheme 15).⁸⁴ The Cp* ligands bound to the gallium centers change their hapticity from η³ to η¹, in order to relieve the high steric overcrowding in the products.

In a similar way, the olefin complex [Ru(η², η²-COD)(η⁶-COT)] reacts with Cp*Ga to yield the addition product [(η², η²-COD)(η⁴-COT)Ru(GaCp*)] (**109**) in quantitative yields.¹⁰³ However, when hydrogenolytic conditions are used, the substitution reaction takes place, leading to the formation of [(η², η²-COD)Ru(GaCp*)₃] (**110**) in good yields (Scheme 16).⁹⁷

The reaction of the platinum precursor [(dcpe)Pt(H)-(CH₂^tBu)] (dcpe = bis(dicyclohexylphosphino)ethane)¹⁰⁴ with Cp*E (E = Al, Ga, In) and [GaC(SiMe₃)₃] can be regarded as an addition reaction, if the formation of a reactive 14-valence-electron intermediate of the formula [(dcpe)Pt] is considered during the process.¹⁰⁵ Thus, the electron-deficient species is stabilized by further ligand coordination, namely, the addition of two RE^I ligands, to yield the tetrahedral complexes [(dcpe)Pt(ECp*)₂] (E = Al (**111**), E = Ga (**112**), E = In (**113**)) and [(dcpe)Pt(GaC(SiMe₃)₃)₂] (**114**) (Scheme 17).^{46,106}

Very recently, it has been reported that the di- and trinuclear molecules [(Cp*Ru)₂(μ₂-H)₄] and [(Cp*Ru)₃(μ₂-H)₃(μ₃-H)₂] undergo addition of Cp*E (E = Al, Ga) ligands to yield the electron-rich polyhydride clusters [Cp*Ru(μ₂-H)(H)(μ₂-ECp*)₂] (E = Al (**115**), E = Ga (**116**)) and [(Cp*Ru)₃(μ₂-H)₃(μ₃-ECp*)₂] (E = Al (**117**), E = Ga (**118**)) (Figure 13).¹⁰² These complexes are remarkably stable and do not undergo reductive elimination of Cp*H or H₂. Apparently, the anionic hydride ligands decrease the electrophilic character of the transition-metal center, so that the Cp* transfer reactions are prevented.

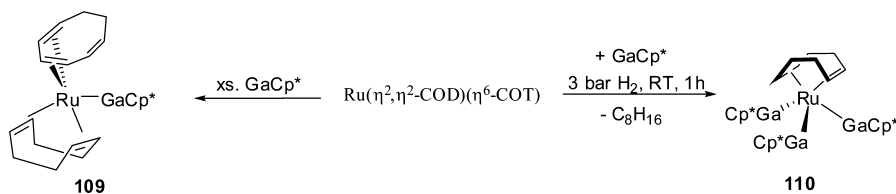
4.1.3. Redox Reactions. Other than the substitution and addition reactions described in sections 4.1.1 and 4.1.2, redox reactions can also be employed to isolate transition-metal complexes of group 13 RE^I ligands. The first complex containing a bond between aluminum and a transition metal was reported as early as 1994, when [Cp*(η²-C₂H₄)Co(μ₂-Al(C₂H₅))₂] (**119**) was isolated as a byproduct in the reaction

Scheme 14. Synthesis of $[\text{Ru}(\text{PCy}_3)_2(\text{GaCp}^*)_2(\text{H})_2]$ (**105**) and $[\text{Ru}(\text{COD})(\text{H})(\text{GaCp}^*)_3][\text{BAR}^{\text{F}}_4]$ (**106**)Scheme 15. Addition of Cp^*Ga to $[\text{CpM}(\text{CO})_2]_2$ ($\text{M} = \text{Mo}, \text{W}$) (Reprinted with permission from Cokoja, M.; Steinke, T.; Gemel, C.; Welzel, T.; Winter, M.; Merz, K.; Fischer, R. A. Ligand properties of Cp^*Ga : New examples of Mo–Ga and W–Ga complexes. *J. Organomet. Chem.* 2003, 684 (1–2), 277–286.⁸⁴ Copyright 2003 Elsevier.)

of $\text{Cp}^*\text{Co}(\text{C}_2\text{H}_4)$ with the Al^{III} precursor $[(\text{C}_2\text{H}_5)_2\text{AlH}]$.¹⁰⁷ $[(\text{CpNi})_2(\text{AlCp}^*)_2]$ (**120**) was later obtained by using Cp^*Al as a reducing agent toward $[\text{Cp}_2\text{Ni}]$.¹⁰⁸ It was the latter reaction which led to the recognition of the high synthetic potential of Cp^*Al as an electron-rich, selective carbenoid. The cobalt complex **119** was formally regarded as two 16-electron $[\text{Cp}^*(\eta^2\text{-C}_2\text{H}_4)\text{Co}]$ units, which are linked by two $[\text{Al}(\text{C}_2\text{H}_5)]$ groups (Figure 14).

The reduction of trivalent precursors led to the first example of a gallium–transition-metal bond in 1997. Robinson and co-workers reported the synthesis of $[(\text{CO})_4\text{Fe}-\text{Ga}(\text{C}_6\text{H}_3\text{Tipp}^*_2)]$ (**121**) ($\text{Tipp}^* = 2,4,6\text{-triisopropylphenyl}$) (Scheme 18) through a (formal) redox reaction between $\text{Na}_2[\text{Fe}(\text{CO})_4]$ and $(\text{Tipp}^*_2\text{C}_6\text{H}_3)\text{GaCl}_2$.⁵³ This synthetic path was also applied by Fischer and co-workers in order to isolate the analogous species $[\text{Cp}^*\text{Al}-\text{Fe}(\text{CO})_4]$ (**122**) (Scheme 18), from the reaction of $[\text{Cp}^*\text{AlCl}_2]_2$ with $\text{Na}_2[\text{Fe}(\text{CO})_4]$ ⁶⁶ and by Ueno and co-workers to obtain $[(\text{Cp}^{\text{X}}\text{Fe}(\text{CO}))_2(\mu_2\text{-CO})(\mu_2\text{-GaMes})]$ ($\text{Cp}^{\text{X}} = \text{Cp}$ (**123**), Cp^* (**124**); $\text{Mes} = 2,4,6\text{-trimethylphenyl}$).¹⁰⁹

The distinction between a redox neutral, nucleophilic substitution and the formation of the $\text{M}-\text{E}$ bond involving some electron transfer may certainly be a matter of debate for reactions shown in Scheme 18. The situation is more clear in

Scheme 16. Addition of Cp^*Ga to $[\text{Ru}(\eta^4\text{-COD})(\eta^6\text{-COT})]$ 

the following cases. In the reaction of $[\text{Pd}(\text{tmeda})(\text{CH}_3)_2]$ ($\text{tmeda} = N,N,N',N'$ -tetramethylethylenediamine) with the corresponding RE^{I} ligand, the homoleptic Pd complexes $[\text{Pd}(\text{GaCp}^*)_4]$ (**81**) and $[\text{Pd}(\text{InC}(\text{SiMe}_3)_3)_4]$ (**125**) have been isolated (Scheme 19).⁸⁹ This reaction can be considered as a ligand substitution reaction, which proceeds via reduction of the transition metal. The Pd(II) center is reduced by the group 13 ligand to Pd(0). The ^1H NMR spectrum of the reaction mixture exhibits a signal at -0.15 ppm, a chemical shift typical for $\text{Ga}-\text{CH}_3$ groups. This evidence reveals that the methyl groups are transferred to Cp^*Ga , forming $[\text{Cp}^*\text{Ga}(\text{CH}_3)_2]$ as a byproduct, rather than the reductive elimination of ethane, as known to happen for the reaction of $[\text{Pd}(\text{tmeda})(\text{CH}_3)_2]$ with phosphines PR_3 ,¹¹⁰ or the elimination of $\text{C}(\text{CH}_3)_4$ in the reactions of $[(\text{dcp})\text{Pd}(\text{H})(\text{CH}_2^t\text{Bu})]$.¹⁰⁵

In 2004, Sharp and co-workers used Cp^*Ga to stabilize the first complex that contains a Au–Ga bond, which is also the first gold cluster complex in which the Au atoms are bonded only to an electropositive main-group metal.¹¹¹ Cp^*Ga was used as a reducing agent when an excess of “ $[\text{Cp}^*\text{Ga}/\text{GaI}]$ ” was reacted with $[(\text{Ph}_3\text{P})\text{AuCl}]$, to afford a yellow solution, from which air-sensitive orange-yellow crystals of the phosphine-free gold–gallium cluster complex $[\text{Au}_3(\mu_2\text{-GaI}_2)_3(\text{GaCp}^*)_5]$ (**126**) were isolated along with a yellow solid that has been identified by spectroscopic data as $[(\text{Ph}_3\text{P})_n\text{Au}]^+$ ($n = 2-3$). Compound **126** was also prepared from $[(\text{Ph}_3\text{P})\text{AuI}]$ and a mixture of Cp^*Ga and GaI_3 , presumably without the formation of the $[(\text{Ph}_3\text{P})_n\text{Au}]^+$ ($n = 2-3$) species as byproducts. The molecular structure of $[\text{Au}_3(\mu_2\text{-GaI}_2)_3(\text{GaCp}^*)_5]$ (**126**) in the solid-state consists of a triangle of gold atoms bridged by GaI_2 units on the edges. Two Au atoms (Au1 and $\text{Au1}'$) are each coordinated by two Cp^*Ga units, whereas the third unique gold atom (Au2) is coordinated by only one Cp^*Ga unit (Ga2). (Figure 15).

Quite interestingly, the redox method has afforded a few examples of compounds containing group 4–group 13 bonds. Either sodium or magnesium has been used as the reducing agent for the reduction of RECl_2 ($\text{E} = \text{Ga}, \text{In}$; $\text{R} = 2,6\text{-}(2,4,6\text{-}^i\text{Pr}_3\text{C}_6\text{H}_2)_2\text{C}_6\text{H}_3$) trivalent compounds and the corresponding $[\text{Cp}_2\text{MCl}_2]$ precursor ($\text{M} = \text{Ti}, \text{Zr}, \text{Hf}$), to afford the

Scheme 17. Synthesis of the Tetrahedral Complexes $[(dcpe)Pt(RE)_2]$ (111–114). (Reprinted with permission from Weiß, D.; Winter, M.; Merz, K.; Knüfer, A.; Fischer, R. A.; Fröhlich, N.; Frenking, G. Synthesis, structure and bonding situation of $[(dcpe)Pt(InCp^*)_2]$ and $\{(dcpe)Pt[GaC(SiMe_3)_3]_2\}$ —Two novel examples of platinum complexes of low valent Group 13 metal species. *Polyhedron* 2002, 21 (5–6), 535–542. ¹⁰⁶ Copyright 2002 Elsevier.)

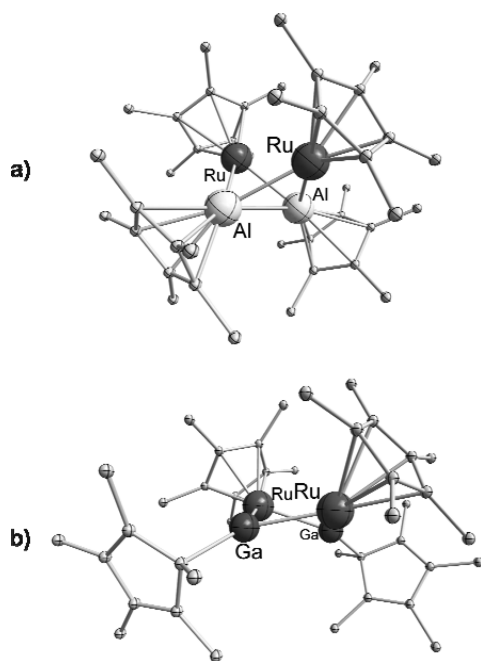
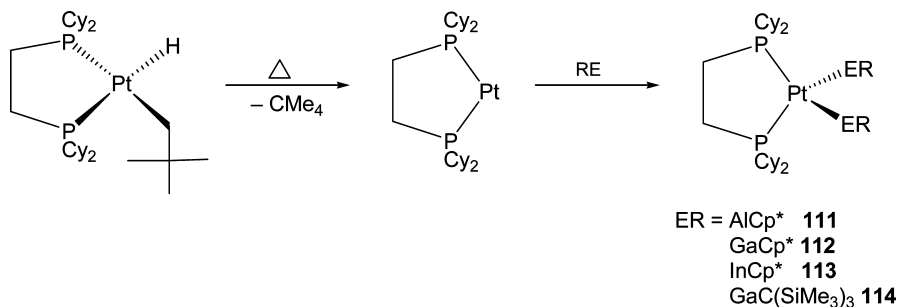


Figure 13. Molecular structure of $[Cp^*Ru(\mu_2-H)(H)(\mu_2-ECp^*)_2]$: (a) E = Al (115) and (b) E = Ga (116).

complexes $[Cp_2M(ER)_2]$ (M = Ti, E = Ga (127), In (128); M = Zr, E = Ga (129), In (130); M = Hf, E = Ga (131), In (132)) (Scheme 20).^{112–114} These complexes are considered analogous to other 18-electron species, such as $[Cp_2M(CO)_2]$,

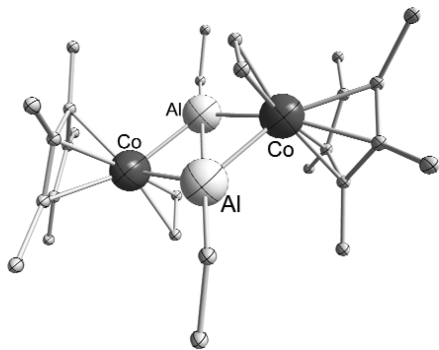
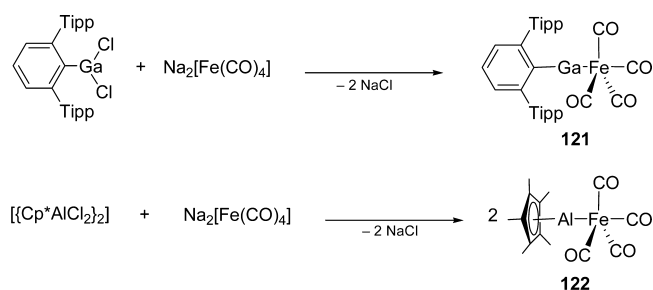


Figure 14. Molecular structure of $[Cp^*(\eta^2-C_2H_4)Co(\mu_2-Al(C_2H_5))_2]$ (119).

Scheme 18. Formation of Transition-Metal Complexes by Reduction of Trivalent Group 13 Precursors

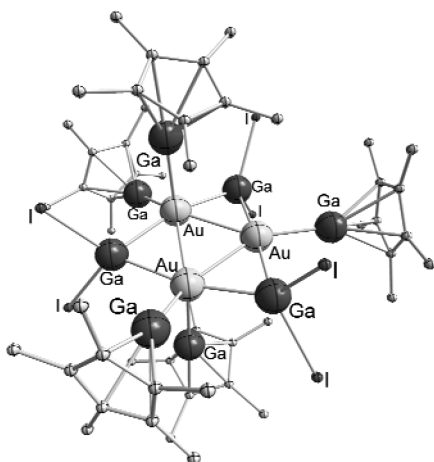
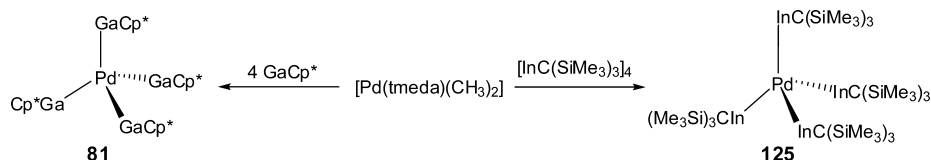
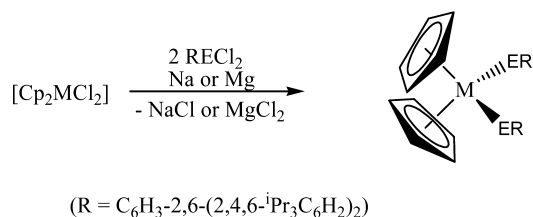


in that the RE^I fragments essentially act as two-electron donating species to the group 4 metal.

The solid-state structures of **127–132** have V-shaped E–M–E trimetallic linkages with relatively short M–E bonds (Zr–Ga, 2.6350(8) Å; Ti–Ga, 2.4921(7) Å; Zr–In, 2.7916(5) Å; Ti–In, 2.6685(8) Å; Hf–Ga, 2.6198(13) Å; Hf–In = 2.7667(10) Å). The transition-metal (M = Zr, Ti, Hf) centers are found in a pseudotetrahedral coordination environment, while the group 13 (E = Ga, In) atoms exhibit a two-coordinated, almost linear geometry (Figure 16). Density functional theory (DFT) computations on the model compounds $[Cp_2M(EPh)_2]$ suggest significant π -back-bonding from the group 4 metals (Zr, Ti, Hf) to the group 13 metals (Ga, In) in these compounds.

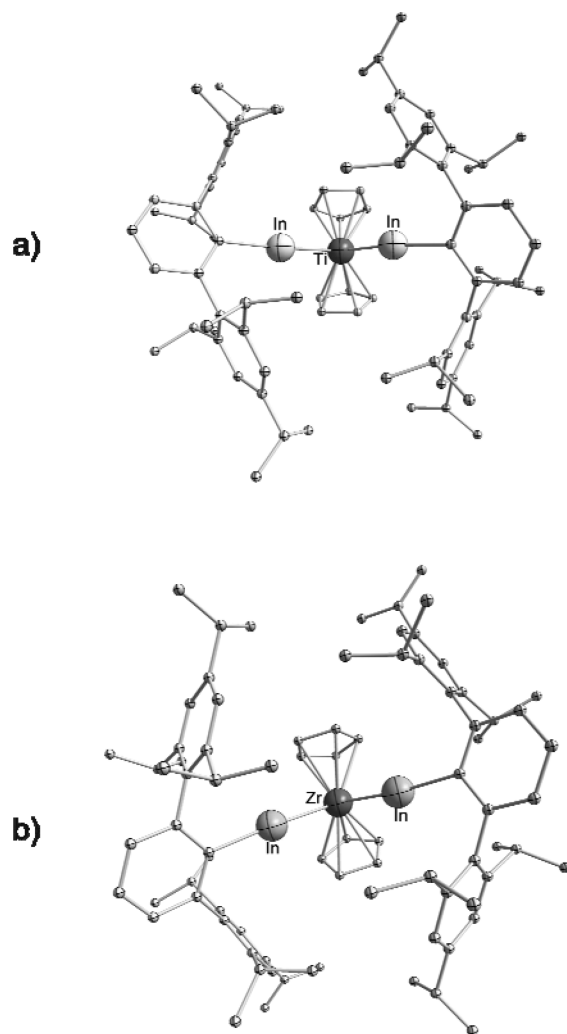
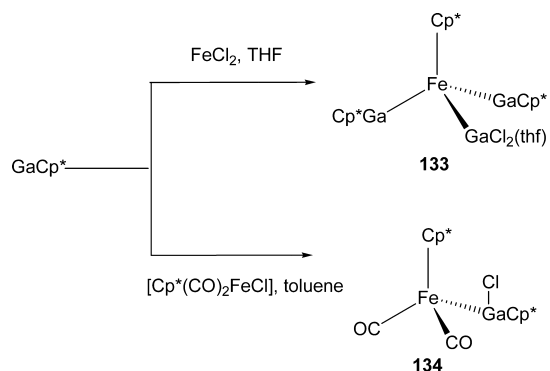
4.1.4. Insertion Reactions. Insertion reactions of monovalent group 13 halides have been known for a long time, particularly with an emphasis on the reactions of InX (X = Cl, Br).¹¹⁵ These studies have shown that insertion reactions of XE^I compounds are extremely sensitive to the reaction conditions and that many possible reaction pathways have to be considered.¹¹⁶ The first example of an insertion of a Cp^*Ga moiety into a metal–chloride bond was reported in 2000, consisting of the synthesis of the iron complexes $[Cp^*Fe(GaCp^*)_2GaCl \cdot THF]$ (133) and $[Cp^*(CO)_2Fe-GaCl(\eta^2-Cp^*)]$ (134).¹¹⁷ In the former case, the insertion into the transition-metal-halide bond in $FeCl_2$ proceeds with a Cp^*/Cl exchange process, followed by σ/π rearrangement of the Cp^* ligand (Scheme 21). In the latter complex, the insertion of the Cp^*Ga ligand proceeds with only a hapticity change of the Cp^* fragment.

The insertion of the $[InC(SiMe_3)_3]_4$ ligand into a metal–metal bond was observed in its reaction with $[(CpNi)_2(\mu_2-CO)_2]$, which afforded the complex $[(CpNi(CO))_2(\mu_2-InC(SiMe_3)_3)]$ (135). Interestingly, the usual CO ligand

Scheme 19. Formation of $[\text{Pd}(\text{GaCp}^*)_4]$ (81) and $[\text{Pd}(\text{InC}(\text{SiMe}_3)_3)_4]$ (125)Figure 15. Molecular structure of the gold cluster $[\text{Au}_3(\mu_2\text{-GaI}_2)_3(\text{GaCp}^*)_5]$ (126).Scheme 20. Synthesis of $[\text{Cp}_2\text{M}(\text{ER})_2]$ ($\text{M} = \text{Ti}$, $\text{E} = \text{Ga}$ (127), In (128); $\text{M} = \text{Zr}$, $\text{E} = \text{Ga}$ (129), In (130); $\text{M} = \text{Hf}$, $\text{E} = \text{Ga}$ (131), In (132))

substitution reaction was observed for the corresponding gallium analogue.⁸⁵ However, the importance of the reaction conditions is highlighted once again, since the reaction in a 4:1 ratio yields the aforementioned complex 135 (Figure 17), while the reaction in a molar ratio of 2:1 leads to the substitution product $[(\text{CpNi})_2(\mu_2\text{-InC}(\text{SiMe}_3)_3)_2]$ (71), as described in the previous section.

The reactions of RE^{I} derivatives with the d^9 -complexes $[(\text{Cp}^*\text{RhCl})_2(\mu_2\text{-Cl})_2]$ and $[(p\text{-cymene})\text{RuCl}_2]_2$ are other examples of insertions into transition-metal–halogenide bonds.^{118–120} The stoichiometry and reaction conditions are key factors for the formation of a wide variety of products. For instance, the reactions of $[(\text{Cp}^*\text{RhCl})_2(\mu_2\text{-Cl})_2]$ with 6 equiv of Cp^*E ($\text{E} = \text{Ga}$, In) or $\text{InC}(\text{SiMe}_3)_3$ yield the corresponding insertion products $[\text{Cp}^*\text{Rh}(\text{ECp}^*)_2(\text{ECp}^*\text{Cl}_2)]$ ($\text{E} = \text{Ga}$ (136), In (137)) and $[\text{Cp}^*\text{Rh}(\mu_2\text{-Cl})_2(\text{InC}(\text{SiMe}_3)_3)_3]$ (138). Meanwhile the reaction with 3 equiv of Cp^*In leads to the ionic compound $[(\text{Cp}^*_2\text{Rh})][(\text{Cp}^*\text{Rh}(\text{InCp}^*)(\text{In}_2\text{Cl}_4(\mu_2\text{-Cp}^*)))]$ (139). In contrast, when Cp^*Ga is used, $[\text{Cp}^*\text{Rh}(\text{GaCp}^*)_2(\text{GaCl}_3)]$ (140) is formed. In all these reactions, the Cp^*E species acts as a reducing agent for the transformation of the Rh^{III} center into a $d^8\text{-Rh}^{\text{I}}$ center, which is stabilized by the formation of a Lewis acid–base adduct (Scheme 22).

Figure 16. Molecular structures of (a) $[\text{Cp}_2\text{Ti}(\text{InR})_2]$ (128) and (b) $[\text{Cp}_2\text{Zr}(\text{GaR})_2]$ (129).Scheme 21. Synthesis of $[\text{Cp}^*\text{Fe}(\text{GaCp}^*)_2\text{GaCl}_2\text{THF}]$ (133) and $[\text{Cp}^*(\text{CO})_2\text{Fe-GaCl}(\eta^2\text{-Cp}^*)]$ (134)

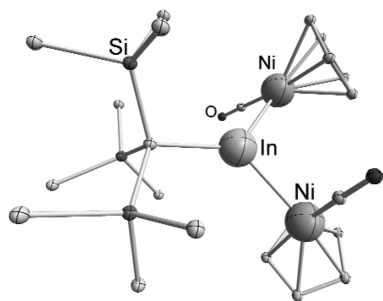
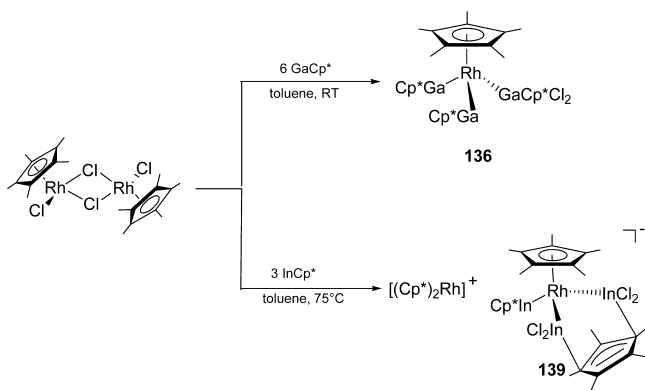


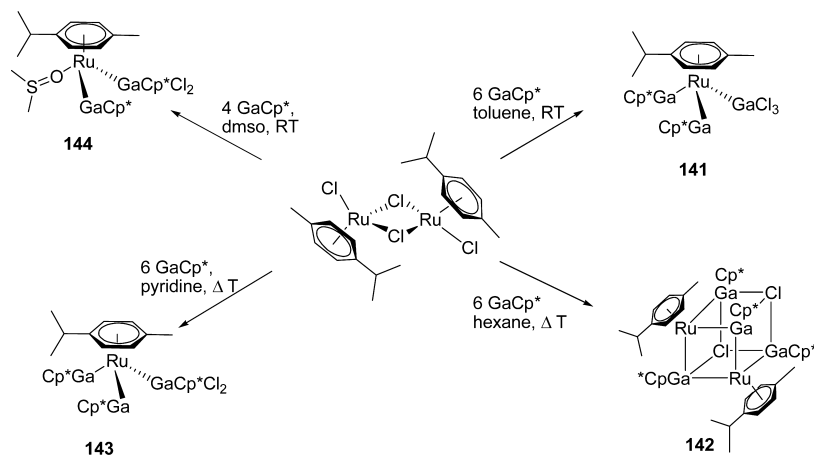
Figure 17. Molecular structure of $[(\text{CpNi}(\text{CO}))_2(\mu_2\text{-InC}(\text{SiMe}_3)_3)]$ (135).

Scheme 22. Reaction of $[(\text{Cp}^*\text{RhCl})_2(\mu_2\text{-Cl})_2]$ with RE^{I} ($\text{E} = \text{Ga, In}$) Compounds



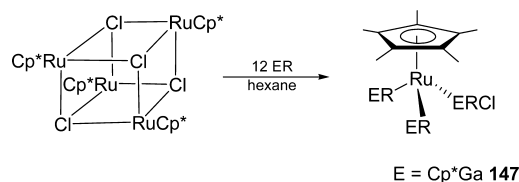
The isolobal ruthenium derivative $[(p\text{-cymene})\text{RuCl}(\mu_2\text{-Cl})_2]$ reacts in toluene with 6 equiv of Cp^*Ga to afford $[(p\text{-cymene})\text{Ru}(\text{GaCp}^*)_2(\text{GaCl}_3)]$ (141). If hexane is used as the solvent, $[(p\text{-cymene})\text{Ru}(\mu\text{-GaCp}^*)_2(\text{GaCp}^*(\mu\text{-Cl})_2)]$ (142) has been obtained as the main product. In the presence of a base such as pyridine, the same reaction affords $[(p\text{-cymene})\text{Ru}(\text{GaCp}^*)_2(\text{GaCp}^*\text{Cl}_2)]$ (143). If the reaction with Cp^*Ga is performed in a 4:1 molar ratio in the presence of dimethylsulfoxide (DMSO), $[(p\text{-cymene})\text{Ru}(\text{GaCp}^*)(\text{GaCp}^*\text{Cl}_2)(\text{DMSO})]$ (144) is isolated. The wide variety of products obtained in this case once again highlights the importance of the kinetic control of the involved processes (Scheme 23).

Scheme 23. Reaction of $[(p\text{-cymene})\text{RuCl}(\mu_2\text{-Cl})_2]$ with Cp^*Ga



Another ruthenium precursor, $[\text{Cp}^*\text{RuCl}]_4$, reacts with RE^{I} derivatives ($\text{RE}^{\text{I}} = \text{Cp}^*\text{Ga, InC}(\text{SiMe}_3)_3$), leading to the isolation of the corresponding insertion products $[\{\text{Cp}^*\text{Ru}(\text{InCp}^*)\}\{(\mu_2\text{-Cl})(\text{InCp}^*)_2\}]$ (145), $[\{\text{Cp}^*\text{Ru}(\text{InC}(\text{SiMe}_3)_3)\}\{(\mu_2\text{-Cl})(\text{InC}(\text{SiMe}_3)_3)_2\}]$ (146), and $[\text{Cp}^*\text{Ru}(\text{GaCp}^*)_2(\eta^1\text{-GaCp}^*\text{Cl})]$ (147), as revealed by their solid-state structures (Scheme 24). The chloride ligand in $[\text{Cp}^*\text{Ru}$

Scheme 24. Reaction of $[\text{Cp}^*\text{RuCl}]_4$ with RE^{I} Ligands



$(\text{GaCp}^*)_2(\eta^1\text{-GaCp}^*\text{Cl})]$ (147) can be removed by the addition of NaBPh_4 , thus leading to the isolation of the ionic compound $[\text{Cp}^*\text{Ru}(\text{GaCp}^*)_3][\text{BPh}_4]$ (148), which is analogous to the product of the reaction of $[(\text{Cp}^*\text{RuCl})_2(\mu_2\text{-Cl})_2]$ with Cp^*Ga , $[\text{Cp}^*\text{Ru}(\text{GaCp}^*)_3][\text{Cp}^*\text{GaCl}_3]$ (149).

The reaction of $[\text{Ru}(\text{PPh}_3)_3\text{Cl}_2]$ with 6 equiv of Cp^*Ga leads to the isolation of an interesting product, $[\text{Ru}(\text{GaCp}^*)_4(\text{Ga}(\text{Cl})\text{Cp}^*)_2]$ (150), albeit in low yields. This might be due to the formation of $[\text{Cp}^*\text{Ru}(\text{H})(\text{PPh}_3)(\kappa^2\text{-}(\text{C}_6\text{H}_4)\text{-PPh}_2)(\text{GaCl}_2)]$ (151) as suggested by the spectroscopic data. The latter is the product of a side-reaction, involving an insertion into the $\text{Ru}\text{-Cl}$ bond, which proceeds via orthometalation of one of the PPh_3 phenyl rings, along with a Cp^* transfer. When $[\text{Ru}(\text{DMSO})_4\text{Cl}_2]$ was used as starting material, the isolated yield of $[\text{Ru}(\text{GaCp}^*)_4(\text{Ga}(\text{Cl})\text{Cp}^*)_2]$ (150) increased significantly (Scheme 25).

The Ru center in 150 is in a distorted octahedral environment, coordinated to six Cp^*Ga ligands. One of the chloride ions occupies a terminal position bound to one of the Cp^*Ga ligands, while the second halide is bridging two gallium centers. The steric crowding around the Ru center causes three of the Cp^* rings to be coordinated in η^5 -mode, while the rest of them are bound to the Ga centers in a η^1 fashion (Figure 18).¹²¹

Insertion reactions have also been observed for the iron complexes $[\text{Fe}(\text{PPh}_3)_2\text{Br}_2]$ and $[\text{Fe}(\text{NCCCH}_3)_2\text{Br}_2]$.¹²¹ The reaction of these complexes with Cp^*Ga proceeds with Cp^*

Scheme 25. Reaction of $[\text{RuCl}_2\text{L}_2]$ ($\text{L} = \text{PPh}_3, \text{DMSO}$) with Cp^*Ga (Reprinted with Permission from Buchin, I. B.; Gemel, C.; Kempter, A.; Cadenbach, T.; Fischer, R. A. Reaction of iron and ruthenium halogenide complexes with GaCp and AlCp : Insertion, Cp transfer reactions and orthometallation. *Inorg. Chim. Acta* 2006, 359 (15), 4833–4839.¹²¹ Copyright 2006 Elsevier.)

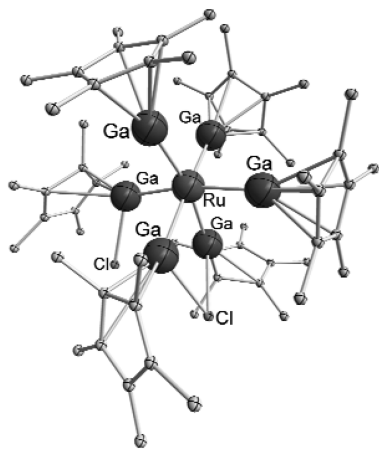
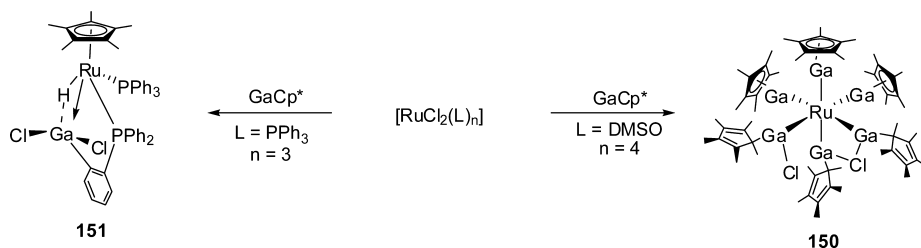
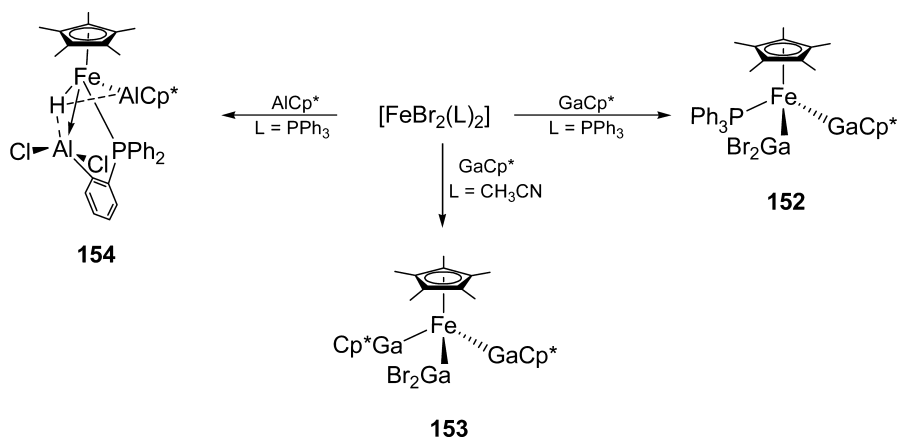


Figure 18. Molecular structure of $[\text{Ru}(\text{GaCp}^*)_6\text{Cl}_2]$ (150).

transfer from the gallium center to iron, leading to the isolation of products $[\text{Cp}^*\text{Fe}(\text{GaCp}^*)(\text{GaBr}_2)(\text{PPh}_3)]$ (152) and $[\text{Cp}^*\text{Fe}(\text{GaCp}^*)_2(\text{GaBr}_2)]$ (153), respectively. The corresponding reaction of $[\text{Fe}(\text{PPh}_3)_2\text{Br}_2]$ with Cp^*Al affords the highly air-sensitive orthometalated $[\text{Cp}^*\text{Fe}(\mu_3\text{-H})(\kappa^2\text{-}(\text{C}_6\text{H}_4)\text{-PPh}_2)(\text{AlCp}^*)(\text{AlBr}_2)]$ (154) (Scheme 26). It is obvious that the Cp^*E ligand significantly influences the course of the reaction, because the reaction of Cp^*Al leads to orthometallation of the remaining phosphine ligand, whereas the reaction of Cp^*Ga does not. This difference in reactivity will be further

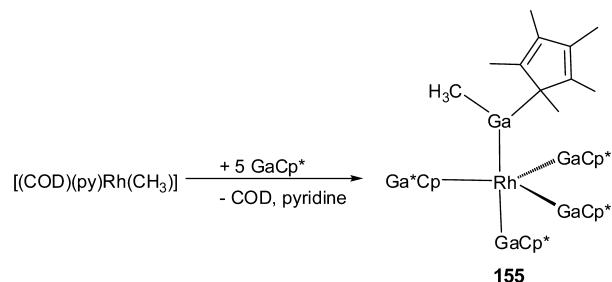
Scheme 26. Insertion Reactions of Cp^*E ($\text{E} = \text{Al}, \text{Ga}$) with Fe Complexes (Reprinted with Permission from Buchin, B.; Gemel, C.; Kempter, A.; Cadenbach, T.; Fischer, R. A. Reaction of iron and ruthenium halogenide complexes with GaCp and AlCp : Insertion, Cp transfer reactions and orthometallation. *Inorg. Chim. Acta* 2006, 359 (15), 4833–4839.¹²⁶ Copyright 2006 Elsevier.)



discussed in the following section devoted to the bond activation by transition-metal complexes containing Cp^*E ligands.

An example of Cp^*Ga insertion into a metal–carbon bond was found in the formation of $[(\text{Cp}^*\text{Ga})_4\text{Rh}(\text{Ga}(\eta^1\text{-Cp}^*)\text{-}(\text{CH}_3))]$ (155) (Scheme 27), where the facile haptotropic shift

Scheme 27. Insertion of Cp^*Ga into Metal–Carbon Bonds



of the Cp^* ring plays an important role.¹²² 155 may undergo selective protolysis, leading to the formation of the ionic species $[(\text{Cp}^*\text{Ga})_4\text{Rh}(\text{GaCH}_3)][\text{BAR}^{\text{F}}_4]$ (156). This reaction has proven to be very useful, because it provides a synthetic route to sterically unshielded alkylgallium^I species, which are unstable and unknown in the free form. For this reason, the protolytic splitting of Cp^*H will be further discussed below as it represents one of the most promising paths for the formation of well-controlled molecular building blocks, which may lead to

the isolation of intermetallic M/E clusters of Hume–Rothery type and nanomaterials.

4.1.5. Hydrogenolysis and Cluster Growth. The principles of the molecular group 13 transition-metal chemistry have been previously applied for the soft chemical synthesis of M/E Hume–Rothery phases because they provide a molecular approach to obtain intermetallic nanomaterials.^{123–126} The hydrogenolysis of Cp* or hydrocarbon ligands has been recognized as a useful method for the synthesis of building blocks for the formation of such species. In an effort to characterize early intermediates that may be involved in this process, the hydrogenolysis of $[\text{Ru}(\eta^2, \eta^2\text{-COD})(\eta^3\text{-C}_4\text{H}_7)_2]$ carried out in the presence of Cp*Ga yields $[(\text{Cp}^*\text{Ga})_4(\text{H})\text{-Ru}(\mu_2\text{-Ga})\text{Ru}(\text{H})_2(\text{GaCp}^*)_3]$ (**157**) along with Cp*H, cyclooctane, and isobutene as side products.¹²⁷ In a similar way, $[\text{Ru}(\eta^2, \eta^2\text{-COD})(\eta^6\text{-COT})]$ was used as the source of Ru to obtain **157**, whereas under slightly different reaction conditions, the intermediates $[(\eta^4\text{-COD})(\eta^4\text{-COT})\text{Ru}(\text{GaCp}^*)]$ (**109**) and $[(\eta^4\text{-COD})\text{Ru}(\text{GaCp}^*)_3]$ (**110**) were formed (Scheme 27). Spectroscopic and structural analyses of **157** provide evidence for two Ru-centers in octahedral coordination environments, which are bridged by a “naked”, substituent-free gallium atom in a quasi-linear arrangement. Seven Cp*Ga and three hydride ligands are coordinated to two Ru-centers, arranged in two different Ru-fragments $[(\text{Cp}^*\text{Ga})_4(\text{H})\text{Ru}(\mu_2\text{-Ga})]$ and $[(\text{Cp}^*\text{Ga})_3(\text{H})_2\text{Ru}(\mu_2\text{-Ga})]$ (Figure 19).

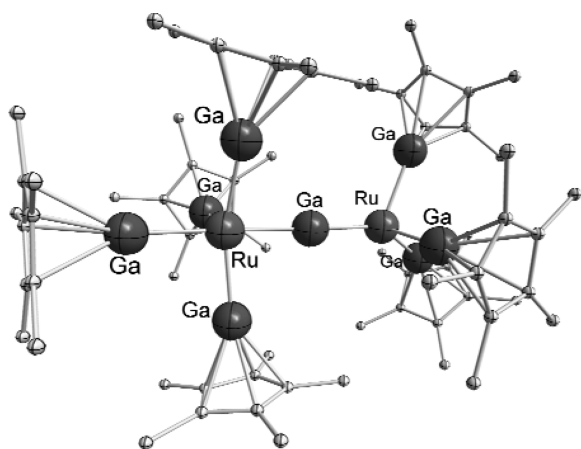


Figure 19. Molecular structure of $[(\text{Cp}^*\text{Ga})_4(\text{H})\text{Ru}(\mu_2\text{-Ga})\text{Ru}(\text{H})_2(\text{GaCp}^*)_3]$ (**157**).

$[(\text{Cp}^*\text{Ga})_4(\text{H})\text{Ru}(\mu_2\text{-Ga})\text{Ru}(\text{H})_2(\text{GaCp}^*)_3]$ (**157**) can be considered as a molecular intermediate in the formation of Ru/Ga nanoparticles during a wet chemical synthesis. Therefore, the hydrogenolysis mechanism of coordinated Cp*Ga releasing Cp*H was studied in detail by applying DFT methods. It was possible to propose a reasonable mechanism in which the key intermediate $[\text{Ru}(\text{GaCp}^*)_4(\text{H})_2]$ (**158**) undergoes a concerted elimination of CpH and through a subsequent association/dissociation equilibrium leads to the model compound $[(\text{GaCp}^*)_4(\text{H})\text{Ru}(\mu_2\text{-Ga})\text{Ru}(\text{H})_2(\text{GaCp}^*)_3]$ (**159**).

5. F-BLOCK COMPLEXES

Compared to the wealth of transition-metal complexes of RE^I ligands, the corresponding chemistry of lanthanides and actinides has only been sparsely investigated. Because of their pronounced Lewis acidity, lanthanides (Nd, Sm, Eu, Yb, and Tm)^{128,129} and actinides (U)¹³⁰ are more readily stabilized by

anionic ligands such as the diazabutenido ligand $[\text{Ga}(\text{ArNCH})_2]^-$ (Ar = 2,6-ⁱPr₂C₆H₃) through the formation of polar Ga–M bonds (Figure 20). A few examples incorporating a neutral RE^I ligand such as Cp*E (E = Al, Ga) have been reported, however. The details of these studies are described below.

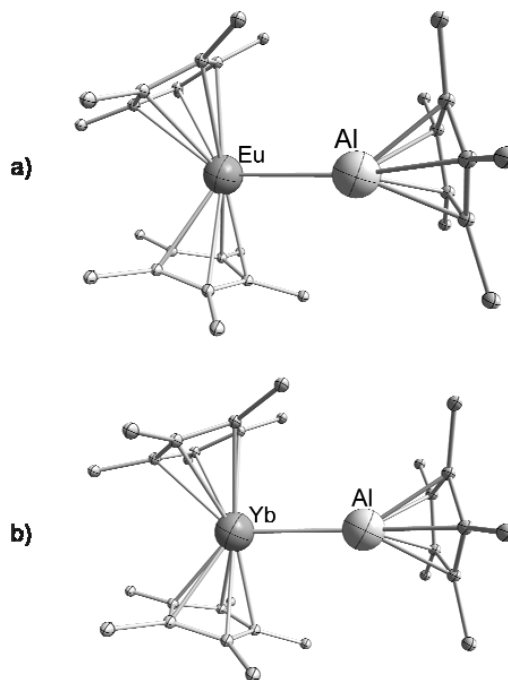
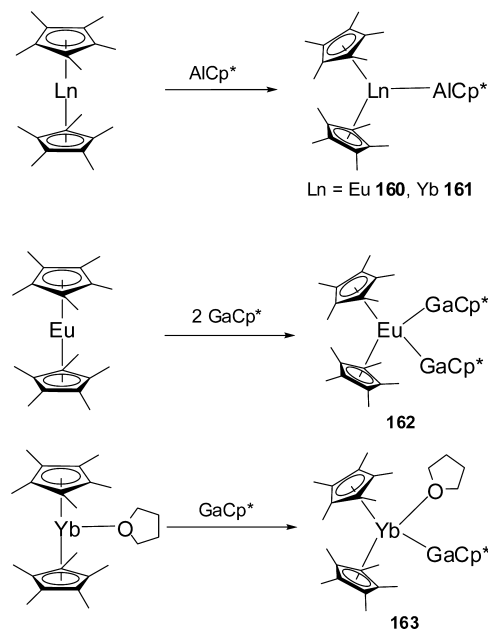


Figure 20. Structure of (a) $[\text{Cp}^*_2\text{Eu}-\text{AlCp}^*]$ (**160**) and (b) $[\text{Cp}^*_2\text{Yb}-\text{AlCp}^*]$ (**161**).

5.1. Lanthanide Compounds

The first examples of complexes containing metal–metal bonds involving rare-earth atoms and a group 13 element were reported only in 2006 (Scheme 28).¹³¹ The complexes

Scheme 28. Synthesis of $[\text{Cp}^*_2\text{Ln}-\text{ECp}^*]$ Complexes



[Cp*₂Ln–AlCp*] (Ln = Eu (160), Yb (161)) were obtained in adequate yields by the solvent-free reaction of the corresponding metallocene with Cp*Al in a sealed ampule at 120 °C for several days. Both products have been found to be extremely air-sensitive and readily decompose in solution. Their solid-state structures determined by single-crystal X-ray diffraction studies reveal them to be Lewis acid–base adducts with no unusually short intermolecular contacts (Figure 20).

The Cp*_{centr}–Al–Ln angle in both complexes [Cp*₂Ln–AlCp*] (Ln = Eu (160), Yb (161)), has been found to deviate significantly from linearity (161.82(1)° (160), 171.79(1)° (161)). These values are, however, in agreement with those found in p-block Lewis acid–base adducts such as [Cp*Al–B(C₆F₅)₃] (24) (Cp*_{centr}–Al–B 172.9(1)°).⁶⁵ The Al–Ln bond lengths of 3.365(1) Å (160) and 3.198(1) Å (161), however, cannot be compared because these are the first examples of metal–metal bonds between aluminum and 4f metals. It is worth mentioning that various spectroscopic and structural analyses were performed to establish that the lanthanide centers maintain their +2 oxidation state even after aluminum coordination, and also to rule out the presence of any bridging hydrido ligands on the f-block element coordination sphere. The low stability of [Cp*₂Ln–AlCp*] (Ln = Eu (160), Yb (161)) in solution can be ascribed to the relatively small energies of the Ln–Al bonds (~30 kJ mol⁻¹) as determined by theoretical calculations (DFT-BP86).¹³² These calculations further confirm the chemical compositions of both complexes and also suggest that the interaction between the [Cp*₂Ln] and [Cp*Al] fragments is essentially electrostatic with insignificant charge-transfer and covalent contributions.

Extending their interest on lanthanide–group 13 metal bonds, P. W. Roesky and co-workers reported on the syntheses of [Cp*₂Eu(GaCp*₂)] (162) and [Cp*₂Yb(THF)GaCp*] (163) (Scheme 28).¹³³ In contrast to the complexes where the ligand is aluminum-based, complexes [Cp*₂Eu(GaCp*₂)] (162) and [Cp*₂Yb(THF)GaCp*] (163) can be obtained in toluene at room temperature. Their relative stability in solution is a quite surprising feature, because Cp*Al is considered to be a stronger base than the analogous gallium-based ligand. To obtain 163, the composition of the starting materials is critical. Compound 163 can be isolated in useful quantities when [Cp*₂Yb(THF)_{1-n}] is reacted with 1 equiv of Cp*Ga in toluene, but when pure [Cp*₂Yb(THF)] is used, fast decomposition of the product is observed. Interestingly, all attempts to obtain a solvent-free Yb species were unsuccessful, and 163 is seemingly less stable in solution than 162. The solid-state structures of 163 and 162 show that both are individual Lewis acid–base adducts with no unusually short intermolecular interactions (Figure 21).

Consistent with their ionic radii, the Eu^{II} center is coordinated to two Cp*Ga units, whereas the Yb^{II} center is bonded to only one unit and hence its coordination sphere is saturated by one solvent molecule. It is worth mentioning that the coordination numbers for the Ln–Al and Ln–Ga differ. Whereas both Ln–Al (Ln = Eu (160), Yb (161)) complexes are 1:1 adducts, the Ln–Ga complexes have additional ligands coordinated to the lanthanide centers. The lanthanide–group 13 metal distances in 162 and 163 can be compared to the corresponding distances in diazabutenido lanthanide complexes 164a–164c and 165 depicted in Figure 22. The Eu–Ga bond lengths in 162 (3.2499 and 3.3907 Å) are comparable to that in [Eu(Ga(ArNCH)₂)₂(tmeda)₂] (164b) (3.3124 Å) (Figure 22), whereas the Yb–Ga distance in 163 (3.2872(4) Å) is longer

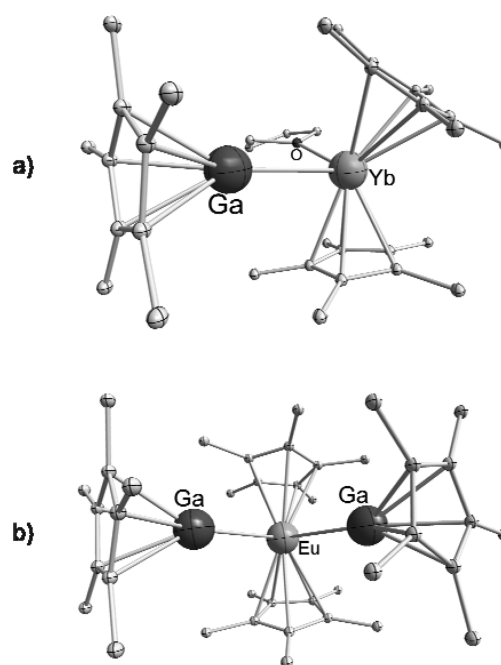


Figure 21. Molecular structures of (a) [Cp*₂Yb(THF)GaCp*] (163) and (b) [Cp*₂Eu(GaCp*₂)] (162).

than that observed for the complex [Yb(Ga(ArNCH)₂)₂(tmeda)₂] (164c) (3.2050 and 3.2473 Å) (Figure 22). As expected for complexes with low covalent contribution, the Ln–Ga distances in 162 and 163 are significantly longer than the sums of the covalent radii (Eu–Ga 3.19 Å, Yb–Ga 3.08 Å).

Recent reports on RE^I complex of the lanthanides by Arnold and co-workers describe the synthesis of [(η⁵-C₅H₄(SiMe₃)₃Ln(ECp*))] (Ln = Nd, E = Al (166), Ga (167); Ln = Ce, E = Al (168), Ga (169)), from the reaction of [(CpSiMe₃)₃Nd] with Cp*Al or Cp*Ga (Scheme 29). However, these species were only identified on the basis of variable-temperature ¹H NMR spectroscopic studies but could not be isolated in pure form.^{134,135}

5.2. Actinide Compounds

Although the bonding in f-element complexes has been traditionally described as electrostatic, in recent times it has been suggested that a certain degree of covalency might be included in metal complexes of the actinides. Arnold and co-workers reported on the synthesis of the first example of an unsupported actinide–group 13 element bond, [(η⁵-C₅H₄(SiMe₃)₃U–AlCp*)] (170) (Figure 23).¹³⁶ This complex was obtained in moderate yields by stirring a mixture of [(η⁵-C₅H₄(SiMe₃)₃U] and Cp*Al in toluene at 60 °C. The analogous complex [(η⁵-C₅H₄(SiMe₃)₃U–GaCp*)] (171) was also subsequently reported.¹³⁴ The complexes 171 and 170 are isostructural.

The U–Al bonds in 170 (3.117(3), 3.124(4) Å) have been found to be close to the sum of covalent radii for the involved elements (3.17 Å), whereas the U–Ga bond lengths in 171 (3.065(1) Å, 3.080(1) Å) are shorter than the sum of the corresponding covalent radii (3.18 Å) and also the observed distance in [(tren^{TMS})U(Ga(NArCH)₂)(THF)] (172) (3.2115(8) and 3.2983(9) Å) (tren^{TMS} = N-(CH₂CH₂NSiMe₃)₃) reported by Liddle, ones, and co-workers.¹³⁰ The short bond distance has been ascribed to a strong

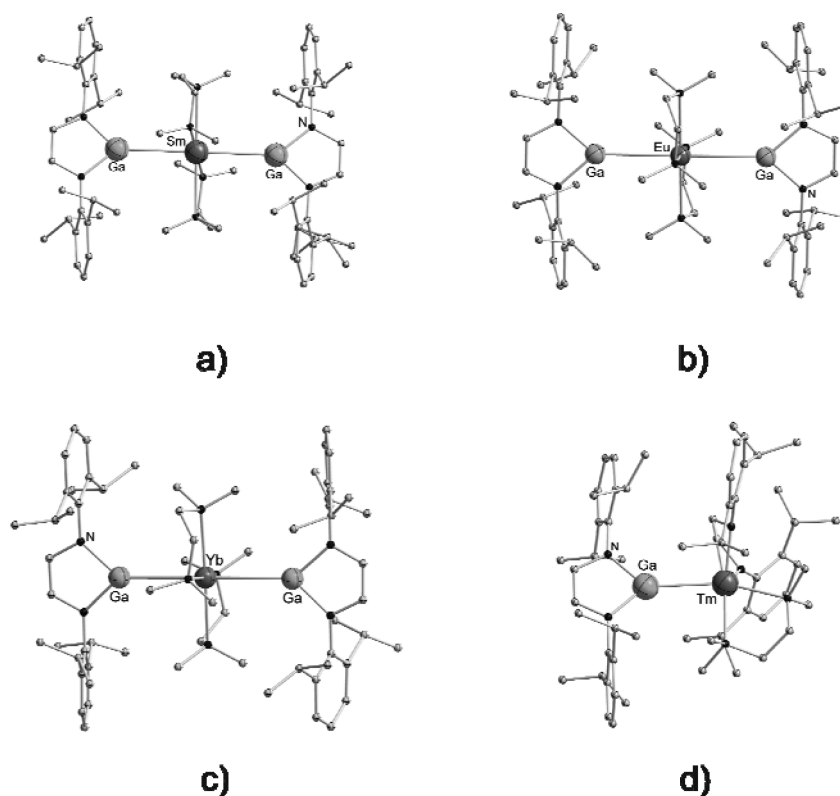


Figure 22. Diazabutenido lanthanide complexes: (a) $[\text{Sm}(\text{Ga}(\text{ArNCH})_2)_2(\text{tmeda})_2]$ (**164a**), (b) $[\text{Eu}(\text{Ga}(\text{ArNCH})_2)_2(\text{tmeda})_2]$ (**164b**), (c) $[\text{Yb}(\text{Ga}(\text{ArNCH})_2)_2(\text{tmeda})_2]$ (**164c**), and (d) $[(\text{tmeda})\text{Tm}(\text{Ga}(\text{ArNCH})_2)(\text{ArNCH})_2]$ (**165**).

Scheme 29. Synthesis of $[(\eta^5\text{-C}_5\text{H}_4(\text{SiMe}_3))_3\text{Ln}(\text{ECp}^*)]$ (**166–169**)

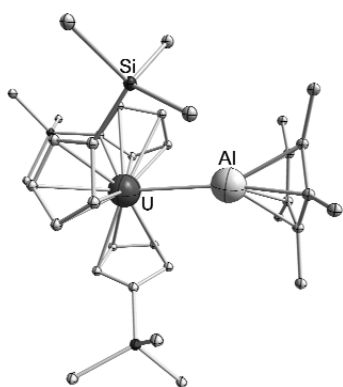
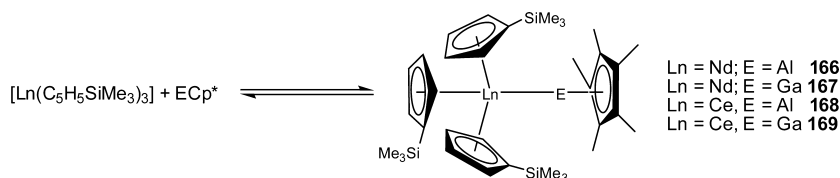


Figure 23. Molecular structures of $[(\eta^5\text{-C}_5\text{H}_4(\text{SiMe}_3))_3\text{U}(\text{AlCp}^*)]$ (**170**).

influence of the crystal packing forces. An NBO/NLMO (natural bond orbital–natural localized molecular orbital) electronic analysis (B3PW91) of the metal–ligand bonding in the model complexes $[\text{Cp}_3\text{U}-\text{ECp}^*]$ (E = Al, Ga) showed that the metal–metal bonding arises predominantly from E \rightarrow U σ -donation, due to the favorable overlap of the lone pair with the 7s/6d acceptor orbitals on U^{III} . A negligible amount of U π -

electron density is donated into the formally empty π -symmetric *p* orbitals on Al or Ga. Density functional theory calculations were undertaken using model complexes $\text{Cp}_3\text{Ln}-\text{ECp}^*$ where Ln = La–Lu and E = Al, Ga. The Ln–E bond distances were predicted to decrease more sharply across the Ln series than those involving hard Lewis bases; however, local increases were observed at Eu and Yb. Electronic analyses were performed in the NBO/NLMO formalism, indicating that the E \rightarrow Ln acceptor orbital is primarily of d-character in all cases. It is proposed that a steric-strain component, which increases with the lanthanide contraction in this case, balances the Ln–E bond-stabilizing effect of core-orbital contraction. All data indicate that the Ln–E bonding interactions are predominantly of covalent or nonpolar donor–acceptor character. However, the formation of a strong covalent bond is not observed because of resistance to reduction of an effectively divalent Ln center.¹³⁵

6. COORDINATION CHEMISTRY OF SUBSTITUENT-FREE GA^+

The extreme redox lability of the Ga^+ species has posed a particular challenge to the development of the organometallic chemistry of this naked cation. The chemistry of In^+ is sparse (vide infra; section 7). Any results on the potentially

homologous chemistry of (extremely reactive) Al^+ have not been reported, yet. The unique $[\text{Ga}_2\text{Cp}^*][\text{BAR}^{\text{F}}_4]$ (**93**)⁹⁶ (Figure 24) species can be easily reduced or oxidized on

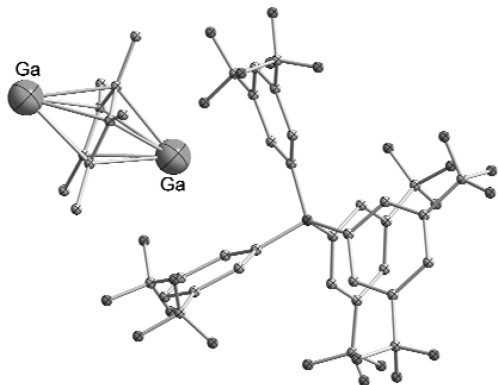


Figure 24. Molecular structure of $[\text{Ga}_2\text{Cp}^*][\text{BAR}^{\text{F}}_4]$.

reaction with numerous reagents containing transition-metal centers. Nevertheless, the naked Ga^+ moiety is a very interesting synthon for unusual complexes $[\text{L}_n\text{M}-\text{GaR}']$ (M = transition metal, R' = anionic ligand, different to Cp^*), which could be obtained either by insertion of Ga^+ into a $\text{M}-\text{R}'$ bond or by addition of a nucleophilic fragment R' into an electrophilic complex $[\text{L}_n\text{MGa}]^+$. Only very recently, the synthesis of the novel species $[\text{Ar}_2\text{Ga}][\text{Al}(\text{OC}(\text{CF}_3)_3)_4]$ (Ar = $\text{C}_6\text{H}_5(\text{CH}_3)$ (**173**), $\text{C}_6\text{H}_5\text{F}$ (**174**)) have been reported. These two derivatives are stable, crystalline, univalent gallium salts, obtained by a simple route where metallic gallium is oxidized by $\text{Ag}[\text{Al}(\text{OC}(\text{CF}_3)_3)_4]$, which contains a weakly coordinating, perfluorinated alkoxy aluminate anion (WCA).¹³⁷

Similar to the Ga^+ -arene salts studied by Schmidbaur, the $[\text{Ga}(\text{C}_6\text{H}_5\text{Me})_2]^+$ cation of **173** adopts a bent sandwich structure. The isolation of these complexes opens up the possibility of exploring the coordination chemistry of Ga^+ ligand. So far, only the reaction of triphenylphosphine with **173** has been reported. This reaction affords the first homoleptic gallium^I-phosphine complex, $[(\text{Ph}_3\text{P})_3\text{Ga}][\text{Al}(\text{OC}(\text{CF}_3)_3)_4]$ (**175**), where the gallium center is found in a trigonal-pyramidal coordination environment, which is indicative of the presence of a stereochemically active lone pair (Figure 25).¹³⁸

Concerning the reactivity of the “naked” Ga^+ , the reaction of $[\text{Ga}_2\text{Cp}^*][\text{BAR}^{\text{F}}_4]$ (**93**) with $[\text{Ru}(\text{GaCp}^*)_3(\text{TMM})]$ (**104**) has been studied, and it has been observed to involve the

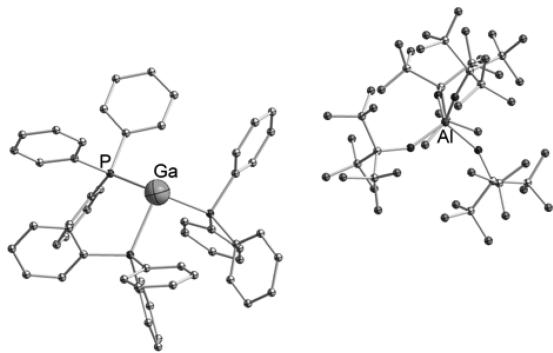


Figure 25. Molecular structure of $[(\text{Ph}_3\text{P})_3\text{Ga}][\text{Al}(\text{OC}(\text{CF}_3)_3)_4]$ (**175**).¹³⁷

nucleophilic attack of a carbon atom to the electrophilic Ga^+ ion, with formation of a RGa^+ species, which “switches on” the free electron-pair at the Ga^+ center.¹⁰⁰ Thus, the electrophilic Ga^+ ion is converted into a basic RGa^+ fragment. This leads to the coordination of a monovalent gallium unit to a neighboring Ru-center and subsequent formation of the dimer $[\text{Ru}(\text{GaCp}^*)_3(\eta^3-(\text{CH}_2)_2\text{C}(\text{CH}_2(\mu_2-\text{Ga})))_2][\text{BAR}^{\text{F}}_4]_2$ (**176**) (Figure 26).

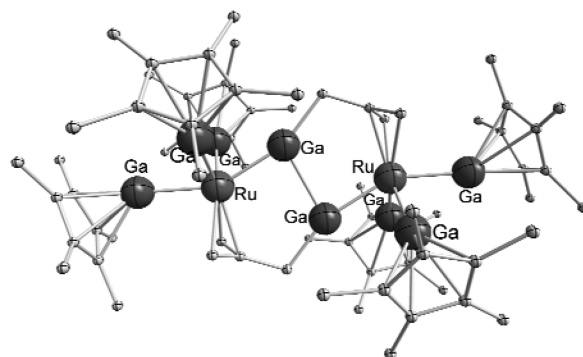


Figure 26. Molecular structure of $[\text{Ru}(\text{GaCp}^*)_3(\eta^3-(\text{CH}_2)_2\text{C}(\text{CH}_2(\mu_2-\text{Ga})))_2][\text{BAR}^{\text{F}}_4]_2$ (**176**).

Compound **176** is stable in the solid state but isomerizes at high temperatures to $[\text{Ru}(\text{GaCp}^*)_3(\eta^3-(\text{CH}_2)(\text{CH}(\mu_2-\text{Ga})(\text{CH}_3))_2][\text{BAR}^{\text{F}}_4]_2$ (**177**) when dissolved in polar solvents such as fluorobenzene. Thereby, the gallium atom is not bound to an aliphatic CH_2 group anymore but to a vinyl group, so that the thermal isomerization of **176** to **177** can be understood as a simple tautomerization of the allyl fragment. The RGa units in **176** and **177** are weakly bound to each other via a closed-shell interaction, which is strong enough to favor the formation of the discrete dimeric structures in **176** and **177**, in contrast to the feasible alternative path to form polymeric chains.

Furthermore, the reaction of $[\text{Ru}(\text{PCy}_3)_2(\text{GaCp}^*)_2(\text{H})_2]$ (**105**) with $[\text{Ga}_2\text{Cp}^*][\text{BAR}^{\text{F}}_4]$ (**93**) selectively leads to the formation of the ionic compound $[\text{Ru}(\text{PCy}_3)_2(\text{GaCp}^*)_2(\text{Ga})][\text{BAR}^{\text{F}}_4]$ (**178**) (Figure 27), with concomitant reductive elimination of H_2 . Complex **178** is the second example of a compound containing a terminal “naked” Ga^+ ligand coordinated to a transition metal. The slightly basic Ru^0 d^8 metal center and the strong σ -/ π -acceptor properties of the Ga^+

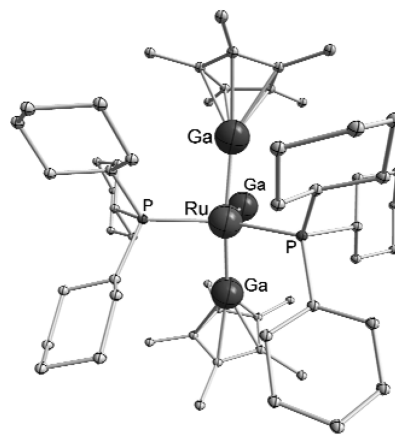
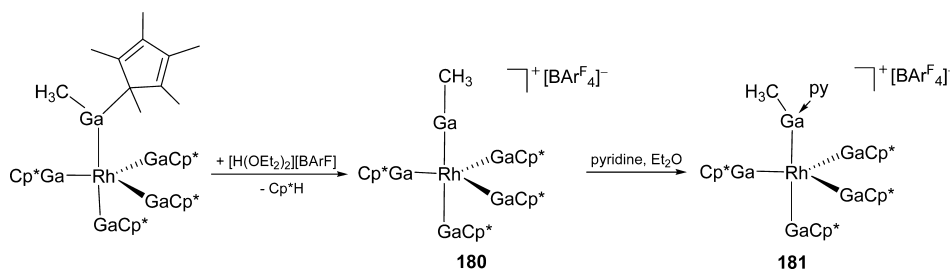


Figure 27. Molecular structure of cation $[\text{Ru}(\text{PCy}_3)_2(\text{GaCp}^*)_2(\text{Ga})]^+$ (**178**).

Scheme 30. Synthesis of $[(\text{Cp}^*\text{Ga})_4\text{Rh}(\text{GaCH}_3)][\text{BAR}^{\text{F}}_4]$ (**180**) and $[(\text{Cp}^*\text{Ga})_4\text{Rh}(\text{Ga}(\text{CH}_3)\text{py})][\text{BAR}^{\text{F}}_4]$ (**181**)

ligand are responsible for the shortest Ru–Ga contact known to date (2.300(2) Å).

7. REMOVAL OF CP* FROM COORDINATED CP*E LIGANDS

The preceding sections of this review have dealt mainly with the coordination chemistry of Cp^*E ligands. In this section we will treat the chemistry of the coordinated ligand Cp^*E with special emphasis on the attack of the $\text{E}-\text{Cp}^*$ bond. The unique property of the Cp^* ligand as an easily removable protecting group was first envisaged by Jutzi et al., who suggested that, because of its leaving-group character, this ligand could offer the option of novel chemistry at the group 13 center.²² As the ensuing discussion would reveal, the transformation of coordinated Cp^*Ga ligands into substituent-free Ga^+ in terminal or bridging positions has been proven possible.

7.1. Protolysis

On the basis of the evidence of the formation of $[\text{Ga}_2\text{Cp}^*][\text{BAR}^{\text{F}}_4]$ (**93**)⁹⁶ and $[\text{GaPt}(\text{GaCp}^*)_4][\text{BAR}^{\text{F}}_4]$ (**179**),¹³⁹ the protolytic cleavage of Cp^*H from coordinated $\text{Ga}(\text{R})\text{Cp}^*$ groups was used to isolate a terminal $[\text{Ga}(\text{CH}_3)]$ ligand in the cationic complex $[(\text{Cp}^*\text{Ga})_4\text{Rh}(\text{GaCH}_3)][\text{BAR}^{\text{F}}_4]$ (**180**) (Scheme 30).¹²²

$[(\text{Cp}^*\text{Ga})_4\text{Rh}(\text{GaCH}_3)][\text{BAR}^{\text{F}}_4]$ (**180**) (Figure 28) is one of a few examples of pseudohomoleptic complexes $[\text{ML}_n]$ with a

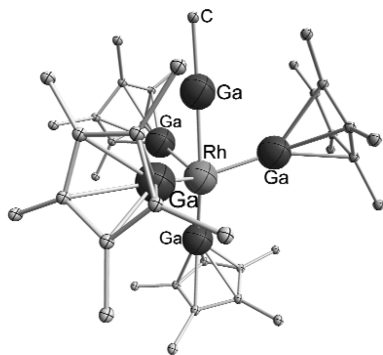


Figure 28. Molecular structure of cation $[(\text{Cp}^*\text{Ga})_4\text{Rh}(\text{GaCH}_3)]^+$ (**180**).

high coordination number ($n > 4$) and ligands that have metal centers as donor atoms.^{90b} $[\text{Ga}(\text{CH}_3)]$, being the smallest alkylgallium(I) fragment, is a good σ -donor, in spite of its poor π -acceptor properties, as proved by the solid-state structure analysis of both **180** and the corresponding pyridine adduct $[(\text{Cp}^*\text{Ga})_4\text{Rh}(\text{Ga}(\text{CH}_3)\text{py})][\text{BAR}^{\text{F}}_4]$ (**181**) (Scheme 30).¹²²

The selective removal of a Cp^* ligand by protonation of the $[\text{Ga}(\eta^1-\text{Cp}^*)(\text{CH}_3)]$ group in $[(\text{Cp}^*\text{Ga})_4\text{RhGa}(\eta^1-\text{Cp}^*)(\text{CH}_3)]$ (**155**), with the concomitant preferential release of

Cp^*H over CH_4 , provides a facile synthetic route to obtain sterically unshielded RGA^{I} species, which are otherwise unstable in their free form and therefore not isolable. The isolobal relationship between the fragments L_4Rh and CH_3 suggests that the cation $[(\text{Cp}^*\text{Ga})_4\text{Rh}(\text{GaCH}_3)]^+$ can be viewed as being composed of a nucleophilic 18-electron fragment $[(\text{Cp}^*\text{Ga})_4\text{Rh}]^-$ and an electrophilic $[\text{GaCH}_3]^{2+}$ ion. On the other hand, if the particular synthesis route is disregarded, the cation $[(\text{Cp}^*\text{Ga})_4\text{Rh}(\text{GaCH}_3)]^+$ as such may be described as a $\text{Rh}^{\text{I}}/\text{Ga}^{\text{I}}$ complex, which is composed of a neutral, carbenoid $[\text{GaCH}_3]$ two-electron donor ligand coordinated to an unsaturated 16-electron $[(\text{Cp}^*\text{Ga})_4\text{Rh}]^+$ ion. DFT calculations for the model complex $[(\text{CpGa})_4\text{Rh}(\text{GaCH}_3)]^+$ (**182**) further substantiate the description of $[(\text{Cp}^*\text{Ga})_4\text{Rh}(\text{GaCH}_3)]^+$ in **180** as a pseudohomoleptic Ga^{I} complex. An energy decomposition analysis (EDA) revealed that a fragmentation into $[(\text{CpGa})_4\text{Rh}]^+$ and $[\text{GaCH}_3]$ ($\Delta E_{\text{int}} = -83.1 \text{ kcal}\cdot\text{mol}^{-1}$) requires much less energy than a homolytic cleavage ($\Delta E_{\text{int}} = -127.4 \text{ kcal}\cdot\text{mol}^{-1}$), whereas the energy needed for the decomposition into $[(\text{CpGa})_4\text{Rh}]^-$ and $[\text{GaCH}_3]^{2+}$ ($\Delta E_{\text{int}} = -457.8 \text{ kcal}\cdot\text{mol}^{-1}$) is very high. Additionally, it was found that the calculated charge on the gallium atom of the GaCH_3 group (1.06) is higher than that on the GaCp ligands (0.78/0.79) but substantially lower than in the cation $[\text{Ga}(\text{CH}_3)_2]^{2+}$ (1.70).

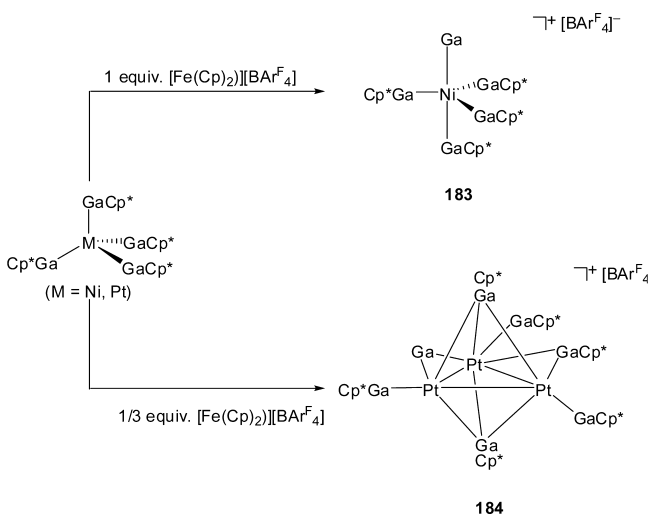
This result highlights the unique properties of the Cp^* group, which are key factors for the stabilization of the low-valent group 13 compounds. When compared with the N,N chelating diketiminate and other analogous ligands, it is obvious that the fluxional behavior at main-group coordinated Cp^* units, as well as the relatively weak bonding between Cp^* and the group 13 atoms, facilitates its use as a protective group. Thus, the obvious question to be addressed is the use of the selective Cp^*H splitting as a deprotection method for compounds of the $[\text{L}_a\text{M}_b(\text{ECp}^*)_c]$ ($\text{E} = \text{Al}, \text{Ga}, \text{In}$) class. Hence, the deeper understanding of this chemistry is a key for the further development of well-controlled molecular building-block chemistry to obtain intermetallic M/E clusters of Hume–Rothery type and nanomaterials.

7.2. Oxidation

Recently, a new and selective method for a facile cleavage of $\text{Ga}-\text{Cp}^*$ bonds has been reported. The treatment of $[\text{M}(\text{GaCp}^*)_4]$ ($\text{M} = \text{Ni}$ (**73**), Pt (**74**))^{83,89} with $[\text{Fe}(\text{C}_5\text{H}_5)_2][\text{BAR}^{\text{F}}_4]$ leads to a surprisingly selective oxidative cleavage of the Cp^* group, leaving the oxidation states of the gallium and transition-metal centers unchanged (Scheme 31).¹⁴⁰

Thus, the BAR^{F}_4 salt of the $[\text{GaNi}(\text{GaCp}^*)_4]^+$ cation was obtained by treatment of $[\text{Ni}(\text{GaCp}^*)_4]$ (**73**) with an equimolar amount of $[\text{Fe}(\text{C}_5\text{H}_5)_2][\text{BAR}^{\text{F}}_4]$. There was no evidence either of the formation of side products that would indicate the oxidation of gallium or the transition metal or of the formation of any gallium–fluorine species.

Scheme 31. Reaction of $[M(\text{GaCp}^*)_4]$ ($M = \text{Ni}$ (73), Pt (74)) with $[\text{Fe}(\text{C}_5\text{H}_5)_2][\text{BAR}^{\text{F}}_4]$



The cation $[\text{GaNi}(\text{GaCp}^*)_4]^+$ (183) exhibits a slightly distorted trigonal-bipyramidal structure with the Ga^+ ligand in an axial position, as in the homologous $[\text{GaPt}(\text{GaCp}^*)_4]^+$ (179) (Figure 29). The bonding situation of substituent-free, terminally coordinated Ga^+ was elucidated in detail and can be described as a main-group-metal equivalent of the proton H^+ .

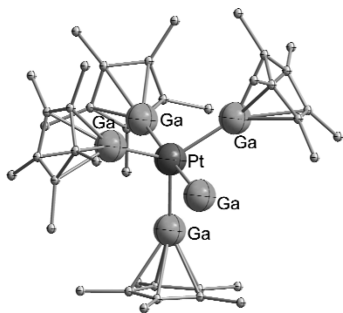


Figure 29. Molecular structure of the cation $[\text{GaPt}(\text{GaCp}^*)_4]^+$ (183).¹³⁹

It is worth noting that the Ga^+ ligand exhibits strong σ - and π -acceptor capacity but no donor properties at all.¹³⁹ In contrast, the reaction of $[\text{Pt}(\text{GaCp}^*)_4]$ (74) with $[\text{Fe}(\text{C}_5\text{H}_5)_2][\text{BAR}^{\text{F}}_4]$ under the same conditions did not yield the analogous monometallic cation but rather the cluster cation $[(\mu_2\text{-Ga})\text{Pt}_3(\mu_3\text{-GaCp}^*)_2(\text{GaCp}^*)_4]^+$ (184). Its molecular structure (Figure 30) consists of a central triangular Pt_3 unit, capped by two $\mu_3\text{-Cp}^*\text{Ga}$ ligands, which are symmetrically equivalent. Each Pt atom bears an additional terminal Cp^*Ga ligand, whereas only two of the three $\text{Pt}\text{-Pt}$ edges are bridged by gallium ligands, that is, one by a Cp^*Ga fragment and the other one by a “naked” Ga^+ moiety. Interestingly, this asymmetric bridging motif leads to differences among the $\text{Pt}\text{-Pt}$ distances. The $\mu_2\text{-GaCp}^*$ bridge leads to the shortest bond of 2.594(2) Å. The $\mu_2\text{-Ga}^+$ bridged $\text{Pt}\text{-Pt}$ bond is 2.691(2) Å, and the remaining ligand-free edge exhibits the longest bond of 2.802(2) Å.

The treatment of $[\text{Pd}(\text{GaCp}^*)_4]$ (81) with $[\text{Fe}(\text{C}_5\text{H}_5)_2][\text{BAR}^{\text{F}}_4]$ affords only an inseparable mixture of products. However, when the trimetallic complex $[\text{Pd}_3(\text{GaCp}^*)_4(\mu_2\text{-GaCp}^*)_4]$ (83)⁹² is used as the metallic precursor, $[(\mu_2\text{-Ga})_2\text{Pd}_3(\text{GaCp}^*)_6][\text{BAR}^{\text{F}}_4]_2$ (185) is obtained, which is the first example of a metal complex or cluster containing more than one substituent-free Ga^+ ligand. The structure of compound 185 in the solid state could not be accurately determined because of poor diffraction data; however, its overall composition and the structural features could be unambiguously established. The structure of the dication 185 can be seen as derived from the structure of the monocation 184, just by attaching a second bridging Ga^+ ligand to the free, nonbridged edge of a hypothetical Pd analogue of 184 (Figure 31).

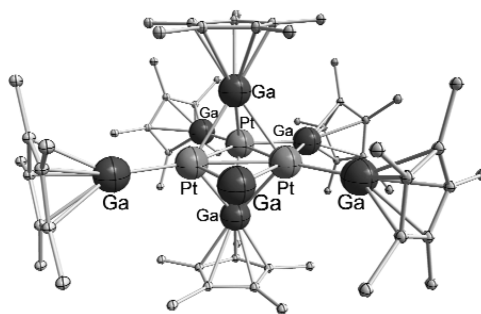


Figure 30. Molecular structure of the cluster cation $[(\mu_2\text{-Ga})\text{Pt}_3(\text{GaCp}^*)_6]^+$ (184).

$[(\mu_2\text{-Ga})_2\text{Pd}_3(\text{GaCp}^*)_6][\text{BAR}^{\text{F}}_4]_2$ (185) is obtained, which is the first example of a metal complex or cluster containing more than one substituent-free Ga^+ ligand. The structure of compound 185 in the solid state could not be accurately determined because of poor diffraction data; however, its overall composition and the structural features could be unambiguously established. The structure of the dication 185 can be seen as derived from the structure of the monocation 184, just by attaching a second bridging Ga^+ ligand to the free, nonbridged edge of a hypothetical Pd analogue of 184 (Figure 31).

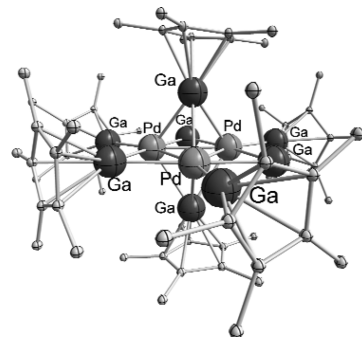


Figure 31. Structure of the cation of $[(\mu_2\text{-Ga})_2\text{Pd}_3(\text{GaCp}^*)_6][\text{BAR}^{\text{F}}_4]_2$ (185).

Using a similar synthetic strategy, a naked In^+ in an organometallic compound has been trapped. The reaction of $\text{Pt}(\text{PPh}_3)_4$ with $\text{In}[\text{BAR}^{\text{F}}_4]$ in fluorobenzene readily yields $[\text{InPt}(\text{PPh}_3)_3][\text{BAR}^{\text{F}}_4]$,¹³⁹ the only example of stabilization of a genuine naked In^+ . There are, however, earlier reports on cationic trimetallic systems featuring indium atom as in $[(\text{Cp}^*\text{Fe}(\text{CO})_2)_2(\mu\text{-In})][\text{BAR}^{\text{F}}_4]$,¹⁴¹ where the formal oxidation state of indium should be +3 in view of the negative charge on the $(\text{Cp}^*\text{Fe}(\text{CO})_2)_2$ fragment.

7.3. Hydrogenolysis

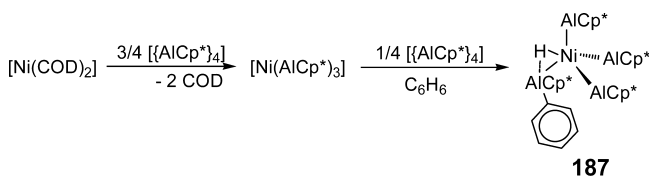
A selective splitting of Cp^* from coordinated Ga centers is also possible by hydrogenolysis as was already discussed in section 4.1.5 on the example of $[(\text{Cp}^*\text{Ga})_4(\text{H})\text{Ru}(\mu_2\text{-Ga})\text{Ru}(\text{H})_2(\text{GaCp}^*)_3]$ (157) as shown in Figure 19. This enhanced reactivity of coordinated Cp^*E in general with respect to the free ligand is important for using Cp^*E in combination with transition-metal complexes as precursors for the soft chemical synthesis of intermetallic nanophases M_xE_y as presented in section 9.

8. REACTIONS AT $[M(\text{ECP}^*)_N]$ FRAGMENTS

8.1. Bond-Activation Reactions

As various theoretical calculations have shown, the greatest contribution to the bonding energy of Cp^*E toward the transition-metal centers originates from the electrostatic interaction between the partial negative charge on the transition-metal atom and the partially positively charged group 13 metal.^{42,43,45,48,66,85} Therefore, the bond strength decreases in the expected order $\text{Al} > \text{Ga} > \text{In}$. The abilities of these ligands do not only dramatically increase the electron density of a metal atom but also act as electrophilic centers for the coordination of weak polar substrates and should provide an outstanding basis for bond-activation reactions. Whereas there is only one example of C–H bond activation by a (DDP) Ga complex, namely, for the formation of the Ni complex $[(\mu_2\text{-GaDDP})\text{Ni}(\text{C}_2\text{H}_4)_2\text{Ni}(\mu_2\text{-CH}=\text{CH}_2)(\text{H})]$,¹⁴² Cp^*E complexes have been shown to have a richer reactivity. The reaction of $[\text{Ni}(\text{COD})_2]$ with 4 equiv of Cp^*Al in benzene does not yield the expected $[\text{Ni}(\text{AlCp}^*)_4]$ (**72**) complex, but $[\text{Ni}(\text{AlCp}^*)_3(\text{H})(\text{Cp}^*\text{AlPh})]$ (**187**) through activation of a C–H bond of the benzene molecule is formed (Scheme 32).⁸⁷

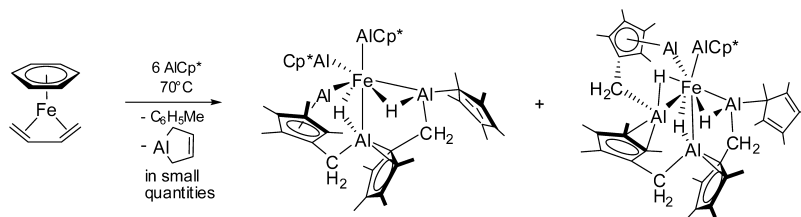
Scheme 32. Formation of $[\text{Ni}(\text{AlCp}^*)_3(\text{H})(\text{AlCp}^*\text{Ph})]$ (**187**) by C–H Bond Activation



The activation of the benzene molecule possibly proceeds with the formation of the unsaturated fragment $[\text{Ni}(\text{AlCp}^*)_3]$ (**188**) through the key intermediate $[(\text{Cp}^*\text{Al})_3\text{Ni}(\text{H})(\text{C}_6\text{H}_5)]$ (**189**). The driving force of this reaction originates from the subsequent migration of the phenyl group to a Cp^*Al ligand, with the concomitant oxidation of the aluminum atom and formation of a strong Al–C bond, along with the coordination of the fourth Cp^*Al ligand. The 16-electron fragment **188** can be trapped by the reaction with other reaction partners, such as HSiEt_3 . Thus, in the presence of HSiEt_3 , the hydrosilyl complex $[\text{Ni}(\text{AlCp}^*)_3(\text{H})(\text{SiEt}_3)]$ (**190**) is obtained through the activation of a Si–H bond.

A further example of the C–H bond activation was observed in the reaction of $[(\eta^6\text{-C}_6\text{H}_5\text{CH}_3)\text{Fe}(\eta^4\text{-C}_4\text{H}_8)]$ with Cp^*Al .¹⁰³ In this reaction, C–H activated isomers of $[\text{Fe}(\text{AlCp}^*)_5]$ (**191a** and **191b**) are formed in which the central iron atom exhibits a distorted trigonal-bipyramidal geometry (Scheme 33). In the process, an unusual tridentate chelate system $[\text{Cp}^*\text{Al}-\text{CH}_2(\text{C}_5\text{Me}_4)\text{Al}-\text{CH}_2(\text{C}_5\text{Me}_4)\text{Al}]$ (**192**) is formed. The hydride occupies a bridging position between the iron and

Scheme 33. Formation of Isomers of the Hypothetical Compound $[\text{Fe}(\text{AlCp}^*)_5]$ (**191**)



aluminum centers. Furthermore, the activation of Cp^*Al is not restricted to Fe–Al species: $[\text{Ru}(\eta^4\text{-COD})(\eta^6\text{-COT})]$ reacted with Cp^*Al , yielding the RuAl_5 complex **193**, which is isostructural to **191a**.

C–C bond activation has been observed to occur in the reaction of $[\text{Cp}^*\text{Rh}(\text{CH}_3)_2\text{L}]$ ($\text{L} = \text{DMSO}$, pyridine) with Cp^*Ga and Cp^*Al .^{143,144} The reaction with Cp^*Ga , for example, yields the isolable intermediate $[\text{Cp}^*\text{Rh}(\text{GaCp}^*)(\text{CH}_3)_2]$ (**194**) (Figure 32), which subsequently undergoes C–

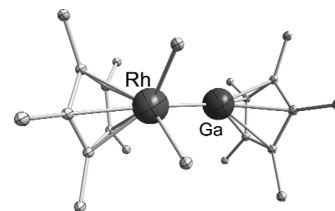
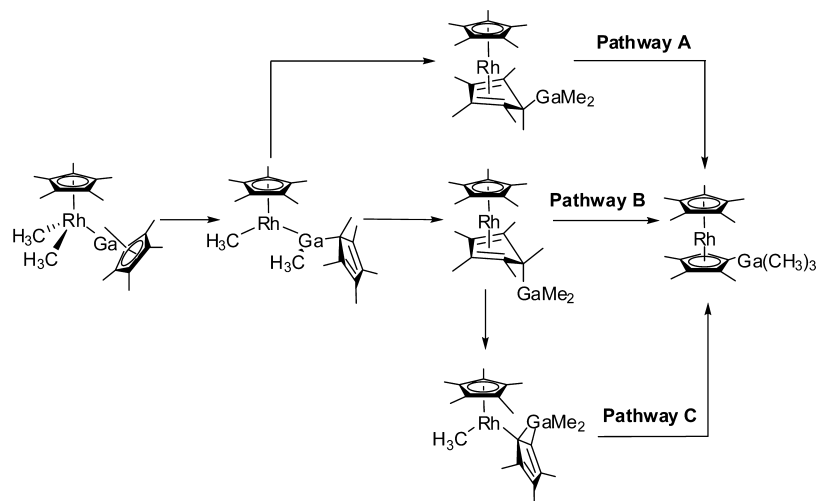
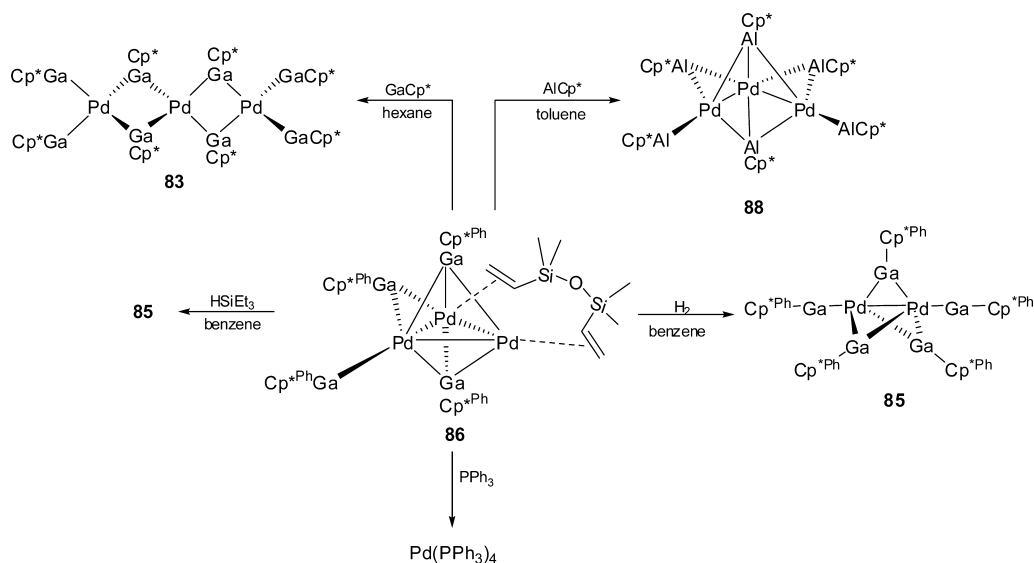


Figure 32. Molecular structure of $[\text{Cp}^*\text{Rh}(\text{GaCp}^*)(\text{CH}_3)_2]$ (**194**).

C bond activation both in solution and in solid state, to yield the zwitterionic species $[\text{Cp}^*\text{Rh}((\text{CpMe}_4)\text{Ga}(\text{CH}_3)_3)]$ (**195**). Similarly Cp^*Al also reacts with $[\text{Cp}^*\text{Rh}(\text{CH}_3)_2(\text{DMSO})]$, giving the complex $[\text{Cp}^*\text{Rh}(\text{CpMe}_4)\text{Al}(\text{CH}_3)_3]$ (**196**).

On the basis of kinetic studies by NMR spectroscopy and detailed DFT calculations, a reaction mechanism has been suggested in which the activation of a C–C bond by the main-group element Ga is assisted by the Rh center. Hence, in the first step, one molecule of DMSO or pyridine is substituted by one Cp^*Ga , leading to the formation of **194** (Figure 32). In the next step, the Rh– CH_3 groups migrate to the gallium center. In the resultant key intermediate, a unit of $\text{Cp}^*\text{Ga}(\text{CH}_3)_2$ coordinates as a neutral diene (in a η^2, η^2 -mode of coordination) to a Rh^1Cp^* fragment (Scheme 34). The actual C–C bond activation with formation of the end products originates from this key intermediate (energetically favorable, 17.4 kcal/mol). This reaction is the first example of a C–C bond activation at a main-group metal in solution under mild conditions. Both experimental and theoretical evidence led to the conclusion that the bond activation takes place at the gallium atom. However, the electronic contribution can be traced back to the cooperative effect between the electron-rich Rh atom and the electrophilic Ga center. This argument can also be applied to explain the formation of $[\text{Cp}^*\text{Ru}(\text{H})(\text{PPh}_3)(\kappa^2\text{-}(\text{C}_6\text{H}_4)\text{-PPh}_2)(\text{GaCl}_2)]$ (**151**) and $[\text{Cp}^*\text{Fe}(\mu_3\text{-H})(\kappa^2\text{-}(\text{C}_6\text{H}_4)\text{PPh}_2)(\text{AlCp}^*)(\text{AlBr}_2)]$ (**154**), because it can be assumed that the actual C–H bond-rupture process takes place directly on the acidic E^{III} center, which is created along with the insertion and Cp^* transfer reaction. Although **154** is formed from the reaction of $[\text{Fe}(\text{PPh}_3)_2\text{Br}_2]$ with Cp^*Al , the reaction with Cp^*Ga does not lead to orthometalation. This observation could be explained by the fact that, in the course of the reaction, a GaBr_2 center is

Scheme 34. Mechanism of Formation of $[\text{Cp}^*\text{Rh}((\text{CpMe}_4)\text{Ga}(\text{CH}_3)_3)]$ (195)Scheme 35. Ligand-Exchange Reactions of $[\text{Pd}_3(\text{GaCp}^*\text{Ph})(\alpha_2\text{-GaCp}^*\text{Ph})(\alpha_3\text{-GaCp}^*\text{Ph})_2(\text{dvds})]$ (86)

formed that is supposed to be less acidic than AlBr_2 . Therefore the formation of an agostic $\text{Ga}-\text{C}_6\text{H}_5$ interaction is prevented, successfully suppressing the rupture of the $\text{C}-\text{H}$ bond.¹²¹

8.2. Substitution of Cp^*E Ligands

Until now, only a little is known about substitution reactions of RE ligands by other 2e donor ligands L, because the $\text{M}-\text{E}$ bonds are relatively strong particularly when $\text{E} = \text{Al}$, Ga and also the steric hindrance rendered by RE ligands is relatively high. Therefore, the monomeric complexes $[\text{M}(\text{ECp}^*)_4]$ are sterically and electronically saturated and thus kinetically inert.⁸⁷ On the other hand, the multinuclear unsaturated complexes $[\text{M}_a(\text{ER})_b]$ ($b > a > 1$) react with a variety of ligands L (CO, phosphines, isonitriles, and also other Cp^*E , i.e., Cp^*Al), to yield bi- and trinuclear substitution products.⁹² In good agreement with quantum-chemical calculations, which prove that the substitution of Cp^*Ga or Cp^*In with Cp^*Al is thermodynamically favored for the homoleptic complexes,⁴⁵ the reactions of $[\text{M}_2(\text{GaCp}^*)_2(\mu_2\text{-GaCp}^*)_3]$ ($\text{M} = \text{Pt}$ (79), Pd (82)) with Cp^*Al yield the trimetallic compound $[\text{Pt}_2(\text{GaCp}^*)_2(\mu_2\text{-AlCp}^*)_3]$ (197) and the product of the complete substitution $[\text{Pd}_2(\text{AlCp}^*)_2(\mu_2\text{-AlCp}^*)_3]$ (198), re-

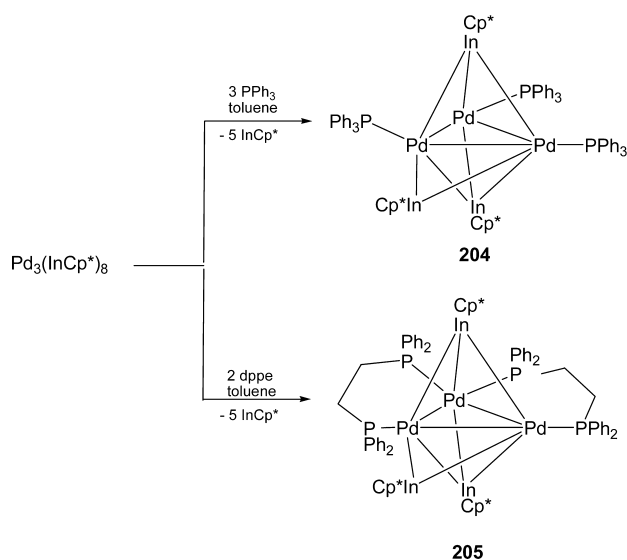
spectively (see Scheme 11). Additionally, the substitution reaction of $[\text{Pd}_3(\text{GaCp}^*\text{Ph})(\mu_2\text{-GaCp}^*\text{Ph})(\mu_3\text{-GaCp}^*\text{Ph})_2(\text{dvds})]$ (86), with the relatively less bulky Cp^*Ga , leads to the formation of the trinuclear species $[\text{Pd}_3(\text{GaCp}^*)_4(\mu_2\text{-GaCp}^*)_4]$ (83). This product can also be obtained by the direct reaction of $[\text{Pd}_2(\text{dvds})_3]$ with Cp^*Ga . Similarly, $[\text{Pd}_3(\text{AlCp}^*)_2(\mu_2\text{-AlCp}^*)_2(\mu_3\text{-AlCp}^*)_2]$ (88) is obtained from the reaction of 86 with Cp^*Al (Scheme 35).³⁰

The reaction of $[\text{M}_2(\text{GaCp}^*)_2(\mu_2\text{-GaCp}^*)_3]$ ($\text{M} = \text{Pt}$ (79), Pd (82)) with PPh_3 yields the mono- and disubstituted complexes $[\text{MPT}(\text{GaCp}^*)(\text{PPh}_3)(\mu_2\text{-GaCp}^*)_3]$ ($\text{M} = \text{Pt}$ (199), Pd (200)) and $[\text{Pd}_2(\text{PPh}_3)_2(\mu_2\text{-GaCp}^*)_3]$ (201), with the complete preservation of the central metallic core. Because of the fluxional behavior in solution, which permits the exchange of the terminal and bridging ligands, a dissociative mechanism of the bridging ligands is considered plausible, so that an unsaturated metallic core is generated as the intermediate. However, the reaction of 86 with PPh_3 proceeds with the complete substitution of both $[\text{Ga}(\text{C}_5\text{Me}_4\text{Ph})]$ and olefin ligands, yielding $[\text{Pd}(\text{PPh}_3)_4]$.³⁰ In contrast to the reactions of the complexes $[\text{M}_2(\text{GaCp}^*)_2(\mu_2\text{-GaCp}^*)_3]$ ($\text{M} = \text{Pt}$ (79), Pd

(82) with PR_3 ($\text{R} = \text{Me}, \text{Ph}$), the analogous reactions with the chelating phosphane-ligand dppe (dppe = bis(diphenylphosphinoethane)) yield the monomeric complexes $[\text{M}(\text{dppe})_2]$ ($\text{M} = \text{Pd}, \text{Pt}$), by complete substitution of the Cp^*Ga units. The reaction of $[\text{Pt}_2(\text{GaCp}^*)_2(\mu_2\text{-GaCp}^*)_3]$ (79) with strong π -acceptors like CN^tBu and CO yields the doubly substituted products $[\text{Pt}_2(\text{CN}^t\text{Bu})_2(\mu_2\text{-GaCp}^*)_3]$ (202) and $[\text{Pt}_2(\text{CO})_2(\mu_2\text{-GaCp}^*)_3]$ (203), in which the Cp^*Ga units remain on the bridging positions.

Although the molecular structure in all substitution reactions of the binuclear complexes $[\text{M}_2(\text{GaCp}^*)_2(\mu_2\text{-GaCp}^*)_3]$ ($\text{M} = \text{Pt}$ (79), Pd (82)) is preserved, the reaction of $[\text{Pd}_3(\text{InCp}^*)_4(\mu_2\text{-InCp}^*)_4]$ (87)⁹³ with the phosphane ligands PPh_3 and dppe proceeds with a rearrangement of the linear Pd_3 core. Thus, the triangular Pd_3 clusters $[\text{Pd}_3(\mu_3\text{-InCp}^*)_2(\mu_2\text{-InCp}^*)(\text{PPh}_3)_3]$ (204) and $[\text{Pd}_3(\mu_3\text{-InCp}^*)_2(\mu_2\text{-InCp}^*)(\text{dppe})_2]$ (205) are formed (Scheme 36). In both cases, a

Scheme 36. Synthesis of $[\text{Pd}_3(\mu_3\text{-InCp}^*)_2(\mu_2\text{-InCp}^*)(\text{PPh}_3)_3]$ (204) and $[\text{Pd}_3(\mu_3\text{-InCp}^*)_2(\mu_2\text{-InCp}^*)(\text{dppe})_2]$ (205)



trigonal-bipyramidal polyhedron is formed, in which two Cp^*In fragments lie above and below the triangular plane defined by the three Pd atoms. An additional Cp^*In ligand occupies a bridging position in the same Pd_3 plane, along with the terminal phosphane ligands.

8.3. Exchange of the Two-Electron Ligands Cp^*E against One-Electron Ligands MR^{\cdot}

Very recently, homoleptic transition-metal complexes of Cp^*Ga (and Cp^*Al) have been successfully used as starting materials to obtain highly coordinated transition-metal–zinc cluster compounds, which represents a novel strategy to link the molecular organometallic chemistry with the synthesis of solid-state intermetallic Hume–Rothery phases.^{145,146} Considering the soft and flexible binding properties of the Cp^* substituents and the inherent reducing power of the RGa^{I} compound, $[\text{L}_m\text{M}(\text{GaCp}^*)_n]$ complexes were treated with ZnR_2 ($\text{L} = \text{CO}$ and/or all hydrocarbon ligands; $\text{R} = \text{Me}, \text{Et}$). Thus, reaction of the transition-metal precursors $[\text{Mo}(\text{GaCp}^*)_6]$ (78), $[(\text{Cp}^*\text{Ga})_4(\text{H})\text{Ru}(\mu_2\text{-Ga})\text{Ru}(\text{H})_2(\text{GaCp}^*)_3]$ (157)¹²⁷ or $[\text{Ru}(\text{GaCp}^*)_6\text{Cl}_2]$ (150),¹²¹ $[(\text{Cp}^*\text{Ga})_4\text{Rh}(\text{Ga}(\eta^1\text{-Cp}^*)(\text{CH}_3))]$ (155),¹²² and $[\text{M}(\text{GaCp}^*)_4]$ ($\text{M} = \text{Ni}$ (73), Pt

(74), Pd (81))⁸⁹ with excess of ZnMe_2 or ZnEt_2 in toluene solution at temperatures of 80–110 °C afforded selectively compounds 206–217 with general formula $[\text{M}(\text{ZnR})_n]$ ($n = 8\text{--}12$; $\text{M} = \text{Mo}, \text{Ru}, \text{Rh}, \text{Ni}, \text{Pd}, \text{Pt}$; $\text{R} = \text{CH}_3, \text{Cp}^*$) in good yields (Figure 33). It is instructive to note that parallel to $\text{Ga}/$

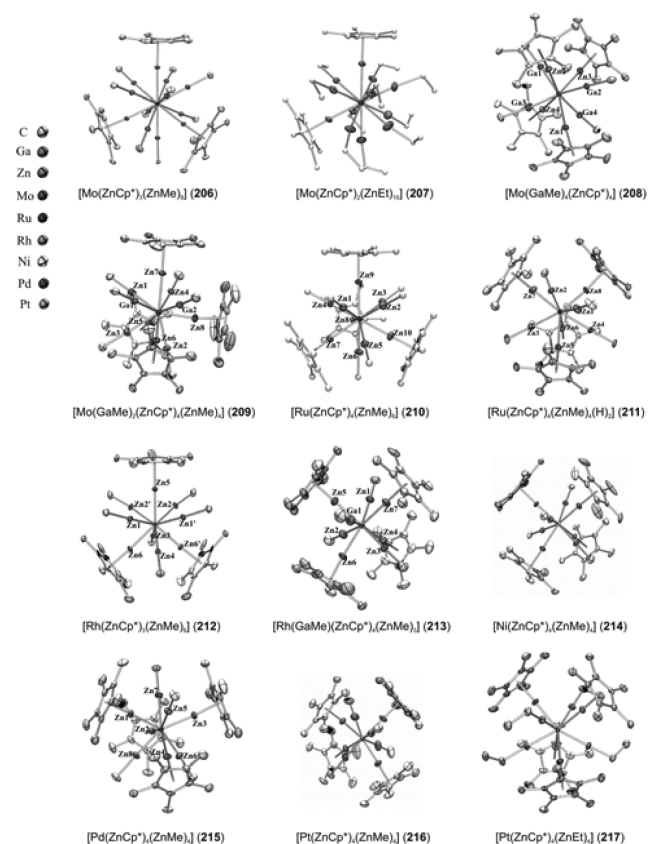
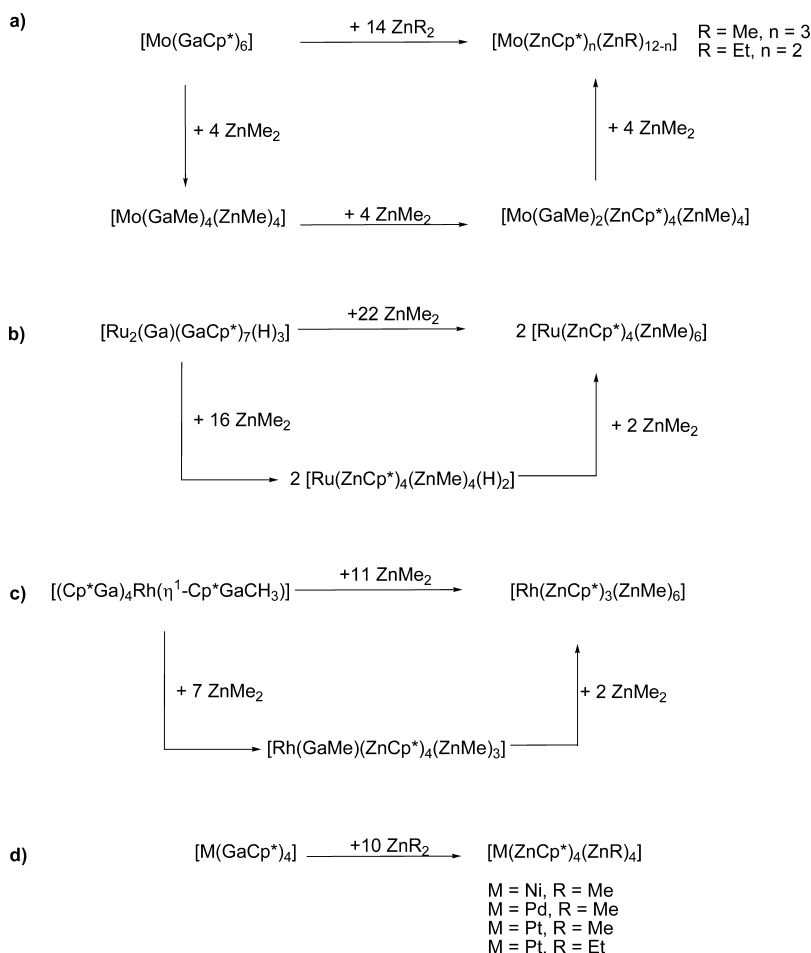


Figure 33. Molecular structures of 206–217.¹⁴⁶ Reprinted and adapted with permission from ref 146. Copyright 2009 American Chemical Society.

Zn substitution, exchange of the R substituents takes place, leading to transfer of the Cp^* group from gallium to zinc. The resulting monovalent zinc fragments, ZnMe , ZnEt , and ZnCp^* , are efficiently trapped by coordination to a transition-metal center. Hence, the formal substitution of one RGa ligand always leads to two ZnR ligands attached to the transition-metal center. If ZnR groups are considered as one-electron ligands and the RGa groups are considered as two-electron ligands, it can be concluded that all compounds 206–217 fulfill the formal 18-electron rule at the central metal.¹⁴⁷ The number of gallium ligands present in the starting material limits the total number of Zn ligands in the complexes. Thus, treatment of the precursors $[\text{M}(\text{GaCp}^*)_n]$ with an excess larger than $2n$ equiv of ZnR_2 leads to the pseudohomoleptic compounds $[\text{M}(\text{ZnCp}^*)_a(\text{ZnR})_b]$ ($a + b = 2n$) (Scheme 37). The syntheses of 206–217 involve (formal) reduction of Zn^{II} to Zn^{I} with the concomitant oxidation of Ga^{I} to Ga^{III} . The corresponding byproduct Me_2GaCp^* and GaMe_3 were observed by spectroscopic methods. Thus, the driving force of the reaction is certainly related to the facile oxidation of Ga^{I} to Ga^{III} , combined with the very similar electronic and steric properties of the monovalent RGa and ZnR ligands at a given transition-metal center. These results should be seen in light of the recent discovery of Zn^{I} compounds of the type $[\text{RZn}^{\text{I}}\text{--ZnR}]$ ($\text{R} =$

Scheme 37. Synthesis of the Compounds $[M(\text{ZnCp}^*)_a(\text{ZnR})_b]$ ($a + b = 2n$)¹⁴⁶ (Reprinted and Adapted with Permission from Ref 146. Copyright 2009 American Chemical Society.)



Cp*, DDP, etc.), and along with the similar electronegativities and covalent radii for Zn and Ga, a rich chemistry of organometallic Zn^I species is suggested, similar to the Ga^I analogues.^{90a,148,149} We discussed these similarities and in particular the bonding properties of the respective complexes in another recent review and will therefore keep our summary short herein.⁵³ The molecular structures (Figure 33) of compounds 206–217 correspond to typical deltahedral coordination polyhedra, namely, icosahedron, bicapped square antiprism, capped square antiprism, and dodecahedron, in accordance with a straightforward deduction from the VSEPR (valence shell electron pair repulsion) concept. The question of the assignment of oxidation states for these compounds is not easy to answer and has been addressed in detail in a previous review.⁵⁴

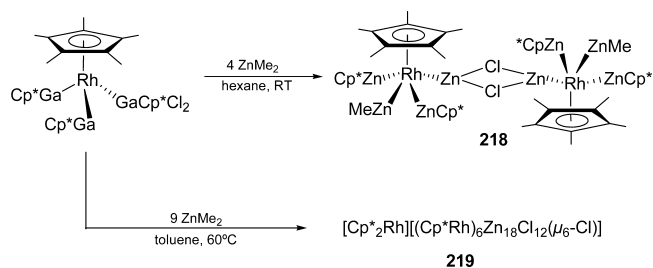
Because the Cp* and the alkyl substituents R at gallium and zinc centers are known to be fluxional and/or transferable,^{122,139} a larger excess of ZnR₂ (R = Me or Et) is likely to allow for the formation of truly homoleptic compounds of the type $[M(\text{ZnR})_n]$ in case of a quantitative exchange of Cp* by R. The bonding analysis at the DFT level of theory of some prototypes, e.g., the icosahedral $[\text{Mo}(\text{ZnCp}^*)_3(\text{ZnMe})_9]$ (206) and the singly capped square antiprismatic $[\text{Rh}(\text{ZnCp}^*)_3(\text{ZnMe})_6]$ (212), as well as the coordination geometry of these kind of highly coordinated compounds suggested these compounds should be considered as novel links between mixed metal complexes and clusters on the one hand

and the respective solid-state intermetallic phases, i.e., Hume–Rothery-type alloys, on the other side.^{90a,145} Experimental and theoretical studies suggest that the reaction principle can be extended to other monovalent (one electron donor) ligands MR' being isolobal to the RZn^I units (M = Cd, Hg, and Mg and R' = alkyl, aryl; M = Au and R' = PMe₃, PPh₃, etc.).¹⁵⁰

Very recently, using similar synthetic protocols, the syntheses of two unusual compounds, $[\text{Cp}^*\text{Rh}(\text{ZnCp}^*)_2(\text{ZnMe})(\text{ZnCl})_2]$ (218) and $[\text{Cp}^*_2\text{Rh}][(\text{Cp}^*\text{Rh})_6\text{Zn}_{18}\text{Cl}_{12}(\mu_6\text{-Cl})]$ (219), have been reported (Scheme 38).¹⁵¹

These derivatives exhibit closed-shell 18-electron square-pyramidal Cp*RhZn₄ building units and were obtained by combined Ga/Zn, Me/Cp*, and Me/Cl exchange upon treatment of $[\text{Cp}^*\text{Rh}(\text{GaCp}^*)_2(\text{GaCp}^*\text{Cl}_2)]$ (136) with

Scheme 38. Synthesis of $[\text{Cp}^*\text{Rh}(\text{ZnCp}^*)_2(\text{ZnMe})(\text{ZnCl})_2]$ (218) and $[\text{Cp}^*_2\text{Rh}][(\text{Cp}^*\text{Rh})_6\text{Zn}_{18}\text{Cl}_{12}(\mu_6\text{-Cl})]$ (219)



ZnMe₂. The molecular structure of [Cp*₂Rh(ZnCp*)₂(ZnMe)(ZnCl)]₂ (218) (Figure 34) consists of two nearly square-

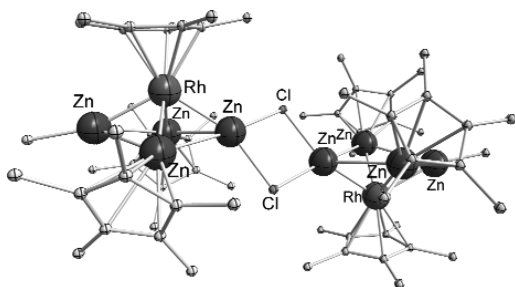


Figure 34. Molecular structure of [Cp*₂Rh(ZnCp*)₂(ZnMe)(ZnCl)]₂ (218).

pyramidal Cp*₂Rh(ZnR)₄ units (R = (μ₂-Cl), Cp*, and Me), which are combined via a planar, bridging Zn(μ-Cl)₂Zn moiety. The unit [Cp*₂Rh(ZnR)₄] is formally derived from [Cp*₂Rh-(GaCp*)₂] by the Ga/Zn and Cp*/R (R = Cl, Me) exchange discussed previously.

Compound [Rh(Cp*₂)₂][(Cp*₂Rh)₆Zn₁₈Cl₁₂(μ₆-Cl)] (219) has been obtained selectively when 9 equiv of ZnMe₂ were used and the reaction mixture was gently heated. The anionic part of 219 is built around a central Zn₆ octahedron, which hosts an interstitial anion Cl_i⁻. The respective Zn-Cl_i distances (2.733(2) and 2.813(2) Å) are significantly longer than the rest of the Zn-Cl_t contacts (average 2.167 Å) and are thus regarded as almost nonbonding. Six terminal ZnCl_t moieties are capping six faces of the central octahedron, while the remaining two opposite faces are bridged by three Cl ligands (average 2.405 Å). Together with the interstitial Cl atom, these Cl atoms form two corner-sharing tetrahedra within an overall cubelike structure. Another six Zn atoms, bearing no Cl atoms, are bridging the terminal ZnCl_t units. The Cp*₂RhZn₄ building units in 219 appear to be interconnected by linear Rh-Zn-Rh bonds in addition to the Zn-Cl-Zn bridges. On the basis of the theoretical bonding analysis of [M(ZnR)_n] species, all Zn...Zn contacts are likely to be only very weakly attractive, whereas the Rh-Zn interactions might be regarded as strong covalent bonds.

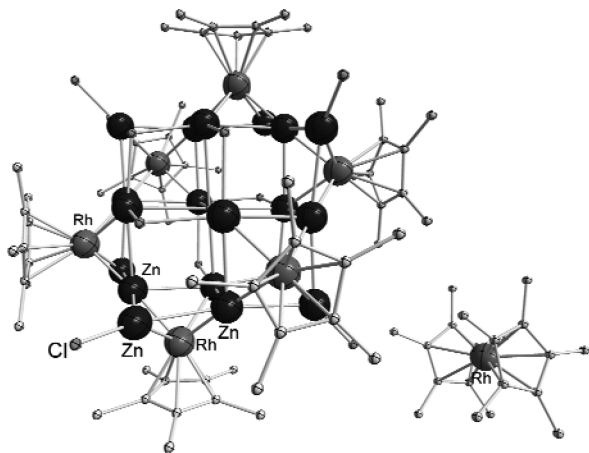


Figure 35. Molecular structure of [Rh(Cp*₂)₂][(Cp*₂Rh)₆Zn₁₈Cl₁₂(μ₆-Cl)] (219).

9. PRECURSOR CHEMICAL NANOMETALLURGY: FROM FUNDAMENTALS TO APPLICATIONS

This section of the review intends to present a perspective of potential applications of some aspects of the above-discussed fundamental chemistry between transition metals M and metals of group 13. However, it will not provide a full coverage of the respective materials chemistry literature. Rather it will present selected examples and suggest directions of further research based on this discussion.

Early work on the use of volatile (sublimable) transition-metal-substituted alanes, gallanes, and indanes of the general formula [L_nM]_{3-a}ER_a(Do)_b (E = Al, Ga, In; L = CO, Cp; Do = neutral O, N atom Lewis base donor, e.g., alkyl amine, ether with a = 0–3 and b = 0–2) were connected with the concepts of metallorganic chemical vapor deposition (MOCVD) and aimed at the deposition of single-phased intermetallic thin films such as β-CoGa, ε-NiIn, PtGa₂, etc.^{152,153} At that time, in the early 1990s, such kind of thin-film materials were discussed as thermodynamically stable gate metallizations and Schottky Barriers for III/V compound semiconductors (i.e., GaAs, InP) allowing the fabrication of atomically abrupt interfaces between the intermetallic phase and the semiconductor.¹⁵⁴ Seen from a more general point of view of molecular (single-source) precursor chemistry, there are, however, limitations associated with this family of precursors [L_nM]_{3-a}ER_a(Do)_b for respective M/E intermetallic materials, because they do not allow straightforward access to group 13 metal-rich phases. This is clearly different for the prototypical compounds of formula [M_a(ECp*)_b] (b > a) being primarily reviewed in this article. Nevertheless, none of these latter compounds can be transported in the gas phase without significant undesired decomposition, and this rules out use in conventional MOCVD. However, the chemistry outlined in the above sections and in particular the soft and flexible binding modes of the Cp* protecting substituent can be regarded as a solid basis for systematic investigation of the still largely unexplored precursor chemistry of [M_a(ECp*)_b]-type compounds to derive the respective M/E intermetallic nanomaterials by employing nonaqueous solution chemical routes. In general, there are only very limited studies on alloy and intermetallic nanoparticles containing metals such as Al, Ga, Zn, etc., of which components are not easily accessible by reduction of salts and other precursors by chemical means in organic solvents (including ionic liquids).¹⁵⁵ A more recent review article in this journal by Ferrando et al. entitled “Nanoalloys: From Theory to Applications of Alloy Clusters and Nanoparticles” should be particularly quoted here. In its section 5.5, this article summarizes the knowledge on transition-metal main-group-metal nanoparticles (emphasizing Ni/Al, Cu/Zn, and Cu,Ag,Au/main-group metal).¹⁵⁶ Herein, we now will discuss a few cases that directly relate to the previously outlined molecular chemistry.

Typically, substitution-labile (ideally “all-hydrocarbon” ligand-substituted) and reactive transition-metal compounds are combined in inert solvents with Cp*₂E in the presence of hydrogen to achieve complete hydrogenolytic cleavage of all the ancillary ligands from both metal centers M and E (compare with sections 4.1.5, 7.3, and 9). A first instructive example is the soft chemical synthesis of Ni_{1-x}Al_x nanoparticles (0.09 ≤ x ≤ 0.50) by cohydrogenolysis of [Ni(cod)₂] with Cp*₂Al. The treatment of equimolar amounts of the two precursors in mesitylene solution under 3 bar of H₂ at 150 °C

resulted in formation of a colloidal solution of intermetallic β -NiAl particles, characterized by transmission electron microscopy/energy-dispersive X-ray analysis (TEM/EDX) and powder X-ray diffraction (PXRD). These β -NiAl colloids were treated postsynthetically with 1-adamantanecarboxylic acid (ACA) as a surface-capping group, giving nearly monodisperse α -NiAl colloids that were stable under argon at room temperature for weeks (Figure 36).¹²⁶

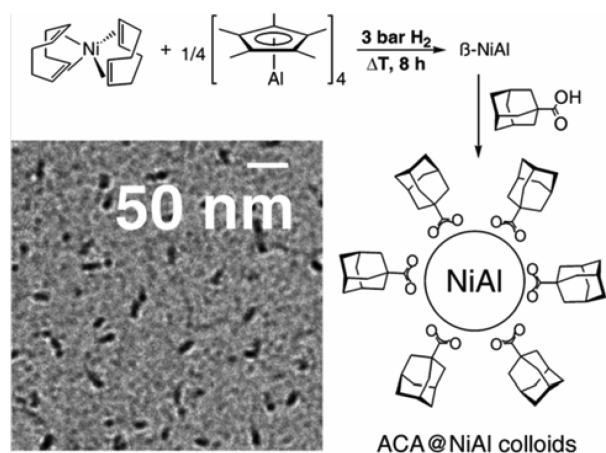


Figure 36. Preparation of adamantanecarboxylic acid (ACA)-stabilized NiAl nanoparticles (see TEM image) by cohydrogenolysis of $[\text{Ni}(\text{cod})_2]$ with $[(\text{Cp}^*\text{Al})_4]$ in mesitylene.¹²⁶ Reprinted with permission from ref 126. Copyright 2007 American Chemical Society.

Similarly, nano brass colloids were obtained by cohydrogenolysis of $[\text{CpCu}(\text{PMe}_3)]$ and $[\text{ZnCp}^*_2]$ at similar conditions as for the Ni/Al case. Deep red to violet colloids of α/β -CuZn nanoparticles were stabilized in the presence of poly(2,6-dimethyl-1,4-phenylene oxide) (PPO) as surfactant. The presence and alloying of Cu and Zn in the β -CuZn sample as a representative example of the series was confirmed by extended X-ray absorption fine structure spectroscopy (EXAFS). In particular, the oxidation behavior of the alloyed nanoparticles was investigated by EXAFS, PXRD, and UV-vis spectroscopy, indicating that the nano brass particles showed preferential oxidation of the Zn component, which results in core-shell particles of the type $(\text{ZnO})_\delta @ \text{Cu}_{1-x}\text{Zn}_{x-\delta}$.¹²⁴ This specific feature of preferential oxidation of the more electro-positive part of the alloy nanoparticles can be used to protect the as-synthesized nanoparticles against further oxidation. The magnetic properties of β -CoAl alloy nanoparticles derived from cohydrogenolysis of $[\text{Co}(\eta^4\text{-C}_8\text{H}_{12})(\eta^3\text{-C}_8\text{H}_{13})]$ and Cp^*Al in mesitylene were studied in dependence of the surface structure. These nanoparticles (NPs) were very air-sensitive, giving rise to a fast aluminum segregation upon exposure to air and development of an alumina shell similar to the Ni/Al and Cu/Zn cases. This leads to a strong enhancement of the magnetization of the NPs as a result of the formation of an aluminum-depleted cobalt core (Figure 37).¹⁵⁷

These few examples may illustrate the concept of using the knowledge obtained from the fundamental study of synthesis, structure, and reactivity of transition-metal compounds bearing the carbenoid group 13 metal ligands Cp^*E for soft chemical synthesis of M/E alloyed and intermetallic nanomaterials. This also includes the related materials involving Zn (and Cd, etc.). In fact, a whole range of intermetallic phases known as Hume-Rothery phases,¹⁵⁸ which are formed between the (late)

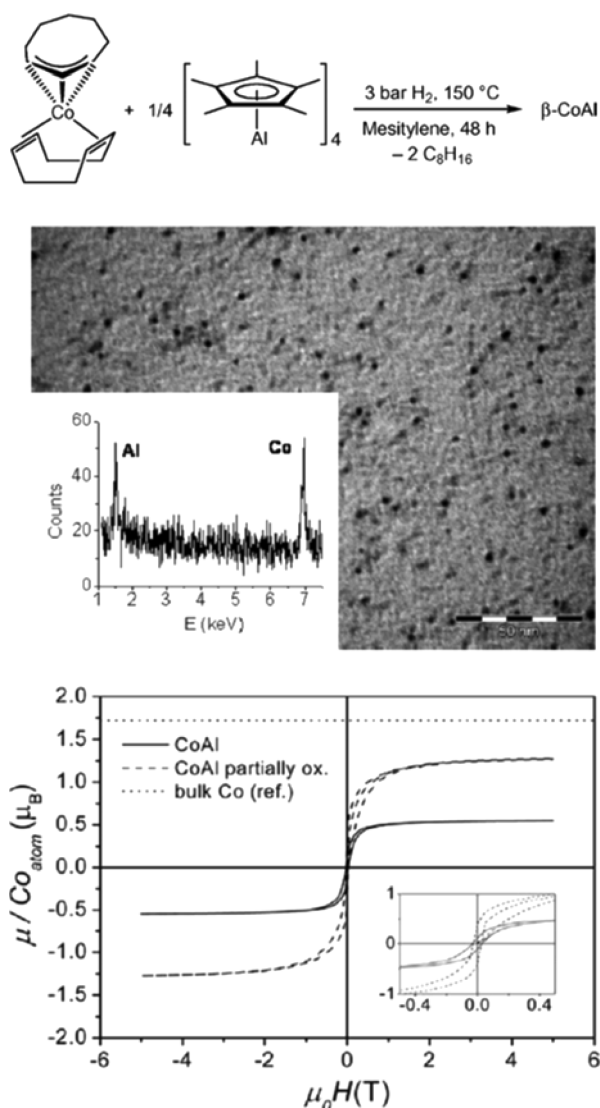


Figure 37. Organometallic synthesis of β -CoAl nanoparticles, TEM (dimensions bar = 50 nm) image and EDX analysis and magnetization cycles recorded at 2 K on CoAl NPs; inset, enlargement displaying the coercive field (dotted line, partially oxidized CoAl; solid line, CoAl).¹⁵⁷ Reproduced by permission from ref 157. Copyright 2010 John Wiley and Sons.

transition metals (A2) and the main-group metals (B1, i.e., Zn, Cd, Hg; Al, Ga, In, Tl; Sn, Pb), may be accessible as nanomaterials by using and further developing the chemistry described in this review. Besides unusual physical properties involving composition, size, and shape dependencies (e.g., for use in plasmonics), applications of M/E nanoparticles in catalysis may be particularly interesting. For example, the binary, stoichiometric PtZn intermetallic (nano) phase has been shown to be very effective for the chemoselective hydrogenation of crotonaldehyde.¹⁵⁹ Noble-metal catalysts based on Pd, Pt, Au, etc. often involve the modification of the active metal by a second metal, e.g., Sn, to increase selectivity.¹⁶⁰ Depending on the catalyst preparation method employed, the resulting noble-metal-based catalyst may contain (a) an auxiliary phase of a metal oxide that exerts a synergistic SMSI effect (strong metal support interaction) and (b) surface alloys or intermetallic compounds or (c) a mixture of (a) and (b).¹⁶¹ For instance, this latter case (c) is true for Cu/ZnO

biphase nanocatalysts that were discovered by exploring the potential of the nano brass materials mentioned previously for application in liquid-phase methanol synthesis from CO and H₂.^{162,163}

In the case of the single-phase intermetallic PtZn catalyst, interestingly enough, the authors have ruled out any contribution of ZnO components and SMSI effects but have attributed the activity and selectivity to an intrinsic feature of the intermetallic compound itself. Similar observations were made for PdGa and Pd₃Ga₇ materials obtained by ball milling as catalysts for the selective hydrogenation of acetylene. The gallium oxide layer introduced during the milling procedure was removed from the particle surface by etching and washing with ammonia. Compared to reference catalysts, the Pd/Ga catalysts exhibited a similar activity per surface area but higher selectivity and stability.¹⁶⁴ The superior catalytic properties are attributed to the isolation of active Pd sites in the crystallographic structure of PdGa and Pd₃Ga₇ according to the so-called active-site isolation concept, which involves geometric, steric, and electronic effects of alloy (nano) catalysts.¹⁶⁵ In addition to M/E nanoparticles, molecular-size M/E clusters may also be quite interesting for catalysis. The activity and selectivity of (Pt/Ga)@ZSM-5 (ZSM-5, Zeolite Socony Mobil-5) in the aromatization of ethane was studied.¹⁶⁶ Pt/Ga clusters localized inside the zeolite channels were observed after high-temperature treatment of a mixture of platinum-containing zeolites with gallium oxides. The interaction of gallium with the H-form of ZSM-5 zeolites was shown to result in the formation of cationic centers containing reduced single-charged gallium cation, i.e., Ga⁺ (note the connection to the coordination chemistry of substituent-free, “naked” Ga⁺ discussed in sections 6 and 7).

10. CONCLUSIONS AND PERSPECTIVES

The main goal of this review was a comprehensive treatment of synthesis, structure, and reactive properties of metal complexes of RE^I ligands of aluminum, gallium, and indium with special emphasis on R = Cp*, although it turns out that the coordination chemistry of Cp*Al and Cp*Ga is far more developed than the corresponding chemistry of Cp*In or any other RIn^I ligand (Table 2). Many aspects of the coordination chemistry of Cp*E ligands are similar to the respective complexes being formed with *N,N* chelating substituents, which has been reviewed recently by Asay et al.⁷ However, the steric bulk of Cp* is less and the binding properties are more flexible, which favors a rich chemistry of compounds of the general formula [M_a(ECp*)_b] including the unique option to use Cp* as a removable “protecting” group of the mixed M_aE_b core structures. This feature links the fundamental work on the coordination chemistry of Cp*E at metal centers with the quite different world of intermetallic solid-state compounds and the respective nanomaterials.

The selected examples discussed in section 9 may have put the otherwise quite exotic coordination chemistry of carbenoid group 13 compounds ER and the related chemistry of monovalent ZnR species at transition-metal centers into a potentially fruitful context, which may stimulate further research. Smoothly removable, all-hydrocarbon substituents R, in particular Cp*, seem to be the key to success in this area. Certainly, if only soft-chemical synthesis of intermetallic M/E phases from labile metal–organic precursors is the target, a simpler access may be possible and the need of using sophisticated metal-rich molecules as precursors, which are in part difficult to synthesize, will not be necessary. For example,

Table 2. Structurally Well-Characterized RIn^I Complexes

complex	ref
Cp*In complexes	
[Cp*In–Al(^t Bu) ₃] (36)	71
[Cp*In–Ga(^t Bu) ₃] (37)	71
[Cr(CO) ₅ (InCp*)] (61)	82
[Pd ₃ (InCp*) ₄ (μ ₂ -InCp*) ₄] (87)	93
[(dcpe)Pt(InCp*) ₂] (113)	106
[Cp*Rh(eta-1-Cp*InCl)(Cp*In)(eta-3-Cp*In(μ-Cl))] (137)	118
[Cp* ₂ Rh][Cp*Rh(InCp*){In ₂ Cl ₄ (μ-κ ₂ -Cp*)}] (139)	120
[Cp*Ru(InCp*)((μ-Cl)(eta-3-InCp*) ₂)] (145)	119
[Pd ₃ (μ ₂ -InCp*)(μ ₃ -InCp*) ₂ (PPh ₃) ₃] (204)	92
[Pd ₃ (dppe) ₂ (μ ₂ -InCp*)(μ ₃ -InCp*)] (205)	92
In(C(SiMe ₃) ₃) complexes	
[(CpNi(CO)) ₂ {μ-In(C(SiMe ₃) ₃)}] (35)	85
[Mn ₂ (CO) ₈ (μ ₂ -In{C(SiMe ₃) ₃ })] (39)	74
[Co ₂ (CO) ₆ (μ-CO){μ ₂ -In(C(SiMe ₃) ₃)}] (40)	75
[Co ₂ (CO) ₆ {μ ₂ -(In(C(SiMe ₃) ₃)) ₂ }] (41)	75
[Fe ₂ (CO) ₆ {μ ₂ -In(C(SiMe ₃) ₃)} ₃] (58)	80
[(CpNi) ₂ (μ-InC(SiMe ₃) ₃)] (71)	85
[Ni{In(C(SiMe ₃) ₃) ₄ }] (76)	86
[Pt{In(C(SiMe ₃) ₃) ₄ }] (77)	88
[Pd{In(C(SiMe ₃) ₃) ₄ }] (125)	89
[Cp*Rh][{In(C(SiMe ₃) ₃) ₃ (μ ₂ -Cl) ₂ }] (138)	118
[Cp*Ru{In(C(SiMe ₃) ₃) ₃ }{(μ-Cl)(In(C(SiMe ₃) ₃)) ₂ }] (146)	119
In(2,6-Trip ₂ C ₆ H ₃) complexes	
[Cp ₂ Hf–In(2,6-Trip ₂ C ₆ H ₃)] (32)	114
[CpMn(CO) ₂ In(2,6-Trip ₂ C ₆ H ₃)] (66)	34
[Cp ₂ Ti–In(2,6-Trip ₂ C ₆ H ₃)] (128)	113
[Cp ₂ Zr–In(2,6-Trip ₂ C ₆ H ₃)] (130)	113

phase-pure, polycrystalline θ-CuE₂ powder materials can be derived simply by combining [CuMes]₅ (Mes = 1,3,5 trimethylphenyl = mesityl) with H₃EL (E = Al, Ga; L = NR₃) under hydrogen pressure in refluxing mesitylene.¹²⁵ However, if molecular control over the composition of very small intermetallic nanoparticles or larger molecular clusters is targeted, we think that some of the metal-rich molecules presented in this review may offer unique possibilities as well-defined, single-source precursors.

Last but not least, ternary Hume–Rothery-like intermetallic clusters and nanoparticles represent a virtually virgin field of research. However, data from theory suggest a significant dependence of properties on composition and structure.¹⁶⁷ For example, alloy nanoclusters like (Ni,Co)–Mn–Ga are of current interest for recording media and actuators involving the magnetic shape memory effect, respectively.¹⁶⁸ Also trimetallic nanoclusters are of special interest for catalysis because the third element can be used to achieve higher catalytic and selective properties compared to the corresponding monometallic and bimetallic clusters. Interestingly, it is difficult to synthesize binary clusters Fe–Pt and Co–Pt below a critical size, because the L12 structure with its technologically relevant high magnetocrystalline anisotropy is difficult to stabilize. For trimetallic systems, however, like the Heusler alloy Ni–Mn–Ga, the rather versatile properties of the bulk material can be used to achieve shape changes or magneto-caloric effects (depending on the composition) also in nanoclusters. With this review we therefore like to suggest novel molecular approaches to compositionally and structurally defined clusters and nanoparticles of binary M/E, ternary M/M'/E, and even multinary systems as interesting and

challenging topics for future research linking molecular organometallic chemistry with intermetallics.

AUTHOR INFORMATION

Corresponding Author

*E-mail: roland.fischer@rub.de.

Notes

The authors declare no competing financial interest.

Biographies



Sandra González-Gallardo studied Chemistry at the National University of Mexico, where she developed her doctoral research under the supervision of Prof. Mónica Moya-Cabrera. After receiving her Ph.D. in 2008, she was awarded a DAAD Research Grant for Postdoctoral Studies at the Ruhr-Universität Bochum, in the research group of Prof. Dr. Roland A. Fischer. Since 2010, she is a research assistant at the Karlsruhe Institute of Technology, with Prof. Dr. Frank Breher. Her research interests focus on main group chemistry and the synthesis of multimetallic complexes stabilized by ligands featuring dual functionality.



Timo Bollermann studied Chemistry at the Ruhr-Universität Bochum, where he received his B.Sc. in 2006 and his M.Sc. in 2008. In 2011 he received his Ph.D. under the supervision of Prof. Dr. Roland A. Fischer, supported by the Ruhr University Research School and by a fellowship from the German Chemical Industry Fund. His research interests focus on the coordination chemistry of low-valent group 12/13 metals and the formation of metal-rich molecules.



Roland A. Fischer studied chemistry at the Technische Universität München (TUM) and received his Ph.D. in 1989 under the guidance of Wolfgang A. Herrmann. After a postdoctoral collaboration with Herb D. Kaesz at the University of California, Los Angeles (UCLA), he returned to TUM in 1990, where he obtained his Habilitation in 1995. In 1996 he was appointed Associate Prof. at the Ruprecht-Karls Universität in Heidelberg. In 1998 he moved to the Ruhr-Universität Bochum where he took the chair in Inorganic Chemistry II. He was Dean of the Ruhr University Research School (2006–2009). His research interests focus on group 13/transition-metal compounds, precursor chemistry for inorganic materials, chemical vapour deposition (CVD), thin films, nanoparticles, colloids, and the supramolecular host guest chemistry of porous coordination polymers (MOFs).



Ramaswamy Murugavel received his BSc and MSc degrees from University of Madras and his Ph.D. from Indian Institute of Science. He carried out postdoctoral research in Göttingen and subsequently joined IIT—Bombay as an Assistant Professor in December 1997, where he is a Full Professor since 2005. He has been a DFG Mercator Professor in Ruhr-Universität-Bochum during 2009–2010. Murugavel's research focus is in the area of synthetic organometallic and main group chemistry applied to materials science and catalysis including the rational design of porous solids. He is a Fellow of Indian Academy of Sciences.

REFERENCES

- (1) (a) Arduengo, A. J. *Acc. Chem. Res.* **1999**, *32*, 913. (b) Bourissou, D.; Guerret, O.; Gabbai, F. P.; Bertrand, G. *Chem. Rev.* **2000**, *100*, 39. (c) Hahn, F. E. *Angew. Chem., Int. Ed.* **2006**, *45*, 1348. (d) Hahn, F. E.; Jahnke, M. C. *Angew. Chem., Int. Ed.* **2008**, *47*, 3122. (e) Alder, R. W.; Blake, M. E.; Chaker, L.; Harvey, J. N.; Paolini, F.; Schütz, J. *Angew. Chem., Int. Ed.* **2004**, *43*, 5896. (f) Canac, Y.; Soleilhavoup, M.; Conejero, S.; Bertrand, G. *J. Organomet. Chem.* **2004**, *689*, 3857. (g) Kirmse, W. *Angew. Chem., Int. Ed.* **2004**, *43*, 1767.

- (2) Dohmeier, C.; Loos, C.; Schnöckel, H. *Angew. Chem., Int. Ed.* **1996**, *35*, 129.
- (3) Rao, M. N. S.; Roesky, H. W.; Anantharaman, G. *J. Organomet. Chem.* **2002**, *646*, 4.
- (4) Asay, M.; Jones, C.; Driess, M. *Chem. Rev.* **2011**, *111*, 354.
- (5) Roesky, H. W. *Inorg. Chem.* **2004**, *43*, 7284.
- (6) Roesky, H. W.; Kumar, S. S. *Chem. Commun.* **2005**, 4027.
- (7) (a) Fischer, R. A.; Weiss, J. *Angew. Chem., Int. Ed.* **1999**, *38*, 2830.
(b) Gemel, C.; Steinke, T.; Cokoja, M.; Kempter, A.; Fischer, R. A. *Eur. J. Inorg. Chem.* **2004**, *21*, 4161.
- (8) Linti, G.; Schnöckel, H. *Coord. Chem. Rev.* **2000**, *206–207*, 285.
- (9) (a) Baker, R. J.; Jones, C. *Coord. Chem. Rev.* **2005**, *249*, 1857.
(b) Jones, C.; Stasch, A. In *The Group 13 Metals Aluminium, Gallium, Indium and Thallium. Chemical Patterns and Peculiarities*; Downs, A.J., Aldridge, S., Eds.; Wiley-Blackwell: Chichester, U.K., 2011; Chapter 5.
- (10) Roesky, P. W. *Dalton Trans.* **2009**, 1887.
- (11) Fischer, E. O.; Hofmann, H. P. *Angew. Chem.* **1957**, *69*, 639.
- (12) Meister, H. *Angew. Chem.* **1957**, *69*, 533.
- (13) Beachley, O. T.; Blom, R.; Churchill, M. R.; Faegri, K.; Fetting, J. C.; Pazik, J. C.; Victoriano, L. *Organometallics* **1989**, *8*, 346.
- (14) Uhl, W.; Graupner, R.; Layh, M.; Schütz, U. *J. Organomet. Chem.* **1995**, *493*, C1.
- (15) Dohmeier, C.; Robl, C.; Tacke, M.; Schnöckel, H.-G. *Angew. Chem., Int. Ed.* **1991**, *30*, 564.
- (16) Tacke, M.; Schnöckel, H. *Inorg. Chem.* **1989**, *28*, 2895.
- (17) Beachley, O. T.; Pazik, J. C.; Noble, M. J. *Organometallics* **1994**, *13*, 2885.
- (18) Loos, D.; Schnöckel, H.; Gauss, J.; Schneider, U. *Angew. Chem., Int. Ed.* **1992**, *31*, 1362.
- (19) Loos, D.; Schnöckel, H. *J. Organomet. Chem.* **1993**, *463*, 37.
- (20) Loos, D.; Baum, E.; Ecker, A.; Schnöckel, H.; Downs, A. J. *Angew. Chem., Int. Ed.* **1997**, *36*, 860.
- (21) Schulz, S.; Roesky, H. W.; Koch, H. J.; Sheldrick, G. M.; Stalke, D.; Kuhn, A. *Angew. Chem., Int. Ed.* **1993**, *32*, 1729.
- (22) Jutzi, P.; Neumann, B.; Reumann, G.; Stamm, H.-G. *Organometallics* **1998**, *17*, 1305.
- (23) Schormann, M.; Klimek, K. S.; Hatop, H.; Varkey, S. P.; Roesky, H. W.; Lehmann, C.; Röpken, C.; Herbst-Irmer, R.; Noltemeyer, M. *J. Solid State Chem.* **2001**, *162*, 225.
- (24) Schnitter, C.; Roesky, H. W.; Ropken, C.; Herbst-Irmer, R.; Schmidt, H.-G.; Noltemeyer, M. *Angew. Chem., Int. Ed.* **1998**, *37*, 1952.
- (25) Uhl, W.; Jantschak, A. *J. Organomet. Chem.* **1998**, *555*, 263.
- (26) Uhl, W.; Hiller, W.; Layh, M.; Schwarz, W. *Angew. Chem., Int. Ed.* **1992**, *31*, 1364.
- (27) Purath, A.; Schnöckel, H. *J. Organomet. Chem.* **1999**, *579*, 373.
- (28) Buehler, M.; Linti, G. *Z. Anorg. Allg. Chem.* **2006**, *632*, 2453.
- (29) Buchin, B.; Steinke, T.; Gemel, C.; Cadenbach, T.; Fischer, R. A. *Z. Anorg. Allg. Chem.* **2005**, *631*, 2756.
- (30) Buchin, B.; Gemel, C.; Cadenbach, T.; Fischer, R. A. *Inorg. Chem.* **2006**, *45*, 1789.
- (31) Linti, G. *J. Organomet. Chem.* **1996**, *520*, 107.
- (32) Jutzi, P.; Schebaum, L. O. *J. Organomet. Chem.* **2002**, *654*, 176.
- (33) Niemeyer, M.; Power, P. P. *Angew. Chem., Int. Ed.* **1998**, *37*, 1277.
- (34) Haubrich, S. T.; Power, P. P. *J. Am. Chem. Soc.* **1998**, *120*, 2202.
- (35) Hardman, N. J.; Wright, R. J.; Phillips, A. D.; Power, P. P. *J. Am. Chem. Soc.* **2003**, *125*, 2667.
- (36) Su, J.; Li, X.-W.; Crittendon, R. C.; Robinson, G. H. *J. Am. Chem. Soc.* **1997**, *119*, 5471.
- (37) Twamley, B.; Power, P. P. *Angew. Chem., Int. Ed.* **2000**, *39*, 3500.
- (38) Li, X.-W.; Pennington, W. T.; Robinson, G. H. *J. Am. Chem. Soc.* **1995**, *117*, 7578.
- (39) Cui, C.; Roesky, H. W.; Schmidt, H.-G.; Noltemeyer, M.; Hao, H.; Cimpoesu, F. *Angew. Chem., Int. Ed.* **2000**, *39*, 4274.
- (40) Hardman, N. J.; Eichler, B. E.; Power, P. P. *Chem. Commun.* **2000**, 1991.
- (41) (a) Braunschweig, H. *Angew. Chem., Int. Ed.* **1998**, *37*, 1786.
(b) Braunschweig, H.; Colling, M.; Englert, U. *Angew. Chem., Int. Ed.* **1998**, *37*, 3179.
(c) Braunschweig, H.; Colling, M. *Coord. Chem. Rev.* **2001**, *223*, 1.
(d) Braunschweig, H.; Colling, M. *Eur. J. Inorg. Chem.* **2003**, 393.
(e) Braunschweig, H.; Whittell, G. R. *Chem.—Eur. J.* **2005**, *11*, 6128.
(f) Braunschweig, H.; Radacki, K.; Rais, D.; Seeler, F. *Angew. Chem., Int. Ed.* **2006**, *45*, 1066.
(g) Braunschweig, H.; Kollann, C.; Rais, D. *Angew. Chem., Int. Ed.* **2006**, *45*, 5254.
(h) Braunschweig, H.; Radacki, K.; Uttinger, K. *Angew. Chem., Int. Ed.* **2007**, *46*, 3979.
(i) Braunschweig, H.; Burzler, M.; Kupfer, T.; Radacki, K.; Seeler, F. *Angew. Chem., Int. Ed.* **2007**, *46*, 7785.
- (42) Uhl, W.; Benter, M.; Melle, S.; Saak, W.; Frenking, G.; Uddin, J. *Organometallics* **1999**, *18*, 3778.
- (43) Boehme, C.; Frenking, G. *Chem.—Eur. J.* **1999**, *5*, 2184.
- (44) Macdonald, C. L. B.; Cowley, A. H. *J. Am. Chem. Soc.* **1999**, *121*, 12113.
- (45) Uddin, J.; Frenking, G. *J. Am. Chem. Soc.* **2001**, *123*, 1683.
- (46) Weiss, D.; Steinke, T.; Winter, M.; Fischer, R. A.; Fröhlich, N.; Uddin, J.; Frenking, G. *Organometallics* **2000**, *19*, 4583.
- (47) Doerr, M.; Frenking, G. *Z. Anorg. Allg. Chem.* **2002**, *628*, 843.
- (48) Uddin, J.; Boehme, C.; Frenking, G. *Organometallics* **2000**, *19*, 571.
- (49) Boehme, C.; Uddin, J.; Frenking, G. *Coord. Chem. Rev.* **2000**, *197*, 249.
- (50) Frenking, G.; Wichmann, K.; Fröhlich, N.; Loschen, C.; Lein, M.; Frunzke, J.; Rayón, V. M. *Coord. Chem. Rev.* **2003**, *238–239*, 55.
- (51) Lupinetti, A. J.; Frenking, G.; Strauss, S. H. *Angew. Chem., Int. Ed.* **1998**, *37*, 2113.
- (52) Gorden, J. D.; Macdonald, C. L. B.; Cowley, A. H. *Chem. Commun.* **2001**, 75.
- (53) Su, J.; Li, X.-W.; Crittendon, R. C.; Campana, C. F.; Robinson, G. H. *Organometallics* **1997**, *16*, 4511.
- (54) González-Gallardo, S.; Prabusankar, G.; Cadenbach, T.; Gemel, C.; von Hopfgarten, M.; Frenking, G.; Fischer, R. A. *Struct. Bonding* **2010**, *136*, 147.
- (55) Jones, C.; Mills, D. P.; Platts, J. A.; Rose, R. P. *Inorg. Chem.* **2006**, *45*, 3146.
- (56) Timoshkin, A. Y.; Schaefer, H. F. *Organometallics* **2005**, *24*, 3343.
- (57) Merino, G.; Beltrán, H. I.; Vela, A. *Inorg. Chem.* **2006**, *45*, 1091.
- (58) Wiecko, M.; Roesky, P. W.; Nava, P.; Ahlrichs, R.; Konchenko, S. N. *Chem. Commun.* **2007**, 927.
- (59) (a) Sanderson, R. T. *J. Am. Chem. Soc.* **1983**, *105*, 2259.
(b) Bonello, O.; Jones, C.; Stasch, A.; Woodul, W. D. *Organometallics* **2010**, *29*, 4914.
- (60) Prabusankar, G.; Kempter, A.; Gemel, C.; Schröter, M.-K.; Fischer, R. A. *Angew. Chem., Int. Ed.* **2008**, *47*, 7234.
- (61) Prabusankar, G.; Gemel, C.; Parameswaran, P.; Flener, C.; Frenking, G.; Fischer, R. A. *Angew. Chem., Int. Ed.* **2009**, *48*, 5526.
- (62) Schulz, S.; Schoop, T.; Roesky, H. W.; Häming, L.; Steiner, A.; Herbst-Irmer, R. *Angew. Chem., Int. Ed.* **1995**, *34*, 919.
- (63) Von Hänisch, C. K. F.; Üffing, C.; Junker, M. A.; Ecker, A.; Kneisel, B. O.; Schnöckel, H.-G. *Angew. Chem., Int. Ed.* **1996**, *35*, 2875.
- (64) Cowley, A. H. *Chem. Commun.* **2004**, 2369.
- (65) Gorden, J. D.; Voigt, A.; Macdonald, C. L. B.; Silverman, J. S.; Cowley, A. H. *J. Am. Chem. Soc.* **2000**, *122*, 950.
- (66) Weiss, J.; Stetzka, D.; Nuber, B.; Fischer, R. A.; Boehme, C.; Frenking, G. *Angew. Chem., Int. Ed.* **1997**, *36*, 70.
- (67) Hardman, N. J.; Power, P. P.; Gorden, J. D.; Macdonald, C. L.; Cowley, A. H. *Chem. Commun.* **2001**, 1866.
- (68) Jutzi, P.; Neumann, B.; Reumann, G.; Schebaum, L. O.; Stamm, H.-G. *Organometallics* **2001**, *20*, 2854.
- (69) Gorden, J. D.; Macdonald, C. L. B.; Cowley, A. H. *Main Group Chem.* **2005**, *4*, 33.
- (70) Romero, P. E.; Piers, W. E.; Decker, S. A.; Chau, D.; Woo, T. K.; Parvez, M. *Organometallics* **2003**, *22*, 1266.
- (71) Schulz, S.; Kuczkowski, A.; Schuchmann, D.; Floerke, U.; Nieger, M. *Organometallics* **2006**, *25*, 5487.
- (72) (a) Haaland, A. *Angew. Chem., Int. Ed.* **1989**, *28*, 992.
(b) Haaland, A. In *Coordination Chemistry of Aluminum*; Robinson, G. H., Ed.; VCH Verlagsgesellschaft: Weinheim, Germany, 1993.

- (73) (a) Woski, M.; Mitzel, N. W. *Z. Naturforsch.* **2004**, *59B*, 269. (b) Cowley, A. R.; Downs, A. J.; Marhant, S.; Macrae, V. A.; Taylor, R. A. *Organometallics* **2005**, *24*, 5702. (c) Kuczkowski, A.; Schulz, S.; Nieger, M. *Appl. Organomet. Chem.* **2004**, *18*, 244. (d) Kuczkowski, A.; Schulz, S.; Nieger, M.; Schreiner, P. R. *Organometallics* **2002**, *21*, 1408.
- (74) Uhl, W.; Keimling, S. U.; Hiller, W.; Neumayer, M. *Chem. Ber.* **1995**, *128*, 1137.
- (75) Uhl, W.; Keimling, S. U.; Hiller, W.; Neumayer, M. *Chem. Ber.* **1996**, *129*, 397.
- (76) Uhl, W.; Benter, M.; Prott, M. J. *Chem. Soc. Dalton Trans.* **2000**, 643.
- (77) Uffing, C.; Ecker, A.; Koppe, R.; Schnöckel, H. *Organometallics* **1998**, *17*, 2373.
- (78) (a) Grachova, E. V.; Jutzi, P.; Neumann, B.; Schebaum, L. O.; Stammer, H.-G.; Tunik, S. P. *J. Chem. Soc., Dalton Trans.* **2002**, 302. (b) Grachova, E. V.; Jutzi, P.; Neumann, B.; Stammer, H.-G. *Dalton Trans.* **2005**, 3614.
- (79) Grachova, E. V.; Linti, G.; Stammer, H.-G.; Neumann, B.; Tunik, S. P.; Wadepohl, H. *Eur. J. Inorg. Chem.* **2007**, 140.
- (80) Uhl, W.; Pohlmann, M. *Organometallics* **1997**, *16*, 2478.
- (81) Yu, Q.; Purath, A.; Donchev, A.; Schnöckel, H.-G. *J. Organomet. Chem.* **1999**, *584*, 94.
- (82) Jutzi, P.; Neumann, B.; Reumann, G.; Schebaum, L. O.; Stammer, H.-G. *Organometallics* **1999**, *18*, 2550.
- (83) Jutzi, P.; Neumann, B.; Schebaum, L. O.; Stammer, A.; Stammer, H.-G. *Organometallics* **1999**, *18*, 4462.
- (84) Cokoja, M.; Steinke, T.; Gemel, C.; Welzel, T.; Winter, M.; Merz, K.; Fischer, R. A. *J. Organomet. Chem.* **2003**, *684*, 277.
- (85) Uhl, W.; Melle, S.; Frenking, G.; Hartmann, M. *Inorg. Chem.* **2001**, *40*, 750.
- (86) Uhl, W.; Pohlmann, M.; Wartchow, R. *Angew. Chem., Int. Ed.* **1998**, *37*, 961.
- (87) Steinke, T.; Gemel, C.; Cokoja, M.; Winter, M.; Fischer, R. A. *Angew. Chem., Int. Ed.* **2004**, *43*, 2299.
- (88) Uhl, W.; Melle, S. Z. *Anorg. Allg. Chem.* **2000**, *626*, 2043.
- (89) Gemel, C.; Steinke, T.; Weiss, D.; Cokoja, M.; Winter, M.; Fischer, R. A. *Organometallics* **2003**, *22*, 2705.
- (90) (a) Cadenbach, T.; Bollermann, T.; Gemel, C.; Fernandez, I.; von Hopffgarten, M.; Frenking, G.; Fischer, R. A. *Angew. Chem., Int. Ed.* **2008**, *47*, 9150. (b) Bollermann, T.; Cadenbach, T.; Gemel, C.; Freitag, K.; Molon, M.; Gwildies, V.; Fischer, R. A. *Inorg. Chem.* **2011**, *50* (12), 5808.
- (91) Weiss, D.; Winter, M.; Fischer, R. A.; Yu, C.; Wichmann, K.; Frenking, G. *Chem. Commun.* **2000**, 2495.
- (92) Steinke, T.; Gemel, C.; Winter, M.; Fischer, R. A. *Chem.—Eur. J.* **2005**, *11*, 1636.
- (93) Steinke, T.; Gemel, C.; Winter, M.; Fischer, R. A. *Angew. Chem., Int. Ed.* **2002**, *41*, 4761.
- (94) Kempster, A.; Gemel, C.; Cadenbach, T.; Fischer, R. A. *Inorg. Chem.* **2007**, *46*, 9481.
- (95) (a) Bollermann, T.; Puls, A.; Gemel, C.; Cadenbach, T.; Fischer, R. A. *Dalton Trans.* **2009**, 1372. (b) Bollermann, T.; Prabusankar, G.; Gemel, C.; Seidel, R. W.; Winter, M.; Fischer, R. A. *Chem.—Eur. J.* **2010**, *16* (29), 8846.
- (96) Buchin, B.; Gemel, C.; Cadenbach, T.; Schmid, R.; Fischer, R. A. *Angew. Chem., Int. Ed.* **2006**, *45*, 1074.
- (97) Cadenbach, T.; Gemel, C.; Bollermann, T.; Fischer, R. A. *Inorg. Chem.* **2009**, *48*, 5021.
- (98) MacFarlane, K. S.; Rettig, S. J.; Liu, Z.; James, B. R. J. *Organomet. Chem.* **1998**, *557*, 213.
- (99) Jones, M. D.; Kemmitt, R. D. W.; Platt, A. W. G. *J. Chem. Soc., Dalton Trans.* **1986**, 1411.
- (100) Cadenbach, T.; Gemel, C.; Bollermann, T.; Fernandez, I.; Frenking, G.; Fischer, R. A. *Chem.—Eur. J.* **2008**, 10789.
- (101) Borowski, A. F.; Sabo-Etienne, S.; Christ, M. L.; Donnadiu, B.; Chaudret, B. *Organometallics* **1996**, *15*, 1427.
- (102) Cadenbach, T.; Bollermann, T.; Gemel, C.; Fischer, R. A. *Dalton Trans.* **2009**, 322.
- (103) Steinke, T.; Cokoja, M.; Gemel, C.; Kempster, A.; Krapp, A.; Frenking, G.; Zenneck, U.; Fischer, R. A. *Angew. Chem., Int. Ed.* **2005**, *44*, 2943.
- (104) (a) Hackett, M.; Ibers, J. A.; Jernakoff, P.; Whitesides, G. M. *J. Am. Chem. Soc.* **1986**, *108*, 8094. (b) Hackett, M.; Ibers, J. A.; Whitesides, G. M. *J. Am. Chem. Soc.* **1988**, *110*, 1436.
- (105) (a) Fischer, R. A.; Kaesz, H. D.; Khan, S. I.; Müller, H.-J. *Inorg. Chem.* **1990**, *29*, 1601. (b) Fischer, R. A.; Behm, J. J. *Organomet. Chem.* **1991**, *413*, C10.
- (106) Weiss, D.; Winter, M.; Merz, K.; Knufer, A.; Fischer, R. A.; Fröhlich, N.; Frenking, G. *Polyhedron* **2002**, *21*, 535.
- (107) Schneider, J. J.; Kruger, C.; Nolte, M.; Abraham, I.; Ertel, T. S.; Bertagnolli, H. *Angew. Chem., Int. Ed.* **1994**, *33*, 2435.
- (108) Dohmeier, C.; Krautschied, H.; Schnöckel, H. *Angew. Chem., Int. Ed.* **1994**, *33*, 2482.
- (109) Yamaguchi, T.; Ueno, K.; Ogino, H. *Organometallics* **2001**, *20*, 501.
- (110) (a) de Graaf, W.; Boersma, J.; Smeets, W. J. J.; Spek, A. L.; van Koten, G. *Organometallics* **1989**, *8*, 2907. (b) Krause, J.; Cestarc, G.; Haack, K. J.; Seevogel, K.; Storm, W.; Pörschke, K. R. *J. Am. Chem. Soc.* **1999**, *121*, 9807.
- (111) Anandhi, U.; Sharp, P. R. *Angew. Chem., Int. Ed.* **2004**, *43*, 6128.
- (112) Yang, X.-J.; Quillian, B.; Wang, Y.; Wei, P.; Robinson, G. H. *Organometallics* **2004**, *23*, 5119.
- (113) Yang, X.-J.; Wang, Y.; Quillian, B.; Wei, P.; Chen, Z.; v. R. Schleyer, P.; Robinson, G. H. *Organometallics* **2006**, *25*, 925.
- (114) Quillian, B.; Wang, Y.; Wei, P.; Robinson, G. H. *New J. Chem.* **2008**, *32*, 774.
- (115) (a) Patmore, D. J.; Graham, W. A. G. *J. Chem. Soc., Chem. Commun.* **1965**, 591. (b) Patmore, D. J.; Graham, W. A. G. *Inorg. Chem.* **1966**, *5*, 1405. (c) Patmore, D. J.; Graham, W. A. G. *Inorg. Chem.* **1966**, *5*, 1586. (d) Hoyano, J.; Patmore, D. J.; Graham, W. A. G. *Inorg. Chem. Nucl. Lett.* **1968**, *4*, 201. (e) Chatt, J.; Eaborn, C.; Kapoor, P. N. *J. Organomet. Chem.* **1970**, *23*, 109. (f) Hsieh, A. T. T.; Mays, M. J. *Inorg. Chem. Nucl. Lett.* **1971**, *7*, 223. (g) Hsieh, A. T. T.; Mays, M. J. *J. Chem. Soc., Dalton Trans.* **1972**, 516. (h) Hsieh, A. T. T.; Mays, M. J. *J. Organomet. Chem.* **1972**, *37*, 9. (i) Hsieh, A. T. T. *Inorg. Chim. Acta* **1975**, *14*, 87.
- (116) (a) Gabbai, F. P.; Schier, A.; Riede, J.; Schmidbaur, H. *Inorg. Chem.* **1995**, *34*, 3855. (b) Gabbai, F. P.; Chung, S.-C.; Schier, A.; Krüger, S.; Rösch, N.; Schmidbaur, H. *Inorg. Chem.* **1997**, *36*, 5699. (c) Weiss, J.; Priermeier, T.; Fischer, R. A. *Inorg. Chem.* **1996**, *35*, 71. (d) Weiss, J.; Frank, A.; Herdtweck, E.; Nlate, S.; Mattner, M.; Fischer, R. A. *Chem. Ber.* **1996**, *129*, 297.
- (117) Jutzi, P.; Neumann, B.; Schebaum, L. O.; Stammer, A.; Stammer, H.-G. *Organometallics* **2000**, *19*, 1445.
- (118) Steinke, T.; Gemel, C.; Cokoja, M.; Winter, M.; Fischer, R. A. *Chem. Commun.* **2003**, 1066.
- (119) Cokoja, M.; Gemel, C.; Steinke, T.; Schröder, F.; Fischer, R. A. *Dalton Trans.* **2005**, 44.
- (120) Steinke, T.; Gemel, C.; Cokoja, M.; Winter, M.; Fischer, R. A. *Dalton Trans.* **2005**, 55.
- (121) Buchin, B.; Gemel, C.; Kempster, A.; Cadenbach, T.; Fischer, R. A. *Inorg. Chim. Acta* **2006**, *359*, 4833.
- (122) Cadenbach, T.; Gemel, C.; Zacher, D.; Fischer, R. A. *Angew. Chem., Int. Ed.* **2008**, *47*, 3438.
- (123) Cokoja, M.; Parala, H.; Schroeter, M.-K.; Birkner, A.; van den Berg, M. W. E.; Gruenert, W.; Fischer, R. A. *Chem. Mater.* **2006**, *18*, 1634.
- (124) Cokoja, M.; Parala, H.; Schroeter, M.-K.; Birkner, A.; van den Berg, M. W. E.; Gruenert, W.; Fischer, R. A. *J. Mater. Chem.* **2006**, *16*, 2420.
- (125) Cokoja, M.; Jagirdar, B. R.; Parala, H.; Birkner, A.; Fischer, R. A. *Eur. J. Inorg. Chem.* **2008**, 3330.
- (126) Cokoja, M.; Parala, H.; Birkner, A.; Shekhah, O.; van den Berg, M. W. E.; Fischer, R. A. *Chem. Mater.* **2007**, *19*, 5721.
- (127) Cadenbach, T.; Gemel, C.; Schmid, R.; Halbherr, M.; Yusenko, K.; Cokoja, M.; Fischer, R. A. *Angew. Chem., Int. Ed.* **2009**, *48*, 3872.

- (128) Arnold, P. L.; Liddle, S. T.; McMaster, J.; Jones, C.; Mills, D. P. *J. Am. Chem. Soc.* **2007**, *129*, 5360.
- (129) Jones, C.; Stasch, A.; Woodul, W. D. *Chem. Commun.* **2009**, 113.
- (130) Liddle, S. T.; McMaster, J.; Mills, D. P.; Blake, A. J.; Jones, C.; Woodul, W. D. *Angew. Chem., Int. Ed.* **2009**, *48*, 1077.
- (131) Gamer, M. T.; Roesky, P. W.; Konchenko, S. N.; Nava, P.; Ahrlrichs, R. *Angew. Chem., Int. Ed.* **2006**, *45*, 4447.
- (132) (a) Becke, A. D. *Phys. Rev. A* **1988**, *38*, 3098. (b) Vosko, S. H.; Wilk, L.; Nusair, M. *Can. J. Phys.* **1980**, *58*, 1200. (c) Perdew, J. P. *Phys. Rev. B* **1986**, *33*, 8822. Erratum: Perdew, J. P. *Phys. Rev. B* **1986**, *34*, 7406.
- (133) Wiecko, M.; Roesky, P. W. *Organometallics* **2007**, *26*, 4846.
- (134) Minasian, S. G.; Krinsky, J. L.; Rinehart, J. D.; Copping, R.; Tyliczszak, T.; Janousch, M.; Shuh, D. K.; Arnold, J. *J. Am. Chem. Soc.* **2009**, *131*, 13767.
- (135) Krinsky, J. L.; Minasian, S. G.; Arnold, J. *Inorg. Chem.* **2011**, *50*, 345.
- (136) Minasian, S. G.; Krinsky, J. L.; Williams, V. A.; Arnold, J. *J. Am. Chem. Soc.* **2008**, *130*, 10086.
- (137) Slattery, J. M.; Higelin, A.; Bayer, T.; Krossing, I. *Angew. Chem., Int. Ed.* **2010**, *49*, 3228.
- (138) Wehmschulte, R. J. *Angew. Chem., Int. Ed.* **2010**, *49*, 4708.
- (139) Buchin, G.; Gemel, C.; Cadenbach, T.; Fernández, I.; Frenking, G.; Fischer, R. A. *Angew. Chem., Int. Ed.* **2006**, *45*, 5207.
- (140) Halbherr, M.; Bollermann, T.; Gemel, C.; Fischer, R. A. *Angew. Chem., Int. Ed.* **2010**, *49*, 1878.
- (141) Bunn, N. R.; Aldridge, S.; Kays, D. L.; Coombs, N. D.; Rossin, A.; Willock, D. J.; Day, J. K.; Jones, C.; Ooi, L.-L. *Organometallics* **2005**, *24*, 5891. (b) Aldridge, S. *Angew. Chem., Int. Ed.* **2006**, *45*, 8097.
- (142) Kempter, A.; Gemel, C.; Cadenbach, T.; Fischer, R. A. *Organometallics* **2007**, *26*, 4257.
- (143) Cadenbach, T.; Gemel, C.; Schmid, R.; Block, S.; Fischer, R. A. *Dalton Trans.* **2004**, 3171.
- (144) Cadenbach, T.; Gemel, C.; Schmid, R.; Fischer, R. A. *J. Am. Chem. Soc.* **2005**, *127*, 17068.
- (145) (a) Kays, D. L.; Aldridge, S. *Angew. Chem., Int. Ed.* **2009**, *48*, 4109. (b) Bollermann, T.; Freitag, K.; Gemel, C.; Seidel, R. W.; von Hopffgarten, M.; Frenking, G.; Fischer, R. A. *Angew. Chem., Int. Ed.* **2011**, *50* (3), 772.
- (146) Cadenbach, T.; Bollermann, T.; Gemel, C.; Tombul, M.; Fernández, I.; von Hopffgarten, M.; Frenking, G.; Fischer, R. A. *J. Am. Chem. Soc.* **2009**, *131*, 16063.
- (147) Pyykkö, P. *J. Organomet. Chem.* **2006**, *691*, 4336.
- (148) (a) Resa, I.; Carmona, E.; Gutierrez-Puebla, E.; Monge, A. *Science* **2004**, *305*, 1136. (b) del Río, D.; Galindo, A.; Resa, I.; Carmona, E. *Angew. Chem., Int. Ed.* **2005**, *44*, 1244. (c) Zhu, Z.; Brynda, M.; Wright, R. J.; Fischer, R. C.; Merrill, W. A.; Rivard, E.; Wolf, R.; Fettingner, J. C.; Olmstead, M. M.; Power, P. P. *J. Am. Chem. Soc.* **2007**, *129*, 10847. (d) Gorrane, A.; Resa, I.; Rodriguez, A.; Carmona, E. *Coord. Chem. Rev.* **2008**, *252*, 1532. (e) Fedushkin, I. L.; Skatova, A. A.; Ketkov, S. Y.; Eremenko, O. V.; Piskunov, A. V.; Fukin, G. K. *Angew. Chem., Int. Ed.* **2007**, *46*, 4302. (f) Wang, Y.; Quillian, B.; Wei, P.; Wang, H.; Yang, X.-J.; Xie, Y.; King, R. B.; Schleyer, P. V. R.; Schaefer, H. F., III.; Robinson, G. H. *J. Am. Chem. Soc.* **2005**, *127*, 11944. (g) Schuchmann, D.; Westphal, U.; Schulz, S.; Florke, U.; Blaser, D.; Boese, R. *Angew. Chem., Int. Ed.* **2009**, *48*, 807. (h) Schulz, S.; Schuchmann, D.; Westphal, U.; Bolte, M. *Organometallics* **2009**, *28*, 1590. (i) Schulz, S.; Schuchmann, D.; Krossing, I.; Himmel, D.; Bläser, D.; Boese, R. *Angew. Chem., Int. Ed.* **2009**, *48*, 5748.
- (149) (a) Cadenbach, T.; Gemel, C.; Fischer, R. A. *Angew. Chem., Int. Ed.* **2008**, *47*, 9146. (b) Bollermann, T.; Schwedler, I.; Molon, M.; Freitag, K.; Gemel, C.; Seidel, R. W.; Fischer, R. A. *Dalton Trans.* **2011**, 40, 12570.
- (150) Bollermann, T.; Cadenbach, T.; Gemel, C.; von Hopffgarten, M.; Frenking, G.; Fischer, R. A. *Chem.—Eur. J.* **2010**, *16*, 13372.
- (151) Molon, M.; Cadenbach, T.; Bollermann, T.; Gemel, C.; Fischer, R. A. *Chem. Commun.* **2010**, 46, 5677.
- (152) (a) Fischer, R. A.; Scherer, W.; Kleine, M. *Angew. Chem., Int. Ed.* **1993**, *32*, 748. (b) Fischer, R. A.; Miehr, A. *Chem. Mater.* **1996**, *8*, 497. (c) Fischer, R. A.; Miehr, A.; Schulte, M. M. *Adv. Mater.* **1995**, *7*, 58. (d) Fischer, R. A.; Miehr, A.; Metzger, T. *Thin Solid Films* **1996**, *289*, 147. (e) Fischer, R. A.; Miehr, A.; Metzger, T.; Born, E.; Ambacher, O.; Angerer, H.; Dimitrov, R. *Chem. Mater.* **1996**, *8*, 1356.
- (153) (a) Maury, F.; Talin, A. A.; Kaesz, H. D.; Williams, R. S. *Chem. Mater.* **1993**, *5*, 84. (b) Fraser, B.; Brandt, L.; Stovall, W. K.; Kaesz, H. D.; Khan, S. I.; Maury, F. J. *Organomet. Chem.* **1994**, *472*, 317.
- (154) (a) Williams, R. S. *Appl. Surf. Sci.* **1992**, *60/61*, 613. (b) Kuo, T. C.; Wang, K. L.; Arghavani, R.; George, T.; Lin, T. L. *J. Vac. Sci. Technol.* **1992**, *B10*, 1923.
- (155) (a) Cable, R. E.; Schaak, R. E. *Chem. Mater.* **2007**, *19*, 4098. (b) Bauer, J. C.; Chen, X.; Liu, Q. S.; Phan, T. H.; Schaak, R. E. *J. Mater. Chem.* **2008**, *18*, 275. (c) Schaefer, Z. L.; Vaughn, D. D.; Schaak, R. E. *J. Alloys Compd.* **2010**, 490, 98.
- (156) Ferrando, R.; Jellinek, J.; Johnston, R. L. *Chem. Rev.* **2008**, *108*, 845.
- (157) Cokoja, M.; Parala, H.; Birkner, A.; Fischer, R. A.; Margeat, O.; Ciuculescu, D.; Amiens, C.; Chaudret, B.; Falqui, A.; Lecante, P. *Eur. J. Inorg. Chem.* **2010**, 1599.
- (158) (a) Hume-Rothery, W. *J. Inst. Met.* **1926**, *35*, 295. (b) Jones, H. *Proc. Phys. Soc.* **1937**, *49*, 250. (c) Paxton, A.; Methfessel, M.; Pettifor, D. *Proc. R. Soc. A* **1997**, *453*, 1493. (d) Ferro, R. A.; Saccone, A. In *Materials Science and Technology, Vol. 1, The Structure of Solids*; Cahn, R. W., Haasen, P., Kramer, E. J., Eds.; VCH: Weinheim, Germany, 1993; p 123.
- (159) Galloway, E.; Armbruster, M.; Kovnir, K.; Tikhov, M. S.; Lambert, R. M. *J. Catal.* **2009**, *261*, 60.
- (160) Marinelli, T.B.L.W.N.; Ponc, V. *J. Catal.* **1995**, *151*, 431.
- (161) (a) Liberikova, K. T.; Touroude, R. *J. Mol. Catal. A* **2002**, *180*, 221. (b) M.J. Consonni, M. J.; Murzin, D. Y.; R. Touroude, R. *J. Catal.* **1999**, *188*, 165.
- (162) Schroeter, M. K.; Khodeir, L.; van den Berg, M. W. E.; Hikov, T.; Cokoja, M.; Miao, S. J.; Gruenert, W.; Muhler, M.; Fischer, R. A. *Chem. Commun.* **2006**, 2498.
- (163) (a) Yan, N.; Xiao, C. X.; Kou, Y. *Coord. Chem. Rev.* **2010**, *254*, 1179. (b) Xiao, C. X.; Yan, N.; Kou, Y. *Chin. J. Catal.* **2009**, *30*, 753. (c) Schimpf, S.; Rittermeier, A.; Zhang, X.; Li, Z.-A.; Spasova, M.; van den Berg, M. W.E.; Farle, M.; Wang, Y.; Fischer, R. A.; Muhler, M. *Chem. Catal. Chem.* **2010**, *2*, 214.
- (164) (a) Osswald, J.; Giedigkeit, R.; Jentoft, R. E.; Armbruster, M.; Girsdiess, F.; Kovnir, K.; Ressler, T.; Grin, Y.; Schlogl, R. *J. Catal.* **2008**, *258*, 210. (b) Osswald, J.; Kovnir, K.; Armbruster, M.; Giedigkeit, R.; Jentoft, R. E.; Wild, U.; Grin, Y.; Schlogl, R. *J. Catal.* **2008**, *258*, 219.
- (165) Ponc, V. *Appl. Catal., A* **2001**, *222*, 31.
- (166) Mikhailov, M. N.; Dergachev, A. A.; Mishin, I. V.; Kustov, L. M.; Lapidus, A. L. *Russ. J. Phys. Chem., A* **2008**, *82*, 612.
- (167) Entel, P.; Gruner, M. E.; Rollmann, G.; Hucht, A.; Sahoo, S.; Zayak, A. T.; Herper, H. C.; Dannenberg, A. *Philos. Mag.* **2008**, *88*, 2725.
- (168) (a) Entel, P.; Buchelnikov, V.; Khovailo, V. *J. Phys. D: Appl. Phys.* **2006**, *39*, 865. (b) Entel, P.; Buchelnikov, V. D.; Gruner, M. E. *Mater. Sci. Forum* **2008**, *583*, 21.